

**Study on electrochemical activation and application  
of novel Mg alloy electrode by tension stress  
application**

**Gang Shi**

**Saitama Institute of Technology**

**February 2018**

Chapter 1 Introduction .....	1
1.1 Current status of battery materials .....	1
1.1.1 Composition of the battery .....	1
1.1.2 The study of the material of the battery .....	2
1.2 Introduction of Primary batteries and secondary batteries .....	3
1.2.1 Classification of the electrochemical cell .....	3
1.2.2 Introduction of the Primary battery .....	4
1.2.3 Introduction of the Secondly battery .....	7
1.3 Expectation to a magnesium alloy battery .....	9
1.3.1 Comparison of characteristics of Mg and Li .....	9
1.3.2 Magnesium alloy air cell (primary) .....	10
1.3.3 The introduction of the second battery of Mg battery .....	12
1.3.4 Effect of Vanadium Oxide inserted in Anode .....	14
1.3.5 Introduction of Magnesium stem cell .....	15
1.4 Electrochemical reaction principle .....	16
1.5 Corrosion reaction of the Battery .....	18
1.5.1 Electrochemistry corrosion .....	18
1.5.2 Application of the stress corrosion .....	21
1.6 Design of magnesium electrode material .....	23
1.6.1 Selection of the added element of a new magnesium alloy .....	23
1.7 Purpose of this study .....	27
1.8 Composition of this paper .....	27
1.9 Conclusion .....	28
Reference .....	29
Chapter 2 Development of magnesium alloy electrode materials and performance evaluation .....	36
2.1 Production of the Mg-Zn-In-Se-MnS alloy .....	36
2.1.1 Vacuum gas replacement furnace .....	36
2.1.2 Fabrication of Mg-Zn-In-Sn-MnS alloy in vacuum gas replacement furnace .....	37

2.2	Production method of magnesium alloy plate.....	37
2.2.1	Twin-roll continuous casting .....	37
2.2.2	Manufacture of the Mg-Zn-In-Sn-MnS alloy sheet.....	38
2.3	Analysis of the magnesium alloy ingredient .....	39
2.3.1	Fluorescence X-rays analysis of the magnesium alloy ingredient .....	39
2.4	Performance evaluation of Mg-Zn-In-Sn-MnS alloy .....	40
2.4.1	Observation of fine structure.....	40
2.5	Experiment of tensile stress .....	41
2.6	Conclusion .....	41
	Reference .....	41
Chapter 3 Evaluation of electrode performance with stress corrosion and clarification of electrochemical stress corrosion mechanism .....		43
3.1	Advantages and mechanisms of manganese sulfide .....	43
3.2	Electrolyte selection and stress corrosion experiment .....	45
3.2.1	CV curve of KCl from 0 MPa to 10 MPa at a distance of 10 mm .....	45
3.2.2	CV curve of KCl from 0 MPa to 10MPa at a distance of 2 mm.....	47
3.2.3	CV curve of AcONa from 0 MPa to 10 MPa at a distance of 10 mm.....	48
3.3	The theory of electro-chemical chemistry and the application of the theory of the value of the study .....	52
3.3.1	Introduction .....	52
3.3.2	Experimental material .....	52
3.3.3	Measurement of Mg concentration .....	53
3.3.4	Proposal of hybrid model.....	54
3.3.5	Mg <sup>2+</sup> concentration changes .....	54
3.3.7	LC calculation .....	56
3.4	Conclusion.....	58
	Reference .....	59
Chapter 4 Application of stress corrosion - Development of primary battery .....		60
4.1	Introduction .....	60
4.2	Experimental.....	61

4.2.1 The electrochemical reaction process of corrosion simulation diagram.....	61
4.2.2 Measurements of single electrode characteristics .....	61
4.2.3 Morphologies of the magnesium alloy electrodes after tensile stress tests ..	62
4.3 Result and discussion .....	63
4.3.1.Measurements of single electrode characteristics.....	63
4.3.2.Estimation of power densities for the magnesium alloy batteries.....	65
4.3.3.Morphologies of the stressed magnesium electrodes .....	66
4.3.4 Magnesium air battery .....	69
4.4 Conclusion.....	70
Chapter 5 Mechanical control of magnesium alloy electrodes under the tensile stress for applications in non-aqueous battery electrolyte solution .....	72
5.1 Introduction .....	72
5.2 Experimental .....	74
5.3 Results and Discussion .....	78
5.4 Conclusion.....	86
References.....	87
Chapter 6 Phosphorous Recovery by the Magnesium Alloy Electrode under Tensile Stress.	88
6.1 Introduction .....	88
6.2 Experimental .....	89
6.3 Results and discussion .....	92
6.4 Conclusion .....	95
References.....	96
Chapter 7 Conclusion .....	97
Acknowledgments .....	100
Related publications .....	101

# Chapter 1 Introduction

## 1.1 Current status of battery materials

### 1.1.1 Composition of the battery

The battery, which is the chemical energy using electrochemical oxidation-reduction reaction (redox reaction) with the battery active material a device that converts directly to the battery energy[1-3]. In the non electrochemical redox reaction, such as corrosion and combustion, electron transfer occurs directly substance conversion without passing through an electric circuit, exothermic only. While the battery is often used as a term representing a battery, its basic cell scientific unit is cell (cell, unit cells). Cell is composed of one or more unit cells, the unit cells according to the output and capacity required are connected in series or parallel. The battery is made up of three key components to shown schematically pictorial in Fig1.1[4-7].

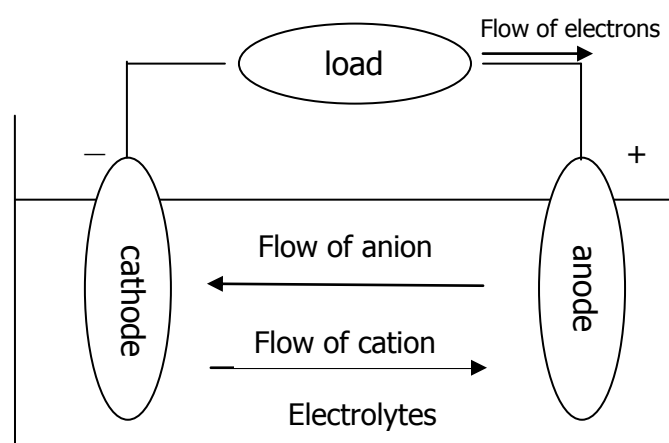


Fig. 1.1 The structure of battery

- a. anode: With a reducing electrode or the fuel electrode, placed accept electrons from the external circuit by an electrochemical reaction itself is reduced.
- b. cathode: Oxidation electrode, I receive an electron, and, with an oxidation electrode, itself is resolved by an electrochemical reaction by an outside circuit

- c. electrolytes: In an ion conductor, it becomes a cathode and the migration of ions medium between anodes. Electrolytes usually dissolved acid, alkali or salt in water and other solvents with a liquid and kept ion conductivity. There is the battery using the solid electrolyte, too, and in this case a solid electrolyte operates in the temperature indicating ion tradition characteristics.

### **1.1.2 The study of the material of the battery**

The combination that light weight, high electromotive force, high capacity are provided is desirable for the materials of the anode and cathode . However, reactivity, the Polari ability with other battery components, the combination that attaches it, and is ideal for reasons of the difficulty, the high cost of the worth by all means may not be practically[7-10]. Hydrogen is a very attractive as the negative electrode material or substance, those for accommodating a gas for state is required, it must be cause an efficient electrochemical reaction in the container. In fact H<sub>2</sub> have been mainly captured by the negative electrode metal material[11-13]. Further zinc with a substance other than a hydrogen have been widely used for a long time because of their useful properties. Lithium is the lightest metal, the development of a suitable electrolyte selection and cell structure in order to control its reactivity, in recent years has become very eye-catching as an attractive anode material. Combined with light weight to have a high performance and low cost, the magnesium alloy is expected as the negative electrode material of all the batteries. Cathode material, stability when in contact simultaneously with the electrolyte and the high oxidant capability, such as a valid operating voltage is required. Oxygen metal oxide taken from the air to direct the cell has been utilized as a positive electrode material, and high voltage, excellent positive electrode material show a high capacity are used in the further improved battery system[14-17]. As the electrode material is stable with little reaction, is that the electrolytic pledge property is almost no temperature dependence. Many electrolyte is an aqueous solution, using a molten salt or a non-aqueous electrolyte as the high temperature battery or electrolyte of a lithium battery as exceptions and prevents the reaction between the negative electrode and the electrolyte. Negative and positive electrodes to prevent internal short circuit of the battery is

electrically isolated, between them are satisfied electrolyte. In fact of the battery mechanically isolates the negative electrode and a positive electrode with a separator, the separator is maintained ionic conductivity for the electrolyte to penetrate. Sometimes, there is a case where the electrolyte is immobilized so as difficult to flow out. Further to reduce the internal resistance of the battery, a method with a conductive grid electrode, or adding a conductive agent into has been used[18-22].

## **1.2 Introduction of Primary batteries and secondary batteries**

### **1.2.1 Classification of the electrochemical cell**

Electrochemical cell is divided into a primary battery by whether it is possible to electrochemically charge (non-rechargeable) and secondary batteries (rechargeable). Primary battery is impossible electrical recharging, is intended to be discarded once the discharge is completed. Many primary battery moistened with electrolyte liquid absorber and a separator (liquid electrolyte is solid), called dry batteries[23]. Primary batteries are relatively inexpensive and lightweight compact power supply, portable electronic devices and appliances, lighting, cameras are used in a wide range of applications such as toys. Generally primary battery, any no need for maintenance in normal use, there is an advantage that excellent storage stability and having a high energy density[24]. In particular, in a storage battery (reserve battery), it is important to keep it in a stable state not activated. In this stable state, it is possible to substantially prevent chemical degradation and self-discharge, which enables long-term storage. At this time, the electrolytic solution is kept isolated[25-29]. Also, in a high temperature battery, it is inactive until the solid electrolyte melts and shows conductivity by heating. Applications are used in weapons systems such as missiles and torpedoes, which require large amounts of energy in a short time. The secondary battery can be electrically recharged and can be restored to the state before the discharge by flowing a current in the opposite direction to the discharge after the discharge. This is a device that saves electric energy and is called the storage battery. Secondary batteries are mainly used for the following two purposes. It is used as an

energy storage medium, is connected to an energy source such as a motor and charged, and discharges as necessary. It is also used for starting power supplies for automobiles and airplanes, emergency batteries, and solid energy storage systems for load leveling. In particular, batteries which are called mechanically rechargeable batteries, in many cases, after discharging, replace the metal of the negative electrode with a new one and recharge it. A metal / air battery is a typical example. Battery as an energy conversion device is classified and it becomes like Fig. 1.2[30,31].

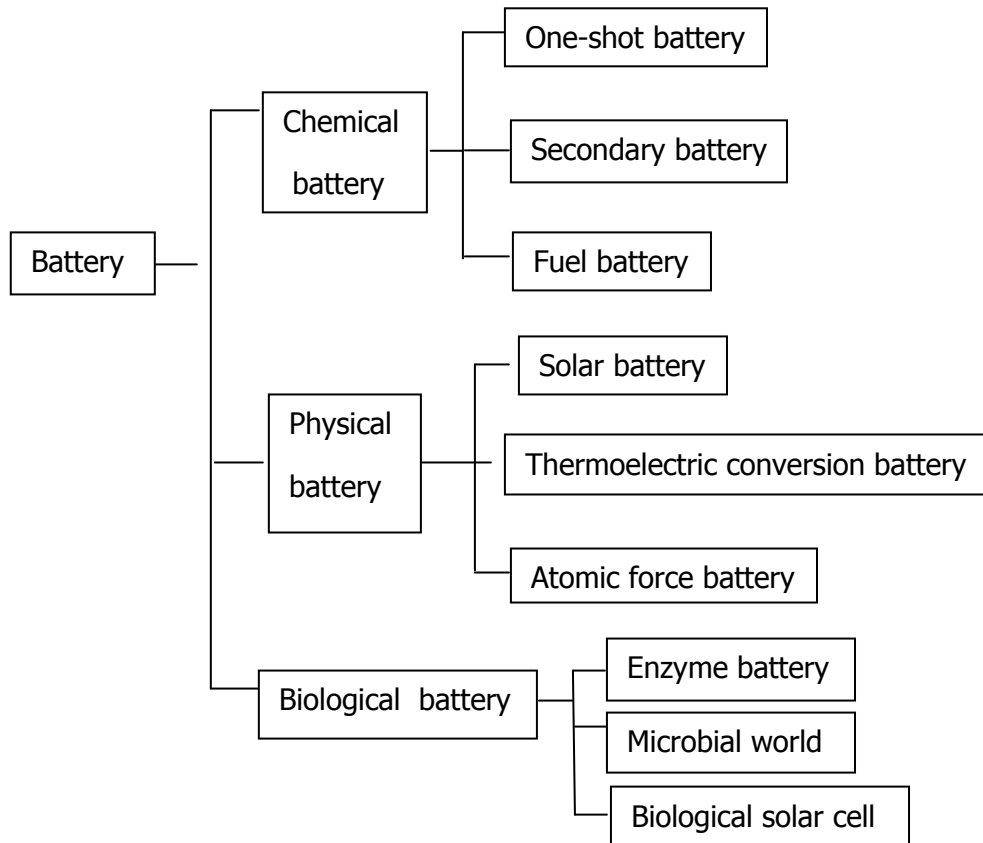


Fig. 1.2 Batteries are categorized from the perspective of energy conversion.

### 1.2.2 Introduction of the Primary battery

Primary batteries are simple power sources independent of public electric power for portable electronic or electrical equipment, lighting, cameras, computers, communication equipment, watches, calculators, memory backup and other various equipment.[32] The maximum advantage of the primary battery is its convenience, it



is easy to use from the viewpoint of structure, but it is not necessary for maintenance. The size and shape can be changed according to the purpose. Other advantages include shelf life, moderate energy density and power density, reliability and affordable will be cost[33,34]. Primary batteries existed 100 years ago, but until 1940 only manganese dry batteries had been used . Battery research developed greatly during World War II and after the war, not only the manganese stem battery system but also an excellent new battery was developed. The capacity has been improved from 50 Wh / Kg or less of the initial manganese stem battery system to 500 Wh / Kg of the current lithium battery. During the Second World War, even if shelf life was preserved under proper temperature, it was one year, but with convenient batteries currently in use has a lifetime of 2 to 5 years, the latest lithium battery Have storage life of more than 10 years even if they are stored at 70 ° C. Operability at low temperature has also been improved from 0 ° C. to -40 ° C and -55 ° C., and the power density has also been improved several times. In the case of a low current battery using a solid electrolyte, the shelf life is more than 20 years[35,36].

With the improvement of such characteristics, many new machines for use of primary batteries have been developed. As a result of the improvement of energy density, the size and weight of the battery were greatly reduced. This reduction contributed to the advancement of electronic technology, and many new desk radio, communication equipment, practical output equipment were made. Improvement of the power density of the primary battery brought about the size and weight of the battery. This reduction contributed to the advancement of electronic technology, and many new desk radio, communication equipment and practical electronic equipment were made. Improvement of the output density of primary batteries not only makes it possible to desktop computers, mobile phones, transceivers, and devices that have required high power of secondary batteries and external power sources, but also has troublesome charging and maintenance Resolved[37]. At present, with respect to primary batteries, the shelf life is further prolonged, while lifespan and reliability are improved at the time of battery operation, on the other hand, it is also used for devices for a long time, such as medical packaging and memory .

Worldwide, the market of primary batteries currently exceeds 10 billion dollars a year, and its growth rate is over 10% a year. Among these primary batteries, the

majority of the primary battery is a general cylindrical or flat plate battery with a capacity of 20 Ah or less. There are few large batteries to reach thousands of Ah, but it is used in special cases such as signaling equipment and military functions that require independent lower power from external power supply.

There are many combinations of a positive electrode and a negative electrode used as a primary battery, but there are considerably few combinations that can be put into practical use. Zinc is the most common negative electrode material due to its electrochemical behavior, high electrochemical equivalent, adversity with electrolyte, long shelf life, low cost and easy to use[38]. Aluminum also exhibits high electrochemical potential and electrochemical equivalence, but since electrostatic behavior is limited due to the formation of passive state, it has not been put into practical use as a primary battery system. At present, a mechanical charging method for exchanging exhausted negative is electrode material, a negative electrode aluminum / air battery and a storage battery system[39-41]. Magnesium is also used as a primary battery due to its characteristic electrochemical properties and low cost. These batteries are used especially for military use because of their high energy density, long shelf life and are commercially restricted. Magnesium is also commonly used as the negative electrode of storage batteries. Lithium has become the subject of interest for the last decade since lithium has the highest energy density in metals and a very large negative standard electrode potential. A battery system using lithium as a negative electrode , a non-aqueous electrolytic solution and a positive electrode material in which lithium can greatly influence the improvement of the behavior characteristics of the primary battery[42-44]. Among them, magnesium shows excellent electrical characteristics, but because of its low storage ability in a part of discharge cells, almost no expectation has been made regarding commercialization, but the magnesium stem cell can be used under non- Due to its long shelf life at high temperature and high energy density, it is widely used as an improved military communication power supply[45]. It is known as one of the general negative electrode materials of magnesium preservation batteries. Also, air / metal batteries are known for their high energy density, but their use is restricted to large low output batteries such as signals and navigation systems. With the improvement of air batteries, rapid discharge of this system is possible, now small button type batteries

are widely used for hearing aids and other electronics equipments[46-48]. These batteries have a very high energy density even without mounting a positive electrode active material. However, there are limits to the expansion of the applications of this battery and the development of large batteries due to their operating characteristics (sensitive to temperature and humidity, short storage life, low power density). Nonetheless, due to the high energy density of this battery, metal / air batteries are considered to be used in a number of applications (desk electrical equipment, electric cars, storage batteries, mechanically charged type).

### **1.2.3 Introduction of the Secondly battery**

Secondary batteries, that is, chargeable / dischargeable batteries, are widely used in many applications. The most familiar uses are used for car startup, lighting, ignition and so on. Others are for industrial use such as forklift, backup for emergency or power failure, etc. Demand for small secondary batteries, which is a power source for tools such as tools, toys, lights, cameras, radios or personal computers, video, mobile phones and other portable devices, is remarkable. Recently, secondary batteries are attracting attention in electric vehicles or applications for leveling power. Also, as appropriate for these applications, plans are underway to improve current battery characteristics and develop new batteries. Applications of secondary batteries can be roughly divided into the following two points.

1. Application for power storage. Used to meet the purpose of supplying the energy as required when the secondary battery is supplied with power from the primary energy source and the primary energy source becomes unusable. Examples include automobiles, airplanes, backups during emergency power outages, storage batteries for power leveling.
2. Application for repeated use that repeats charging and discharging. Used in the same way as the primary battery and intended for recharging after discharge. This secondary battery is used for purposes such as convenience, cost saving or exceeding the capacity of primary batteries. Examples include electrical appliances for consumer use, electric cars and forklifts.

A feature of the secondary battery of a normal aqueous solution is that it can be charged with a high current density, the discharge curve is flat and shows excellent characteristics even at low temperatures. However, the energy density of the secondary battery is lower than that of the primary battery, and self-discharge is large. On the contrary, since the non-aqueous electrolytic solution having a lower electric conductivity than that of the aqueous solution is used as the output density, so excellent characteristics can not be expected[49].

Secondary batteries have a history of over 100 years. Lead storage batteries were invented by Plante in 1859. This battery has been used as a battery for automobiles for many years to improve the characteristics and change the design, and is the most widely used battery all over the world. A nickel-iron battery was invented by Edison as a power source of an early electric vehicle in 1908. However, it is currently used only for industrial transport vehicles, underground construction work vehicles and trains. The reason is that although the cycle characteristics are good and the life is long, the cost is high, maintenance is necessary, and the energy density is low. Utilization is decreasing further[50]. Pocket-type nickel-cadmium batteries were put to practical use in 1909 and were mainly used for industrial applications. When a sintered nickel-cadmium battery capable of high rate discharge and high energy density is put to practical use, it has been used for starting aircraft engines and communication equipment since the 1950's. In addition, due to practical application of hermetically sealed nickel-cadmium battery, it has become a world to be used for portable equipment, and now it has reached about 20% of the sales of secondary batteries. Similarly to primary batteries, secondary batteries have also improved remarkable characteristics, and many new secondary batteries such as silver / zinc, nickel / zinc, hydrogen, lithium, halogen batteries that are used for power supply of portable devices and battery cars has been developed for use. The size of the current secondary battery market exceeds 10 billion dollars. Currently the largest sales are lead-acid batteries, of which automotive batteries account for the majority of the market. However, this share has gradually declined as other uses expand. In the future, the share of alkaline storage batteries will rise to about 25 - 30%, the fastest growing market is the field of small batteries used for mobile devices[51]. If the electric vehicle is successful, the market for secondary batteries will expand dramatically, but

we will predict what sort of time, or what size of the market will be used and what kind of batteries are currently used .

### **1.3 Expectation to a magnesium alloy battery**

#### **1.3.1 Comparison of characteristics of Mg and Li**

In the periodic table, magnesium and Lithium has a diagonal location, so both have a lot of similar chemistry. Magnesium-ion technology is promising for several reasons. First, due to the natural abundance of magnesium in the earth's crust, approximate 10000 times that of lithium, its incorporation into electrode materials is inexpensive (Table 1). Secondly, magnesium is more atmosphere stable and has a higher melting point than lithium, making it safer relative to lithium[52]. The divalent nature of magnesium ions also presents a potential advantage in terms of volumetric capacity (3833mAh/cm<sup>3</sup> for Mg vs. 2046mAh/cm<sup>3</sup> for Li).

Despite these positive attributes, the development of magnesium-ion technology has not kept pace with that of lithium ion technology. One critical issue impeding progress has been development of a suitable electrolyte which will enable reversible release of Mg<sup>2+</sup> ions from a magnesium metal anode. Unlike Li<sup>+</sup> ion conducting surface films formed by polar electrolyte solutions on Li metal electrode, surface films on magnesium metal often block the transport of Mg<sup>2+</sup> ions[53]. Notably, an advancement in this area was reported in 2000 with the development of electrolyte based on magnesium organo-haloaluminate complexes dissolved in tetrahydrofuran or glyme based solvents[54]. These electrolytes allow for electrochemical deposition-dissolution of magnesium and have a stable electrochemical window of 2.5V, thereby allowing for the testing of practical cathode materials[55]. The comparison of characteristics of Mg and Li as shown in Table 1.

Table 1 Comparison of characteristics of Mg and Li

Characteristics	Mg	Li
Pauling Ionic Radius	65	60
Voltage vs. S.H.E.	-2.37	-3.04
Elemental abundance (ppm in earth crust)	2330	20
Volumetric Capacity(mAh/cm <sup>3</sup> )	3833	2046
Gravimetric capacity	2205	3862

### 1.3.2 Magnesium alloy air cell (primary)

The battery which an anode does not consume when I put magnesium and the air pole where a battery giving negative electric potential is an active excellent material scientifically together electrochemically, and it is provided that a battery having the energy density with very big mass or volume in a certain case. As for the magnesium air cell that it was thought that we had such a characteristic, an extremely big energy density was expected, and a great effort has been made by this development. It is primary that in the magnesium air cell, the models such as preservation characteristics, mechanical charge characteristics are devised, and development is pushed forward. The generation of the field film can prevent the water from the reaction of magnesium on a magnesium electrode. It is necessary to create the new naked magnesium surfaces to push forward a reaction. However, the pure magnesium cathode does not show the good electrode performance. Therefore reactive high new magnesium alloy development is performed to get a cathode meeting demand properties.

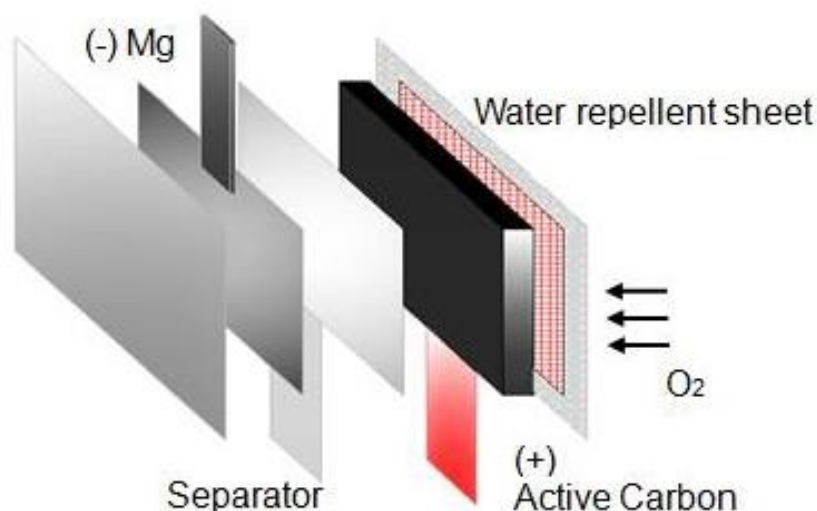


Fig. 1.3 Schematic diagram of Mg air battery

The magnesium air cell has not been yet commercialized in earnest, and the development of the electrode that the magnesium surface has activity as quality of flower arrangement is pushed forward with the dissolved  $O_2$  in seawater recently, as shown in Fig. 1.3. This battery used a magnesium alloy cathode and a film anode, which has been activated by seawater. The best point of this system is that it can get all reactant except the magnesium electrode than seawater, and it achieves an energy density of about 7000WH/Kg. Now it has the results of the application of many batteries, such as the Furukawa battery club has developed a magnesium battery charging panel. The can be used to charge the smart phone device by the USB interface. The electrolyte of the battery was seawater, which were environmental protection and energy conservation. In addition magnesium batteries can also be used in magnesium battery lights. At Kuramoto Works "Fantastic Light" uses magnesium batteries. Illuminate with a small amount of water for over a week. It is an exhausted light thrown away by incombustible garbage. Fuji Sasi Group's Fuji Light Metal Co., Ltd. began joint research on fuel (air) batteries using flame-retardant magnesium alloy. In this collaborative research, we developed an innovative electrode material by casting a flame-retardant magnesium alloy excellent in ignition suppression characteristics on the electrode, and aim for mass production of the same battery.

### 1.3.3 The introduction of the second battery of Mg battery

Magnesium is expected to provide one of the next generation negative battery active materials due to its high electrochemical energy capacity and no dendrite formation of electro-deposited of magnesium on changing, different with lithium ion batteries which employ carbon materials for the intercalation with lithium. Some combinations with positive active materials have been proposed for magnesium secondary batteries.

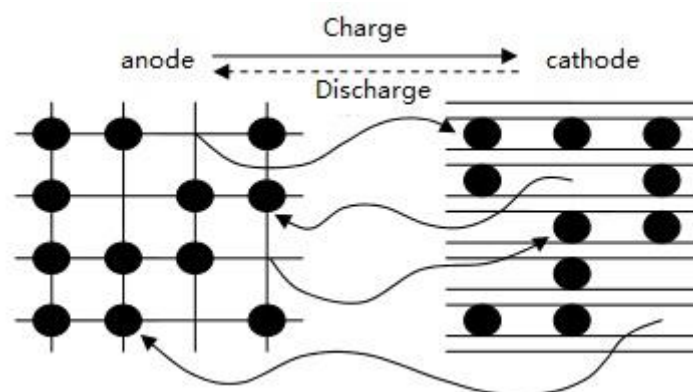


Fig. 1.4 Illustration of rechargeable magnesium battery

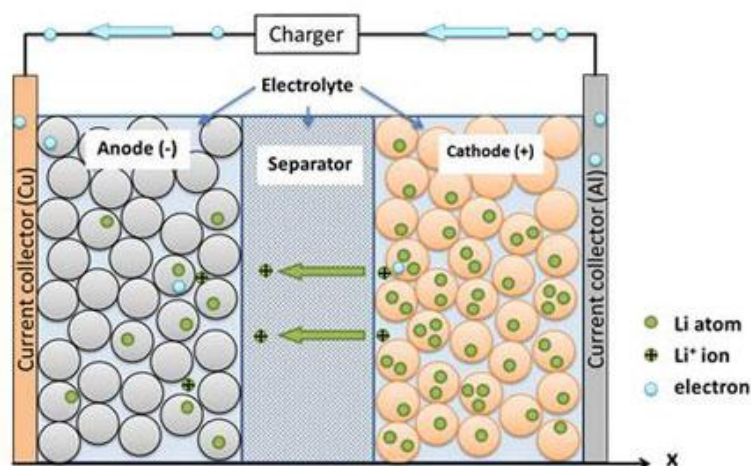


Fig. 1.5 Illustration of rechargeable Li ion battery

Magnesium secondary batteries and Lithium-ion battery works similarly (Figure 1.4), is through the magnesium ions in the positive negative transfer between the battery charge and discharge. While the Illustration of rechargeable Li ion battery is as shown in Fig. 1.5.



When the battery is charged, under the action of external voltage, magnesium ions remove from the cathode material, through the dissolution of the electrolyte, adsorption, transfer and other processes reach the anode, and the negative material deposition; discharge, the magnesium ions are removed from the negative, through the electrolyte back to the positive electrode. Magnesium from sub-respectively in the battery cathode and anode reduction, oxidation reaction, the battery system can be generated in the direction of movement Magnesium ions. Electrolyte solution as a bridge of magnesium ion migration, provide the necessary internal migration of magnesium ions. Due to the large charge density of magnesium, solvation serious, magnesium secondary battery research by the following aspects of the system

Lake of Magnesium: (1) Magnesium has a high chemical activity and tends to form a surface passivation film in most solvents. Magnesium ions are difficult to form through this dense surface film, the reversible deposition and dissolution of magnesium in the electrolyte become very difficult; (2) Magnesium ion charge density, serious solvation, it is difficult to embed in the general matrix, the choice of cathode material Subject to certain restrictions; (3) lack of mediators that mediate  $Mg^{2+}$ .

However, controlling passive states is an important subject to accelerate the development of magnesium batteries especially in organic media. Addition of chloride ions into organic electrolytes was proposed for magnesium and aluminium-magnesium alloy secondary batteries. Chloride ions promotes the anodic electrode reaction for Magnesium alloys, as in the same case of sea water batteries. Corrosive chloride ions seem to be effective to accelerate the anodic reaction of magnesium electrodes, however, deliberate and precise potential control is needed not to evolve chlorine gas from positive electrode on charging. And high output voltages, such as 3V, are different to be obtained due to prevention of chlorine evolution. Intercalation of magnesium is considered to be another important condition for the secondly batteries in the same mechanism as lithium and aluminium. In electrolyte solutions based on Magnesium organohaloaluminate salts, the behavior of essential point magnesium ions was explained which could be intercalated reversibly and with relatively fast kinetics.

The study team of the Yamaguchi University graduate school science and technology studies graduate course developed a magnesium battery with electric capacity of approximately of the used lithium ion battery now theoretically. It is expected that contribution to the mileage is expansion of the electric car. As for the rechargeable battery, anode materials (positive pole) and cathode materials (negative pole) which play a role as the fuel producing energy are comprised of three elements of a medium of the energy between the electrode and the electrolyte . To the rechargeable batteries such as the cell-phones which are generally used, an organic electrolyte use the lithium ion is used for artificial black lead (charcoal), electrolyte to a cobalt-based compound, cathode materials to anode materials mainly now. However, because cobalt and lithium were metals, production cost rose, and the problem for the further spread remained, too.

Because  $\text{Mg}^{2+}$  reacts with a cathode, the magnesium sulfur rechargeable battery is charged and is discharged electricity by reacting with an anode. Because the energy density can produce much energy with less quantity at approximately of the conventional lithium ion rechargeable battery, it is compact, and the manufacture of the lightweighted rechargeable battery is enabled. Furthermore, it is expected that development, the spread of large size batteries to use advances to EV or the solar panel because resources-like problem can be settled cost. Sulfur is a by-product occurring at the time of oil refining, and there is the merit to be able to the effectively utilize resources.

#### **1.3.4 Effect of Vanadium Oxide inserted in Anode**

Intercalation of  $\text{Mg}^{2+}$  into  $\text{V}_2\text{O}_5$  is a slow process, possibly due to chemical modification of the  $\text{V}_2\text{O}_5$  crystal surface[56]. Further,  $\text{V}_2\text{O}_5$  electric conductivity is low. To optimize the diffusional pathways of  $\text{Mg}^{2+}$  during the charging and discharging of  $\text{V}_2\text{O}_5$ , reports have appeared involving the control of crystallite size and the use of conductive additives. Decreasing crystallite size [57-60] and the use of conductive additives. Decreasing crystallite size decreases the diffusion path length within the  $\text{V}_2\text{O}_5$  crystals, improving capacity at higher current rates. This strategy has been utilized in work which investigates nanocrystalline  $\text{V}_2\text{O}_5$  and  $\text{V}_2\text{O}_5$  nanotubes[61.62], although more work needs to be completed to compare the

electrochemistry of the nanocrystalline materials with microcrystalline  $V_2O_5$  in order to accurately assess the effectiveness of this approach. The use of conductive materials has also been tested as a means of improving  $Mg^{2+}$  diffusion. When the electrochemical performance of a composite carbon- $V_2O_5$  xerogel was compared to that of an electrode prepared via a conventional mixture of  $V_2O_5$ , the composite exhibited a higher capacity.

### **1.3.5 Introduction of Magnesium stem cell**

The magnesium stem cell uses a magnesium alloy for the negative electrode and the positive electrode uses manganese dioxide with acetylene black added to give conductivity. To increase the corrosion resistance, chromium salts of barium and lithium are added to the electrolytic solution, and an aqueous solution of magnesium perchlorate is added with magnesium hydroxide (pH 8.5) as a buffer to further improve the storage performance. This battery system has two features compared with manganese / zinc battery. That is, the capacity is doubled, and self-discharge is small even at high temperature. The reason why the storage performance is excellent due to the passive film formed on the surface of the magnesium negative electrode.

Magnesium stem cell is the main application military field transceiver. BA-4386 type battery pack uses 1 LM battery developed for AN / PRC-25 type and AN / PRC-77 type transceiver. Magnesium 1 LM batteries are found to be unsuitable for other military uses. In this application, it was difficult to discharge with a large current, and it was difficult to maintain the shape due to the expansion of the battery due to the discharge, so that an efficient battery was obtained. Characteristics of a military BA-4590 battery pack using a new battery 1601 M is compared with the case of using a 1 LM battery. Especially good characteristics which are good when flowing a large current are compared with the case using 1 LM battery. The BA - 5590 type magnesium stem cell can be used as a substitute for lithium / sulfur dioxide battery field, a more expensive alternative for military training. In the magnesium stem battery, once the discharge is stopped, the protective film of the magnesium negative electrode does not completely restore, and the storage characteristics become worse. Magnesium stem cells have these disadvantages, but because of their low cost, they can be used for training or other military purposes.

## 1.4 Electrochemical reaction principle

The performance of the battery has to meet various demands including not only the output (energy, capacity) but also operation environment and the electrical condition bottom [63]. Nowadays, the battery technology had accomplished progress a lot. The electrochemistry reaction system to join a cathode and an anode together at the same time is improved, and the battery based on a new principle has been developed, but an all-around battery showing superior performance under every condition does not exist again [64]. In order to get a battery of the higher performance, varieties of electrochemistry systems design and batteries development being continued. The battery of the special design is applied for military affairs or industry and is used in environment needing a specific function [65]. An ideal battery is cheap and, with infinite energy, can supply all output levels, and can work under the wide temperature range, and it must be the thing which be superior to the durability, and is also safe. However, there is really life because a chemical reaction and a physical change are caused in the case of preservation and the storage. Besides, as for the performance of the battery, it is acted on temperature and electric discharge speed. In addition, the use of energy storage materials to increase energy output density and a special design push up a price, and a problem in the physical security of the battery corresponds, in addition to this particularly, the prophylaxis is necessary. A study to draw the best performance is essential to choose a battery having highest performance in such a demand, and to use the battery definitely[66].

The device which converts chemical energy into electric energy by the electrochemic oxidation reaction and reduction reaction in the twin cathode and anode directly is a voltaic battery (including the fuel cell). One cell is comprised of a cathode (anode) which the anodal (cathode) reduction reaction that an oxidation reaction happens at the time of an electric discharge happens and the electrolyte that the electric charge transportation by the ion takes place.

The maximum of the energy to be able to take out is equivalent to Gibbs (Gibbs) free energy change  $\Delta G$  of the oxidation-reduction reaction from chemical species (the chemical species which or was supplied to the electrode) made the internal organs to an electric polar body. Of course it is desirable to be able to make good use of all of

this energy at the time of an electric discharge as electric energy, but has a loss due to various polarizations when load electric current  $i$  flows with an electrochemical reaction. I polarize activation to let a reaction progress on the surface of the ,① electrode for the thing included in these energy losses.②There is such concentration polarization due to the density difference of the reactants and products produced between the electrode surface and the bulk as a result of mass transfer. An important factor of greater its influence one the operating characteristics of the cell, there is an internal impedance which results in a reduction of the operating voltage, this is a waste of part of the effective energy as heat loss.

The cell voltage  $E$  when connected to an external load  $R$  can be expressed as the formula

$$E = E_0 - [(\eta_{ct})_a + (\eta_c)_a] - [(\eta_{ct})_c + (\eta_c)_c] - iR_i = iR \quad (1.1)$$

Here, bottom additional character a,c with it out of the parenthesis shows anodal (cathode) cathodal (anode) each. In addition,  $E_0$  circuit voltage of the cell,  $\eta_{ct}$  the activation polarization (charge transfer overvoltage),  $\eta_c$  is the concentration polarization (concentration overvoltage),  $i$  is the load current of the cell,  $R_i$  is the cell internal resistance. As shown in equation 1.1, voltage that the cell can be effectively generated is reduced by the amount by the minute and internal  $iR_i$  drop due to polarization. Theoretically available energy batteries is determined by what cell or a chemical reaction occurs at the two electrodes, the influence factors are charging transfer reaction rate, diffusion rate of the size and the size of the energy loss. Around them, there are important things as how to make electrodes and a design, the transmission rate of the electrolyte and the characteristic of the separator.

## 1.5 Corrosion reaction of the Battery

### 1.5.1 Electrochemistry corrosion

It is to include both chemical conjugation and electrical change, and the characteristic of the electrode reaction is one of the non-homogeneous system reactions. For an electrode reaction, there is the simple thing which only works on the reduction of metal ions in an electrode with a formed metal atom [67]. Even if a reaction is simple in an appearance, the mechanism of the process as a whole is complicated, and it is from the generally plural steps. Prior to an electronic movement process, and it is necessary for active excellent chemical species to be transported by migration or diffusion electrochemically to the electrode surface. In addition, the adsorption of the active kind may affect it on the electrode of the electronic movement process. Furthermore, a chemical reaction may be included in all electrode reactions. In the same way as a general reaction, the speed of the electrochemic process is ruled over consecutively among the reaction processes named the ream by the speed of the slowest step[68]. In the thermal mechanical handling of the electrochemical process, but to define the equilibrium conditions of the system, it cannot be foreseen in relation to non-equilibrium conditions, such as the current based on the polarization (overvoltage) to be added in order to cause a reaction. Examining the Current - overvoltage characteristics experimentally for many systems, it has been found that there is a linear relationship between the logarithm of current density  $i$  and the overvoltage  $\eta$ . Expression of this relationship which was generally described is Tafel.

$$\eta = a + b \log|i| \quad (1.2)$$

Constant  $b$  is usually called Tafel coefficients. The relationship between the Tafel is made of a wide range of overvoltage for many of the system. However, when overvoltage is small, these relations are not managed, and the plot of  $\eta$  vs.  $\log i$  is aberranted the straight line. [69-72]

An expression of Tafel was applicable to many experiments system well, and, in a thing, the kinetics about the electrode reaction process progressed. Because the expression of Tafel is applied when overvoltage is large, as for these relations, which

could be considered that express electric current - overvoltage relations when rather a process progresses in one is natural without applying to it in equilibrium. It means, for example, that a re-reduction process for reverse is a negligible condition in the oxidation process.

$$i = \exp(\pm \frac{a}{b}) \exp \frac{\eta}{b} \quad (1.3)$$

In a more general theory, it is necessary to consider both forward reaction and inverse reaction about the simplified electrolysis reduction process such as Fig. 1.6[73,74]

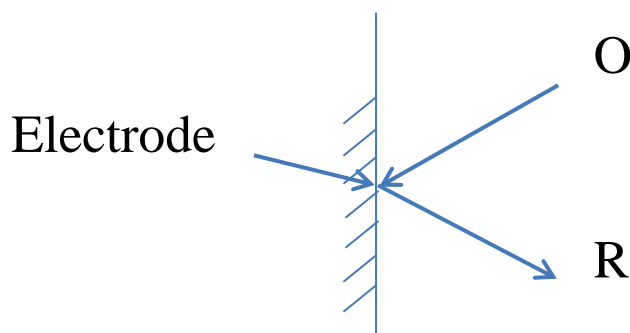


Fig. 1.6 The simplified figure of reduction on the surface of electrode

As shown in this action



Here, O is the oxidant, R represents reductant, n is the number of electrons involved in the electrode reaction. Forward reaction can refer to the speed of the inverse reaction using each speed fixed number  $k_f$ ,  $k_b$  and is given in the product with the speed fixed number and the density of reactant (appropriate using the density in the electrode surface).[75] The density of active chemical species is not often equal to the electrode surface in bulk solutions electrochemically. The speed of the forward reaction is  $K_f C_O$ , while the reverse reaction is  $K_b C_R$ , these are usually transcribed in current density if of the forward reaction, form of current density  $I_b$  of the inverse reaction for convenience.

$$I_f = nFAk_f C_O \quad (1.5)$$

$$I_b = nFAk_b C_R \quad (1.6)$$

Here A is the area of the electrode.

The type is not only the thing which expressed an original direction and the speed of the reverse electrode reaction process simply. It can be considered that the electronic ratio in the electrode reaction process if it can be regarded that the speed fixed number depends on the electrode potential. This dependence is usually expressed based on a supposition that remaining some (1-a) E contributes to restraint of the inverse reaction again aE which is a part of the overvoltage by promotion of the forward reaction.

$$k_f = k_f^0 \exp \frac{-anFE}{RT} \quad (1.7)$$

$$k_b = k_b^0 \exp \frac{(1-a)nFE}{RT} \quad (1.8)$$

Here, a is the transfer coefficient.[76,77] Because the electric current of the original taste does not flow in the equilibrium, As shown in this equation.

$$i_f = i_b = i_0 \quad (1.9)$$

In an expression (1.9) when substituted an expression (1.5) – (1.8) ,

$$E_e = \frac{RT}{nF} \quad (1.10)$$

The standard value E of the formula in potential with concentration rather than the activity of the reaction-participating material can be defined as the equation from (2.9) to(1.11).

$$E_C^0 = \frac{RT}{nF} \ln \frac{k_f^0}{k_b^0} \quad (1.11)$$

$$E_e = E_C^0 + \frac{RT}{nF} \ln \frac{C_O}{C_R} \quad (1.12)$$

The Nernst equation (1.12) is obtained from (1.10) and (1.11).

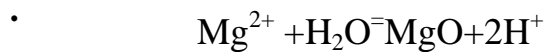
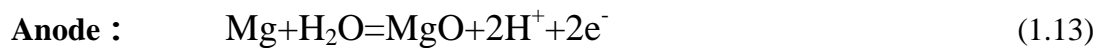


The standard electrode electric potential of magnesium calculated based on the above-mentioned expression is -2.37V, and the primary cell and the rechargeable batteries are the material which is attractive as cathode materials. In addition, from a Nernst type and the expression of the current density, mechanism of the magnesium corrosion became clear[78-80].

### 1.5.2 Application of the stress corrosion

The stress corrosion depends on tensile stress from the inside or the outside and synergism of the corrosion. The characteristic of the stress corrosion is that dissolves a corrosion product and may interfere with the generation of the passivity oxide film.

The generation of a wedge-shaped section by the anodal erosion, and new small anodal appearance occurs, and a process of the stress corrosion advances auto catalytically more, and the formation of the passivation oxide film is restrained, and erosion caused by the corrosion progresses[81]. It seems to show the stress corrosion in Fig. 1.7 schematically and occur when three persons of materials, environment and the stress meet in a specific condition.



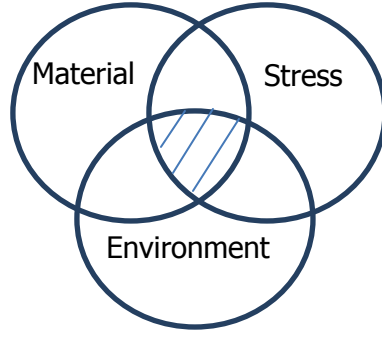


Fig. 1.7 Stress corrosion and factors

When change  $\Delta G$ (per g) of the free energy refers to relations of the stress in an expression (1.15).

$$\Delta G = \frac{\delta^2}{2\rho Y} \quad (1.15)$$

Here,  $\delta$  is the applied stress,  $Y$  is Young's modulus,  $\rho$  is the density of the Mg alloy. And the change of the electric potential is accompanied with a change of the free energy.

$$\Delta E = - \frac{\Delta G}{nF} \quad (1.16)$$

Here,  $n$  is the electronic number,  $F$  of the reaction is the faraday fixed number[82].

Therefore, I show electric potential and relations of the stress in an expression (2.17) from expression (1.16), (1.17).

$$\Delta E = - \frac{\delta^2}{2\rho Y n F} \quad (1.17)$$

With the generation of the immovable oxide film, and using the stress corrosion method, the surface of the magnesium alloy can propel the reaction of the surface of the magnesium alloy and the solution. In addition, it can suppose that the voltage of the magnesium alloy electrode towards the negative direction under the influence of stress. It can be considered that it can improve the battery chemistry performance of the magnesium with the method of stress corrosion.

## 1.6 Design of magnesium electrode material

### 1.6.1 Selection of the added element of a new magnesium alloy

Usually, the magnesium electrode material the addition of trace elements, also has been developed to changes in manufacturing methods and conditions based Nuisance material design of the original, yet corrosion resistance and machinability and electricity further having a microstructure in accordance with the application purpose properties improvement and the chemical properties have been sought. Therefore, in this study, it was first investigated the information about the trace additive element. The conventional magnesium alloys Al, Zn, although Mn element is mainly added, considering the characteristics of the group metal element, as shown in Table 1.1, the characteristics of the magnesium alloy is affected by the addition of another element[83].

Table 1.1 Influences of alloying elements on the properties of Mg alloys

Element alloy	Melting and casting behavior	Mechanical and technological behavior	Corrosion behavior I/M produced
Ag		Improves elevated Temperature tensile and creep properties in the presence of rare earth	Detrimental influence on corrosion behavior
Al	Improves castability, tendency to	Solid solution hardener, precipitation	Minor influence

	microporosity	hardening at low temperature	
Be	Significantly reduces oxidation of melt surface at very low concentrations lead to coarse grains	Improve creep properties	
Ca	Effective grain refining effect, slight suppression of oxidation of the molten metal		Detrimental influence on corrosion behavior
Cu	System with easily forming metallic glasses, Improves castability		Detrimental influence on corrosion behavior, limitation necessary
Fe	Magnesium hardly reacts with mild steel crucibles		Detrimental influence on corrosion behavior, limitation necessary
In	Improves castability, tendency to microporosity	Improves elevated temperature tensile and creep properties, improves ductility, most efficient alloying element	Improve corrosion behavior
Li	Increases	Solid solution	Decreases

	evaporation and burning behavior, melting only in protected and sealed furnaces	hardener at ambient temperatures, reduces density, enhances ductility	corrosion properties strongly, coating to protect from humidity is necessary
Mn	Control of Fe content by precipitating Fe-Mn compound, refinement of precipitates	Increases creep resistivity	Improves corrosion behavior due to iron control effect
Ni	System with easily forming metallic glasses		Detrimental influence on corrosion behavior
Rare earth	Improve castability, reduce microporosity	Solid solution and precipitation hardening at ambient and elevated temperatures	Improve corrosion behavior
Sn	Suppresses microporosity	Improves elevated temperature tensile and creep properties, improves ductility, most efficient alloying element	Improve corrosion behavior
Y	Grain refining effect	Improves elevated temperature tensile and creep properties	Improve corrosion behavior
Zn	Increase fluidity of	Precipitation	Minor influence,

	the melt, weak grain refiner, tendency to microporosity	hardening, improves strength at ambient temperature, tendency to brittleness and hot shortness unless Zr refined	sufficient Zn content compensates for the detrimental effect of Cu
Zr	Most effective grain refiner, incompatible with Si, Al, and Mn, removes Fe, Al, and Si from the melt	Improves ambient temperature tensile properties slightly	

Among general-purpose pure magnesium and magnesium alloy AZ31, AZ91, AZ91 alloy is most used as a magnesium product. The reason is that it has excellent castability (moldability), high strength and high corrosion resistance. In addition, the results of comparing electrochemical performances of pure magnesium AZ31 and AZ91 alloy are that AZ91 has higher voltage and stable current. Therefore, in this study, based on the AZ91 alloy, a new magnesium alloy was developed by adding trace elements. The components of AZ91 alloy are shown in Table 1.2.

Table 1.2 Ingredient of AZ91 alloy

	Al	Zn	Mn	Si	Fe	Mg
AZ91	9.0	0.8	0.22	0.04	0.001	balance

One of the objectives of this research is to produce new Mg alloys with high electrochemical performance, high strength and high corrosion resistance compared with AZ91 alloy by fully demonstrating the advantages of AZ91 alloy. Element was selected from Table 2.1 and added the trace elements Mg - Zn - In - Sn and

Compound MnS which can improve the performance of AZ91 alloy and designed the manufacturing experiment of Mg - Zn - In - Sn - MnS alloy.

## **1.7 Purpose of this study**

Because we had performance such as the recyclability that magnesium was an abundant resources material, and was eco-friendly, so it has been attracted attention as effect materials for a long time. In addition, the magnesium electrode is expected as attractive new energy because it has a low higher cost theory capacity, high energy density and a long-term storage life.

In this study, it has been used of superior performance of magnesium and developed a new magnesium alloy electrode available as an eco-energy source in a generation in sequence. In addition, I succeeded that in improving the electrochemistry performance of the new magnesium alloy electrode by using corrosion promotion action of the stress to find more high efficiency. Furthermore, using the new magnesium alloy electrode, a new magnesium air cell (primary cell) and the secondary battery would be tried to development. Furthermore, by applying stress, ecological problems can also be improved, for example recovery of phosphorus.

## **1.8 Composition of this paper**

This research consists of 8 chapters.

Chapter 1 The history of magnesium, the classification of batteries, the current state of battery materials for next generation, and the primary batteries and secondary batteries currently on the market are introduced, especially from the perspective of new eco energy expectation for application of magnesium batteries Mentioned. The working principle of the battery and examined the reaction principle of the magnesium electrode based on the theory of electrochemical corrosion and stress corrosion was studied. Furthermore, considering the addition of trace elements, a new magnesium alloy was designed.

Chapter 2 A new magnesium alloy was produced. By the observation of the fine structure, the action of the additive element is described. Furthermore, from the viewpoint of practical application, workability and corrosivity of the magnesium alloy electrode were studied.

Chapter 3 In order to improve the electrochemical performance of the alloy electrode, stress was applied to examine the performance of the alloy. Furthermore, by using various electrolytic solutions, the electrochemical performance of the novel magnesium alloy electrode was investigated by the influence of stress corrosion. Corrosion model of magnesium alloy electrode was developed based on the basic principle of stress corrosion method. Also, manganese ions in the solution were simulated using discharge reaction. Furthermore, the voltage and current of the novel magnesium alloy electrode were calculated.

Chapter 4 When stress corrosion is applied, the effect of electrochemical corrosion becomes clear. Based on the principle of stress corrosion, primary batteries are being developed.

Chapter 5 The effect of Magnesium alloy electrodes under tensile stress were examined for magnesium secondary batteries. Besides the charge and discharge performance, the effect of tensile stresses was confirmed by cyclic voltammetric measurements and SEM observations.

Chapter 6 A practical method was studied for phosphorous resource recovery from wastes, such as waste water or many kinds of sludge. It was confirmed that the magnesium alloy electrodes could remove phosphates from the sludge and dissolve them by applying tension stress for phosphate resources recovery.

## **1.9 Conclusion**

In this chapter, based on the working principle of batteries, we applied trial of stress corrosion by studying chemical corrosion reaction. Furthermore, the design of a new magnesium alloy was examined and the following conclusions were obtained.



- (1) The battery discharges by a chemical reaction, and the voltage can be calculated with the Nernst equation.
- (2) It can be inferred that the electrochemical performance of the battery using the principle of stress corrosion can be improved.
- (3) For the magnesium alloy, we examined the advantages and disadvantages of each element and clarified the effect of the added element to the magnesium alloy.

## Reference

- [1] M.Barak.Electrochemical Power Sources-Primary&Secondary Batteries, Peter Peregrinus, Stevenage, U.K.,1980
- [2] B.E.Conway.Theory and Principles of Eletrode Processes,Ronald,NewYork,1965.
- [3] H.Bode.Lead-Acid Batteries (translated from German by R.J.Brodd and K.V.Kordesch), Wiley, New York,1977.
- [4] D. H. Dorghty, B. Vyas, T. Takamura and J. R. Huff, Materials for ELECTROCHEMICAL Energy storage and Conversion-Batteries, Capacitors and Fuel Cells, Materials Eeseach Society, Pittsburgh,1995
- [5] S.U.Falk and A.J. Salkind.Alkaline Batteries, Wiley, New york,1969.
- [6] A.Fleischer and J.J lander.Zinc-OSilver Oxide Batteries, Wiley, New York,1971
- [7] Frost and Sullivan Inc,U.S.Market for Batteries, Summer 1992.New York,1992
- [8] George Consulting International, he world Battery Industry. A Multiclient Study,Concord, Mass., 1992

- [9] The Freedonia Group, Inc., Industry Study 395, Primary and Secondary Batteries, Cleveland, Ohio, Jan. 1992
- [10] R. Samuel, The Evolution of Electric Batteries in Response to Industrial Needs, Dorrance, Philadelphia, 1978
- [11] V. George, Primary Batteries, Wiley, New York, 1950
- [12] N.C. Cahoon and G.W. Heise, The primary Battery, Wiley, New York, 1976.
- [13] H. Richard, Batteries, Dekker, New York, 1974
- [14] A. Kozawa and R.A. Powers, Electrochemical Reactions in Batteries, J. Chem. Ed. 49(1972):587
- [15] R.J. Brodd, A. Kozawa, and K.V. Kordsh, Primary Batteries 1951-1976, J. Electrochem. Soc. 7(1978):125
- [16] M. Bregazzi, Electrochem. Technol., (1967):507.
- [17] C.L. Mantell, Batteries and Energy Systems, McGraw-Hill, New York, 1983.
- [18] American National Standard Specification for Dry Cells and Batteries, ANSI C18.1-1992, American National Standard Institute, New York, 1992.
- [19] Everyday Battery Engineering Data, Everyday Battery Company, St. Louis, Mo., 1992
- [20] M. Dentch and A. Hillier, Progress in Batteries and Solar Cells, Polaroid Corp., 1992
- [21] NEDA Batteries Index, National Electronic Distributors Association, Chicago, 1990
- [22] A.J. Salkind, D.T. Ferrell, and A.J. Hedges, Secondary Batteries 1952-1977, J. Electrochem. Soc. 8(1978):125
- [23] A.J. Salkind, Director, Battery Laboratory, Rutgers University, NJ, 1994
- [24] S.U. Falk and A.J. Salkind, Alkaline Storage Batteries, Wiley, New York, 1969

- [25] L.H.Thaller, Expected Cycle Life vs.Depth of Discharge Relationships of Weii-Behaved Single Cells and Cell Strings,J.Electrochem.Soc.5(1983):130
- [26] R.Udhayan and B.D. Prakash. On the corrosion behavior of magnesium and its alloys using electrochemical techniques[J], J Power Sources, 63(1996):103
- [27] E.J.Wade, Secondary Batteries, The Electrician, London, 1902
- [28] M.Barak(Ed), Electrochemical Power Source, Peter Peregrinus, London,1980
- [29] P. Ruetschi, J. Power Source 42(1993):1.
- [30] F.J.Kruger,J.Russow,G.Sandstede (Eds.), Proceedings of the Annual Meeting of the GDCh-Monographie 12(1998):250
- [31] L.F.Trueb,P.Ruetschi,Batterien and Akkumulatoren, Springer-Verlag, Berlin, Heidelberg, New York, 1998
- [32] D.Berndt, Maintenance-Free Batteries, Wiley, New York, 1993
- [33] J.L. Fricke and H.A.Kiehne, Batterien, in'F.J.Kruger,J.Russow,G. Sandstede(Eds),Proceedings of the Annual Meeting of the GDCh-Fachgruppe Angewandte Elektrochemie in Vienna,9,1997, GDCh-Monographie 12(1998): 472
- [34] D.Linden (Ed.), Handbook of Batteries, second ed., McGraw Hill, New York 1995
- [35] F.Beck, K.J. Euler, Elektrocheemische Energiespeicher, VDE-Verlag, Berlin and Offenbach,1984.
- [36] V.Barsukov, F.Beck(Eds.), New Promising Electrochemical Systems for Rechargeable Batteries, in; Proceedings of the NATO Advanced Research Workshop, Puscha Voditsa near Kiev, Ukraine, May 14-17, 1995, Kluwer Academic Publishers, Dordrecht, 1996.

- [37] F.Beck(Ed.), Elektrochemie der Elektronenleiter-Metalle, Oxide, Polymere, Proceedings of the Annual Meeting of the GDCh-Fachgruppe Angewandte Elektrochemie in Duisburg, 9, 1995, GDCh-Monographie 3(1996).
- [38] C.F. Holmes and A.R.Landgrebe(Eds), Batteries for Portable Applications and Electric Vehicles, Proceedings 48th ISE-Meeting;192nd ECS-Meeting, Paris,9, 1997, The Electrochem. Soc., Pennington, NJ(1998).
- [39] S.C.Levy and M.E.Fiorino, Electrochem. Soc.Interface Winter 5(1995):26
- [40] G.Kortum, Lehrbuch der Elektrochemie, fifth edition, Verlag Chemie, Weinheim, 37(1972):551.
- [41] R.P.Clark, J.L. Chamberlin, H.J. Saxton and P.C. Symons, Power Sources 9, Academic Press, London, 1983
- [42] A. Heinzl, M. Zedda, U. Paschke and M.Barragan, D. Golombowski, Extended Abstracts 50th ISE Meeting, Pavia 9, 1(1999):887
- [43] K.J. Vetter, Chem.-ing.-Techn.45(1973):213.
- [44] M.S. Whittingham,J.Electrochem Soc.123(1976):315.
- [45] B. Scrosati, J. Electrochem. Soc. 139(1992): 2276
- [46] H.A.Liebhafsky, Regenerative EMF Cells, in; C.E. Crouthamel, H.L. Recht(Eds.), Advanced Chemistry Series, Washington 64(1967).
- [47] L.L. Swette,A.B. Laconti and S.A.Mc Catty, J.Power Sources 47(1994): 343.
- [48] J. Giner, A.B. Laconti, New Promisingn Electrochemical Systems for Rechargeable Batteries, in; V.Barsukov, F.Beck(Eds.), Proceedings of the NATO Advanced Research Workshop, Puscha Voditsa near Kiev, Ukraine, May 14-17, 1995, Kluwer Academic Plublishers, Dordrecht(1996):215
- [49] M.N. Golovin, D.P. Wilkinson, J.T.Dudley, D.Holonko and S. Woo, J.Electrochem. Soc. 139(1992):5

- [50] J.Barthel, H.J.Gores,Batterien, in; F.J. Kruger, J.Russow,G. Sandstede (Eds.),  
Proceedings of the Annual Meeting of the GDCh-Fachgruppe, Angewandte  
Elektrochemie in Vienna, 9, 1997, GDCh-Monographie 12(1998):185
- [51] P.Ruetschi, J.Ellectrochem.Soc.139(1992):1347
- [52] E.Bashtavelova,A.Winsel, in; F.J.Kruger, J.Russow, G.Sandstede(Eds.),  
Proceedings of the Annual Meeting of the GDCh-Monographie 12(1998): 121
- [53] H.D. Yoo, I. Shterenberg, Y. Gofer, G. Gershinsky, N. Pour, D. Aurbach,  
Energy Environ. Sci. 6(2013): 2265
- [54] P. Novak, R. Imhof, O. Haas, Electrochim, Acta 45(1999) :351-367
- [55] Z. Lu, A. Schechter, M. Moshkovich, D. Aurbach, J. Electronal. Chem.  
466(1999)203-217
- [56] D. Aurbach, Z. Lu, A. Schechter, Y. Gofer, H. Gizbar, R. Turgeman, Y.  
Cohen, M.Moshkovich, E. Levi, Nature(Lond.)407(2000)724-727
- [57] G. G. Amatucci, F. Badway, A. Singhal, B. Beaudoin, G. Skandan, T.  
Bowmer, J. Pitz, N. Pereira, T. Chapman, R. Jaworski, J. Electrochem. Soc.  
148(2001) :A940
- [58] L. Jiao, H. Yuan, Y. Si, Y. Wang, J. Cao, X. Cao, M. Zhao, X. Zhou, Y.  
Wang, J. Power Sources 156(2006):673-676
- [59] L. Jiao, H. Yuan, Y. –C. Si, Y.-J. Wang, Electrochem. Commun, 7(2005):  
431-436
- [60] L.-F.Jiao,H.-T.Yuan, Y.-C.Si,Y.-J.Wang, Y,-M.Wang, Electrochem.  
Commun. 8(2006):1041-1044
- [61] F.Beck, J.Electrochem. Soc.129(1880): 1982.
- [62] T.J. Clough, R.L. Scheffler, Extended Abstract, 9th Battery and Electrochem.  
Contractors Conference(DOE),11,1989, US Department of  
Energy,Washington,1989.

- [63] J.P.Gabano, Lithium Batteries, Academic Press, London, 1983.
- [64] R.W.Gabam, Secondary Batteries-Recent Advances, Noyes Data Corp, Park Ridge, N.J., 1978
- [65] H.A.Kiehne, Battery Technology Handbook, Kekker, New York, 1989.
- [66] K.V.Kordesch, Manganese Kioxide, vol.II leak-Acid Batteries and Electric Vehicles, Kekker, New York, 1974 and 1977
- [67] C.L.Mantell, Batteries and Energy Systems, McGraw-Hill, New York, 1983
- [68] G. Pistoia, Lithium Batteries, Elsevier, New York, 1950
- [69] H.V. Venkatesetty, Lithium Battery Technology, Wiley, New York, 1984
- [70] G.W.Vinal, Primary Batteries, Wiley, New York, 1950
- [71] Proceedings of the Annual Battery Conference on Applications and Advances, California State University, Long Beach, Calif, 1996.
- [72] Proceedings of the 23rd Intersociety Energy Conversion Engineering Conference, American Chemical Society, Washington, D, C, 1988
- [73] Electric Batteries, a Bibliography, Energy Research and Development Administration, Report no. TID-3359, Washington, 1977
- [74] Fuel Cells, a Bibliography, Energy Research and Development Administration, Report no. TID-3359, Washington, 1977
- [75] Batteries, Fuel Cells, and Related Electrochemistry, Books, Journals, and Other Information Sources, 1950-1979, U.S. Dept. of Energy Rep. DOE/CS-0156, Washington, D.C., 1980
- [76] Fuel Cells, A Handbook, U.S. Department of Energy Rep. DOE/METC-88/6096, Washington, D.C. NASA Handbook of Nickel-Hydrogen Batteries, NASA Ref. Pub. 1314, Sept. 1993.
- [77] Handbook for Handling and Storage of Nickel-Cadmium Batteries. Lessons Learned, NASA Ref. Publ. 1326, Feb. 1994

- [78] Navy Primary and Secondary Batteries-Design and Manufacturing Guidelines, Department of the Navy Publ. NAVSO P-3676, Sept.1991.
- [79] NAVSEA Battery Document; State of the Art, Research and Development, Projections, Environmental Issues, Safety Issues, Degree of Maturity, Department of the Navy Publ.NAVSEA-AH-300, July 1993
- [80] M. Barak, Electrochemical Power Sources-Primary and Secondary Batteries, Peter Peregrinus, Stevenage, U.K.,1980
- [81] H.Bode,Lead-Acid batteries(translated from German by R. J. Brodd and K. V. Kordesch), Wiley , New York, 1977
- [82] B.E. Conway, Theory and Principles of Electrode Processes, Ronald, New York,1965
- [83] R. W. Cahn, P. Hassen and E. J. Kramer, Materials science and technology structure and properties of nonferrous alloys, UCH, New York, 1996

## **Chapter 2 Development of magnesium alloy electrode materials and performance evaluation**

### **2.1 Production of the Mg-Zn-In-Se-MnS alloy**

#### **2.1.1 Vacuum gas replacement furnace**

Magnesium is a chemically active metal and reacts with oxygen in the atmosphere, so ordinary metal melting furnace can not be considered as casting magnesium alloy. Therefore, in order to prevent oxidation of the magnesium alloy during melting, casting experiments were carried out using a vacuum gas replacement furnace in this study. Figure 2.1 shows a vacuum gas replacement furnace SM - 1300. First, the interior of the furnace is evacuated with a directly connected oil rotary vacuum pump, then argon gas is injected to prevent oxidation when the metal dissolves[1]. By controlling with the program PID device, the maximum temperature in the furnace reaches 1300 °C.



Fig. 2.1 Vacuum Gas Substitution Furnace SM-1300



### **2.1.2 Fabrication of Mg-Zn-In-Sn-MnS alloy in vacuum gas replacement furnace**

AZ91 alloy and additive element Zn - In - Sn - MnS were placed in a crucible and placed in a vacuum gas replacement furnace. After this, the furnace was closed and a vacuum was applied before argon gas was added. The casting temperature is set with the program PID control device, the maximum temperature is 680 ° C., the heat retention time is 1 hour. Finally, the inside of the furnace was lowered to room temperature, and a new magnesium alloy Mg - Zn - In - Sn - MnS was produced.

## **2.2 Production method of magnesium alloy plate**

### **2.2.1 Twin-roll continuous casting**

About 50 years have elapsed since the continuous casting and rolling process (cc) was introduced into the aluminum industry, but various methods were developed, various improvements were added, the productivity and product quality were improved, Production volume of thin plates by year increased, and in 1970 it was only 10% of the general DC casting route, but it increased to 30% in 2002[2-5].

Normally, the technology lateral type twin roll continuous casting machine was adopted in the iron-free metal alloy industry, the technology vertical type twin roll continuous casting machine was successfully applied in the steel industry. However, recently, some researchers have focused on technology vertical type twin roll continuous casting machine in order to produce a metal alloy containing no iron. Researchers such as T. HagaT developed a vertical twin roll continuous casting machine in which a thin plate of magnesium alloy is cast at a high speed of 60 to 180 m / min, and the thickness of the alloy reached 3 mm. Also, we believe that forming a semi-solid by rapid condensation improves the microstructure of the metal. Therefore, when manufacturing metal thin plates, a new twin roll continuous casnew magnesium alloy was produced in order to reduce the cost. A pilot vertical twin roll continuous casting machine is shown in the Fig. 2.2[6].

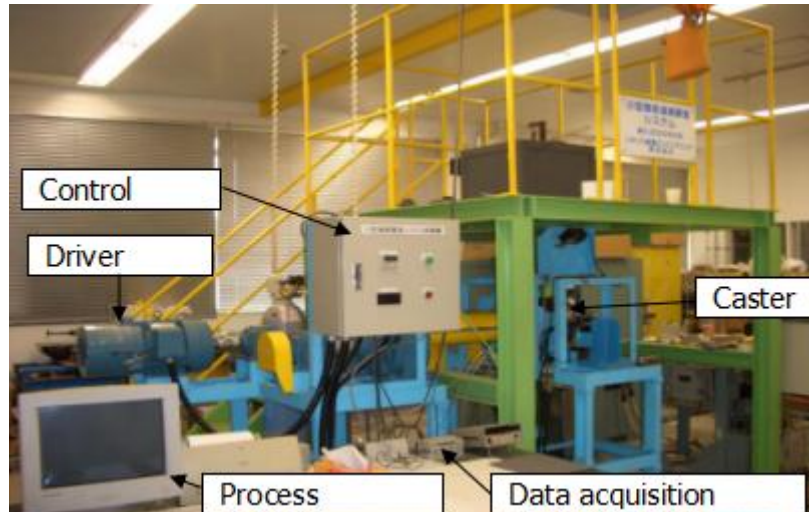


Fig. 2.2 Overview of pilot vertical twin roll caster

### 2.2.2 Manufacture of the Mg-Zn-In-Sn-MnS alloy sheet

A figure of structure of the pilot vertical twin roll continuous casting machine is shown in the Fig. 2.3. The sheet casting process of the magnesium alloy is the phenomenon that is very complicated other than a simple physical change. At first AZ91 alloy and additional element Zn-In-Sn-MnS were mixed in tundish well and the tundish project was controlled and heated up. And it is flowed into the lower oil tank through the twin roll that the liquid which dissolved turns by the tundish. Two shells which hardened go along the place to thicken from the smallest gap of the roll.[7-12].

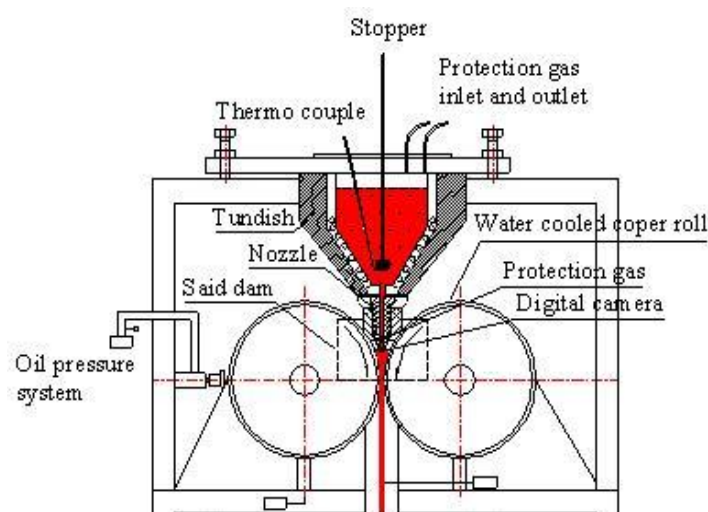


Fig. 2.3 Schematic diagram of the pilot vertical twin roll casting process

## 2.3 Analysis of the magnesium alloy ingredient

### 2.3.1 Fluorescence X-rays analysis of the magnesium alloy ingredient

Mg-Zn-In-Sn alloy and Mg-Sn-In-Sn-MnS alloy ingredient were measured by fluorescence X-rays. Figure 2.4(A) and Fig. 2.4 (B) show a spectrum of the fluorescence X-rays qualitative analysis of Mg-Zn-In-Sn alloy and the Mg-Zn-In-Sn-MnS alloy. Elemental peaks such as Al, Mn, Zn, Sn, and In appeared clearly to show it in Fig. 2.4(B) and were able to confirm that an additional Mn element existed in Mg-Zn-In-Sn-MnS alloy.

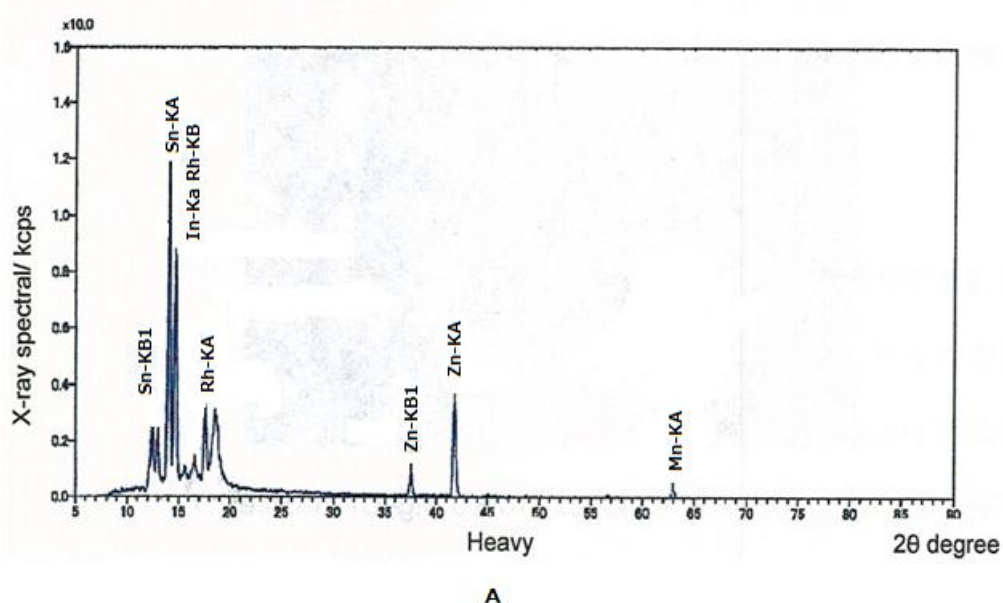


Fig. 2.4(A) Fluorescence X-rays ingredient of Mg-Sn-In-Sn-MnS alloy

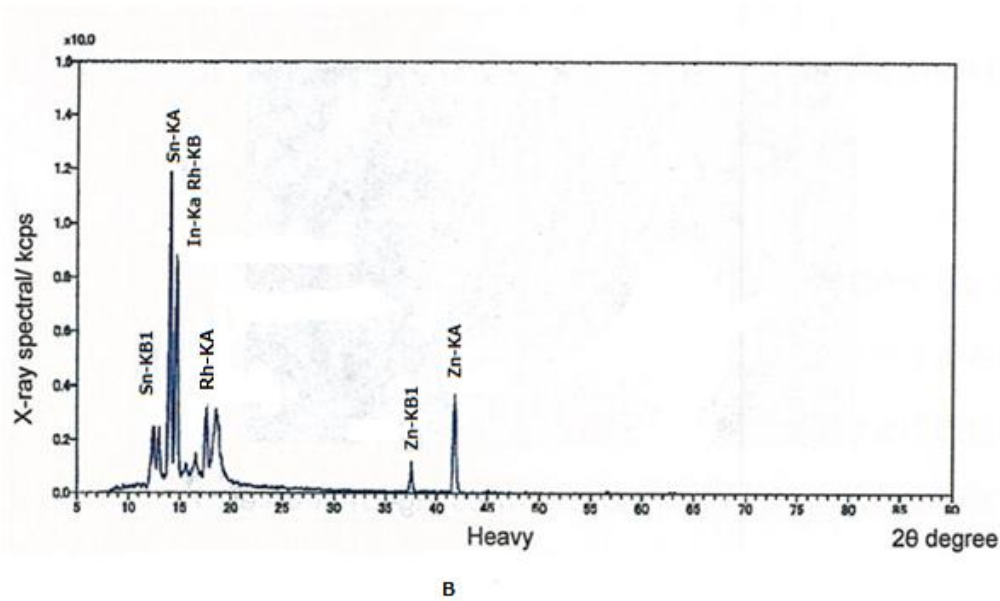


Fig. 2.4(B) Fluorescence X-rays ingredient of Mg-Sn-In-Sn-MnS alloy

## 2.4 Performance evaluation of Mg-Zn-In-Sn-MnS alloy

### 2.4.1 Observation of fine structure

The fine structure of the Mg - Zn - In - Sn alloy and the Mg - Zn - In - Sn - MnS alloy which were casted by twin roll continuously and was observed by using OM ,the photograph is shown in Fig. 2.5. Although Mg - Zn - In - Sn has a grain boundary size of 20-100  $\mu\text{m}$ , Mg - Zn - In - Sn - MnS has a grain boundary size of about 5-10  $\mu\text{m}$  and is found to be extremely small

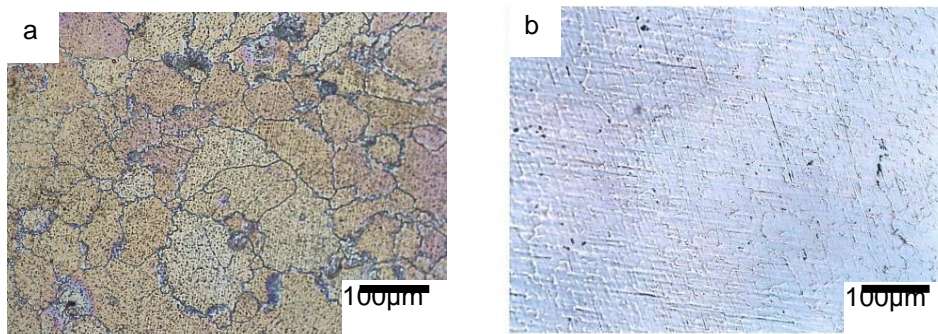


Fig. 2.5 Observation of fine structure of (a) Mg - Zn - In - Sn and (b) Mg - Zn - In - Sn - MnS

## 2.5 Experiment of tensile stress

A thin plate having a thickness of 0.5 mm was produced from a sheet material having a thickness of 3 mm by casting. According to the dimensions of the specimen, the tensile specimens prepared are shown in the Fig. 2.6. The test piece size is 70 mm in total length, the length of the reference point part is 26 mm, and the mark part width is 6 mm. The plate has been designed and produced. Using the tensile testing machine the experiment can be measured.

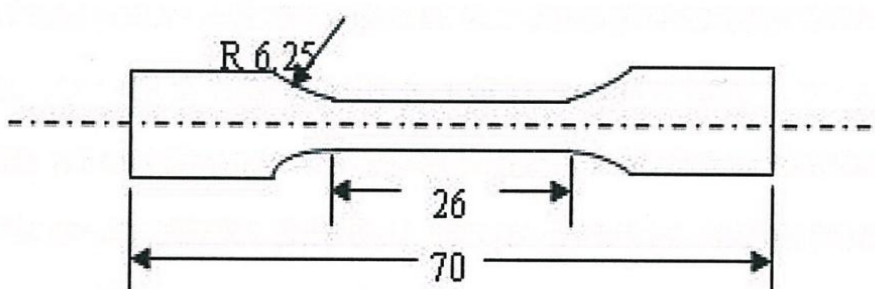


Fig. 2.6 Specimen of Stress-strain Experimentation

## 2.6 Conclusion

In this chapter, a new magnesium alloy Mg - Zn - In - Sn - MnS is prepared by adding a trace element Mn to a magnesium alloy Mg - Zn - In - Sn using a vacuum gas replacement furnace and made it by twin roll continuous casting method. Components of the Mg - Zn - In - Sn alloy were analyzed using fluorescent X-ray. Furthermore, the microstructure of the prepared Mg - Zn - In - Sn - MnS alloy and the Mg - Zn - In - Sn alloy were compared to clarify that the performance of the Mg - Zn - In - Sn - MnS alloy was excellent.

## Reference

- [1] T.Haga et al, Semisolid Strip Casting Using a Vertical Type Twin Roll Caster, Materials Science Forum. 426(2003):477

- [2] T.Haga et al, High Speed Roll Casting of Aluminum Alloy Strip, Materials Science Forum. 475(2005):343
- [3] T.Mizoguc et al, Relation between Surface quality of as-Cast Strips and Meniscus Profile of Molten Pool in the Twin Roll Casting Process, ISIJ International, 36(1996):417
- [4] L. Strezov and J. Herbertson, Experimental Studies of Interfacial Heat Transfer and Initial Solidification Pertinent to Strip Casting, ISIJ International, 38(1998):959
- [5] B.Sun, Characterization of Magnesium Plates Produced by Wheel-band Casting and Horizontal Continuous Casting, materials Science Forum. 488(2007):337
- [6] O.Daland et al, Thin Gauge Twin-roll Casting Process Capabilities and Product Quality, Light Metals, 23(1997):745
- [7] G.Z.Doing, Research on microstructure and properties of highly strengthened wrought magnesium alloys[D], Chongqing; Chongqing University, 2005
- [8] E.F.Horst and B.L.Mordike, Magnesium technology, metallurgy, design data, application[M]. Berlin, Heidelberg; Springer-Verlag, 2006
- [9] G.Abbas, L.Li, U.Ghazanfar and Z.liu, Effect of high power diode laser surface melting on wear resistance of magnesium alloys[J]. Wear, 260(2006):175
- [10] F.W.Bacha and M.Rodmanb, High quality magnesium sheets for automotive applications[J]. Advanced Materials Research, 6(2005):665.
- [11] A.J.Carpenter, Automotive Mg research and development in North America [J]. Materials Science Forum, 546(2007):11
- [12] S.Schunmann, The paths and strategies for increase magnesium application in vehicles[J]. Materials Science Forum, 488(2005):1

## Chapter 3 Evaluation of electrode performance with stress

### corrosion and clarification of electrochemical stress

### corrosion mechanism

## 3.1 Advantages and mechanisms of manganese sulfide

A convenient hydrothermal synthetic route has been successfully developed to prepare stable rock-salt-type structure  $\alpha$ -MnS submicrocrystals under mild conditions. In this synthetic system, hydrated manganese chloride (MnS) was used to supply a highly reactive manganese source. The results revealed that the electrochemical performance of the MnS submicrocrystals may be associated with the degree of crystallinity and particle size of samples. The initial lithiation capacity of the MnS submicrocrystals obtained is  $1327 \text{ mAh g}^{-1}$  at 1.7 V versus  $\text{Mg/Mg}^{2+}$ , which exhibited  $\alpha$ -MnS submicrocrystals is extremely promising anode material for magnesium-ion batteries and has great potential applications in the future. MnS has a large electrostatic capacity. But also has a storage container for batteries.

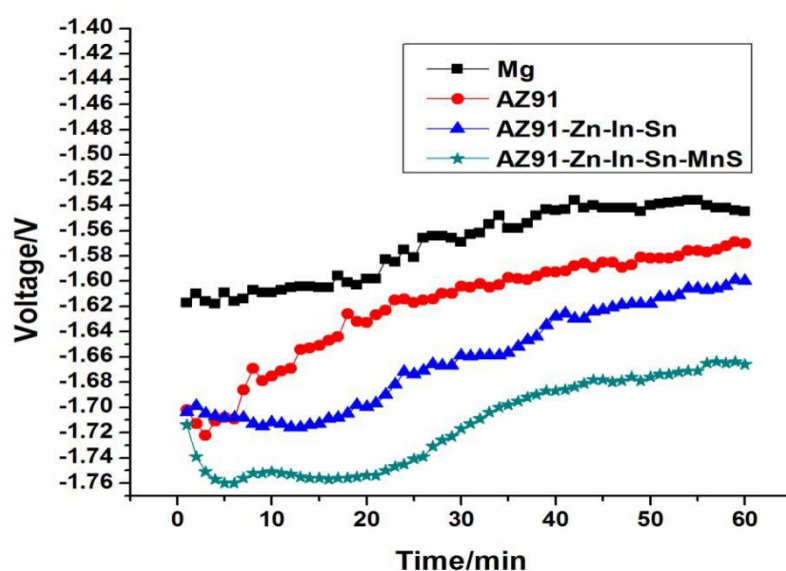


Fig. 3.1 The comparison of voltage value of a variety of Mg alloys.

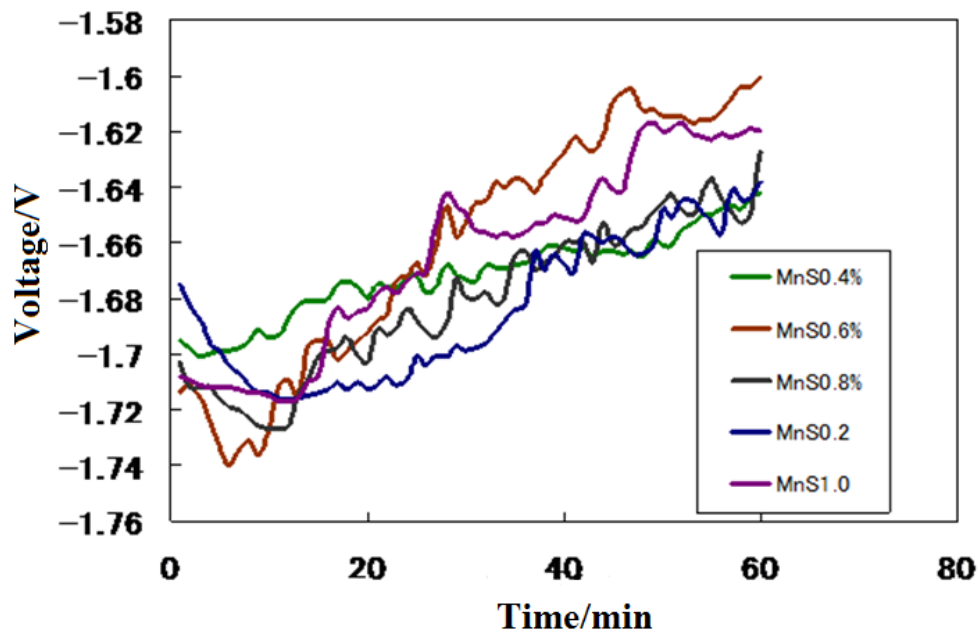


Fig. 3.2 The comparison of voltage value of a variety of MnS concentration in Mg-Zn-In-Sn-MnS alloys.

MnS had added into the Mg-Zn-Sn-In alloy as 0.2%,0.4%, 0.6%, 0.8%,1.0%.The alloy of 0.8% showed the best excellent electrochemical effect of all, both from the current value or stability, as shown in Fig. 3.2 .

The electrode potentials were observed for 4 samples in 3.5% of sodium chloride aqueous solution, as shown in Fig 3.1. In aqueous solutions, dipped magnesium alloys usually show the electrode potentials in the range from -1.5 V to -1.8V vs Ag/AgCl electrode. This simple evaluation seemed to be effective for the screening, since potentials shifts to the positive side suggest the corresponding oxides layer formation, which hinder the electrifitrode reactions.AZ91-Zn-In-Sn-MnS showed negative shifts in this screening tests, and were expected to keep relatively active surface for electrode reactions.



## 3.2 Electrolyte selection and stress corrosion experiment

In this section the two electrolytes and the four loading forces have been set up, and the distance between the cathode and the anode are also distinguished. Here, we use the best electrochemical properties alloy Mg-Zn-In-Sn-MnS which the containing of manganese sulfide was 0.8% for testing. The two electrolytes were 1mol / L ACONa and 1mol / L KCl solution, respectively. The forces applied were 0N, 50N and 100N. The distance between the cathode and the counter electrode is also divided into 10 mm and 2 mm.

### 3.2.1 CV curve of KCl from 0 MPa to 10 MPa at a distance of 10 mm

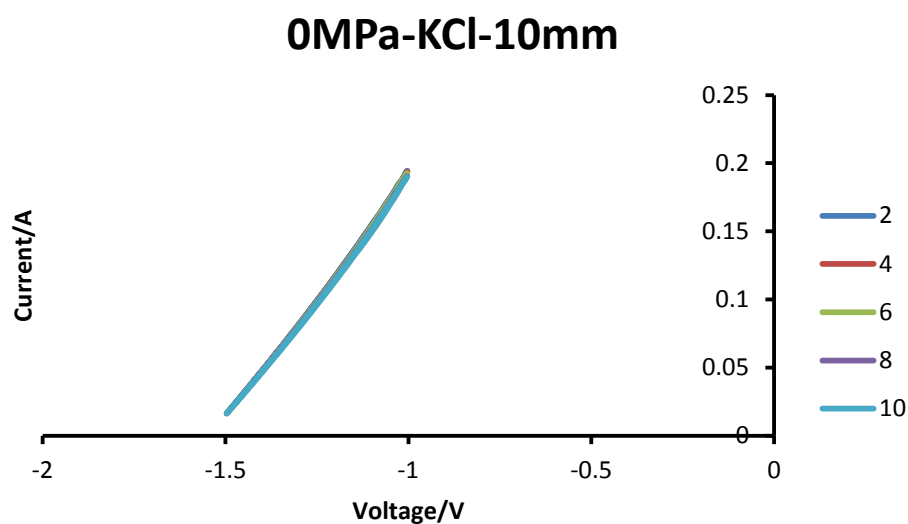


Fig. 3.3 CV curve of KCl for 0 MPa at 10mm

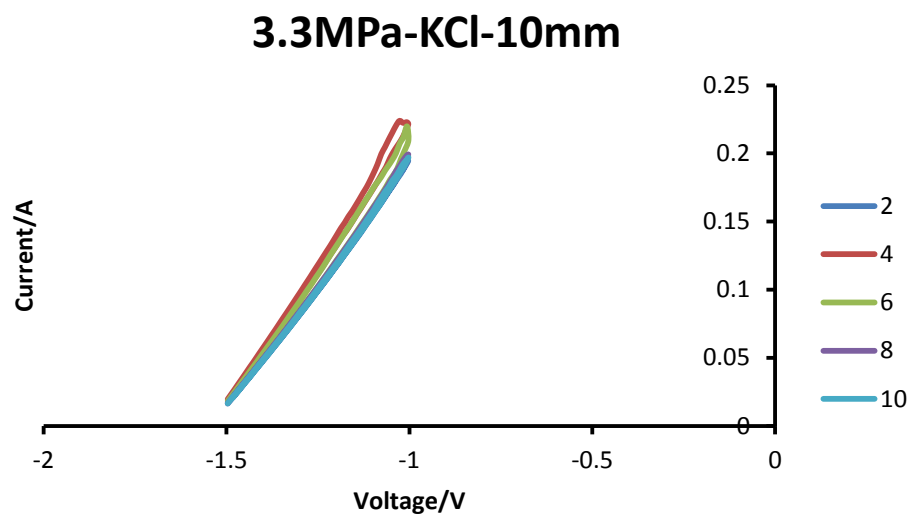


Fig. 3.4 CV curve of KCl for 3.3Pa at 10mm

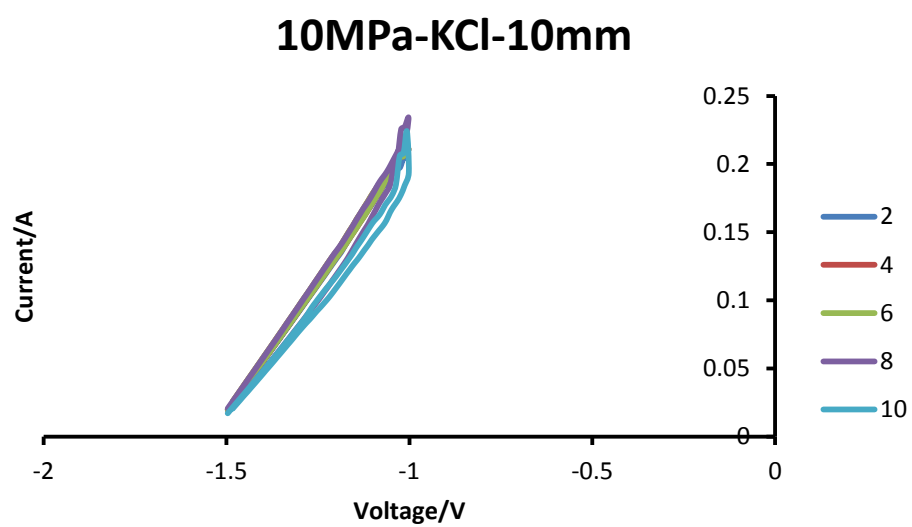


Fig. 3.5 CV curve of KCl for 10MPa at 10mm

### 3.2.2 CV curve of KCl from 0 MPa to 10MPa at a distance of 2 mm

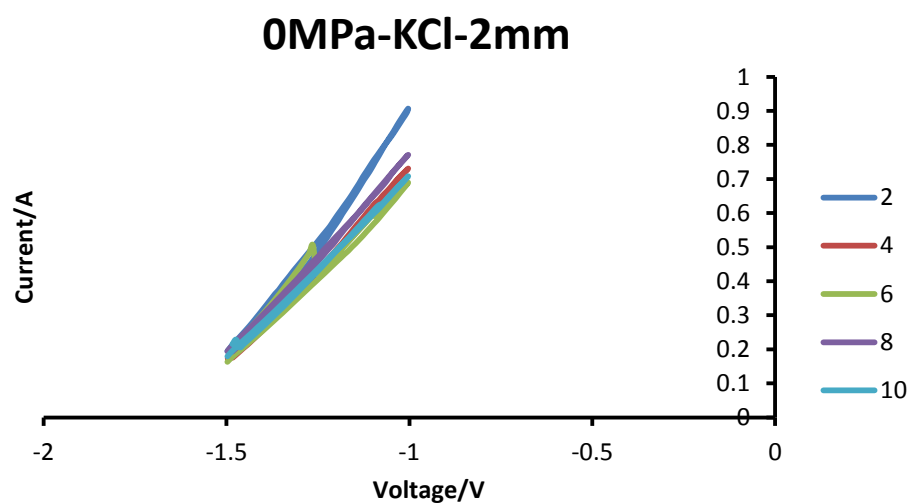


Fig. 3.6 CV curve of KCl for 0MPa at 2mm

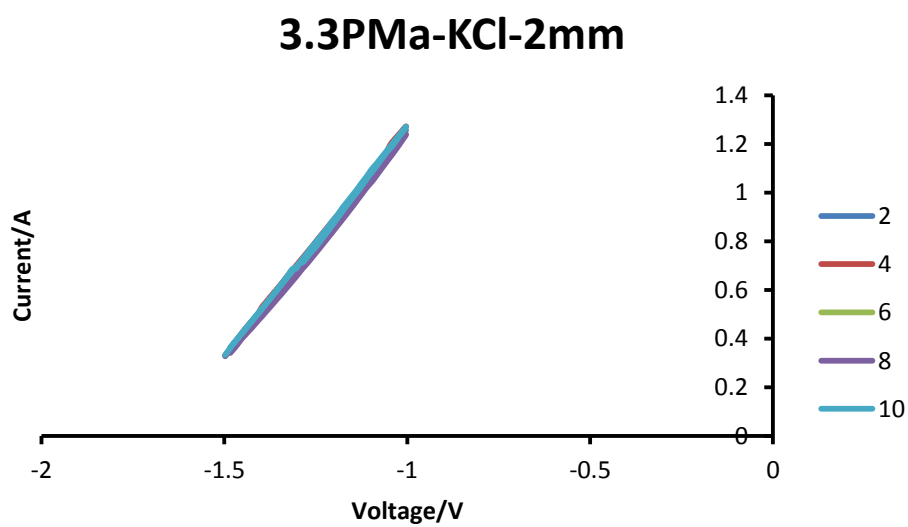


Fig. 3.7 CV curve of KCl for 3.3MPa at 2mm

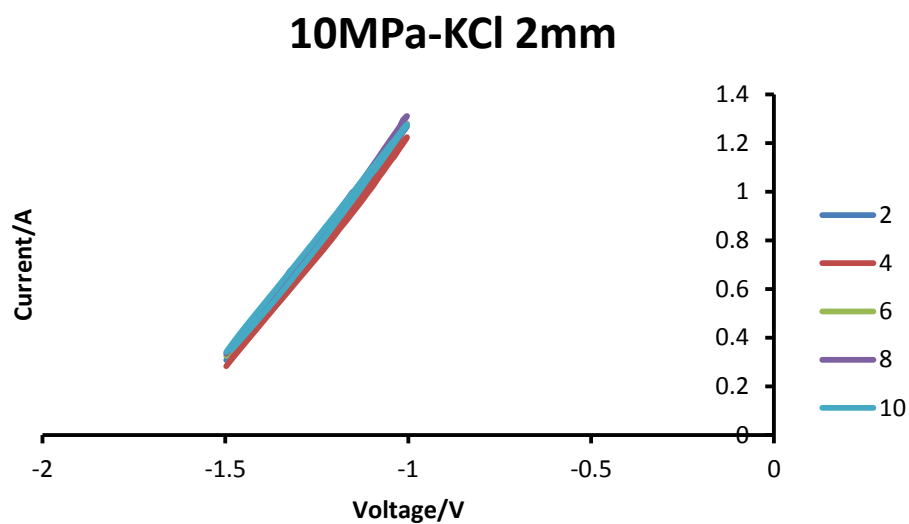


Fig. 3.8 CV curve of KCl for 10MPa at 2mm

### 3.2.3 CV curve of AcONa from 0 MPa to 10 MPa at a distance of 10 mm

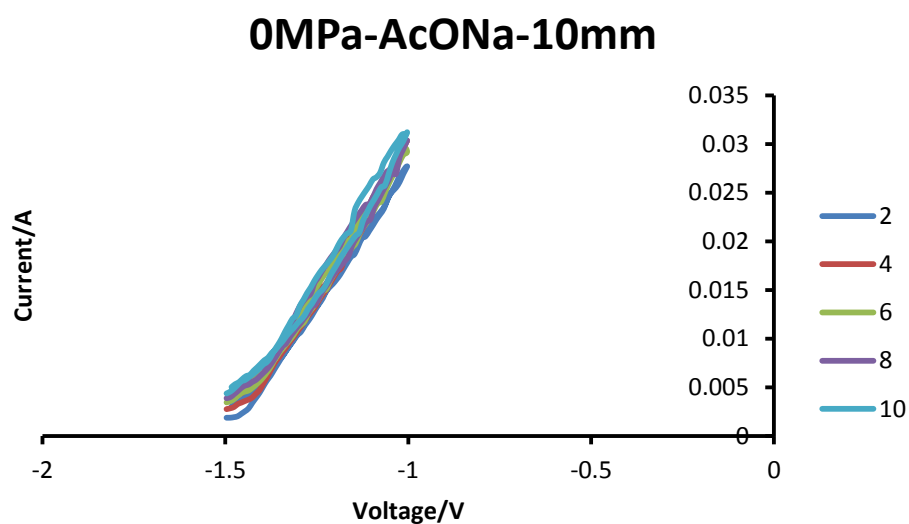


Fig. 3.9 CV curve of AcONa for 0MPa at 10mm

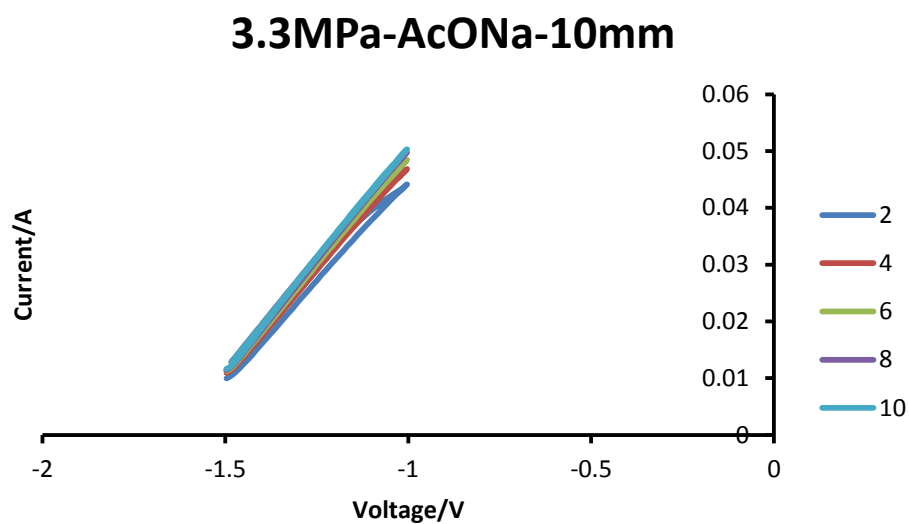


Fig. 3.10 CV curve of AcONa for 3.3 MPa at 10mm

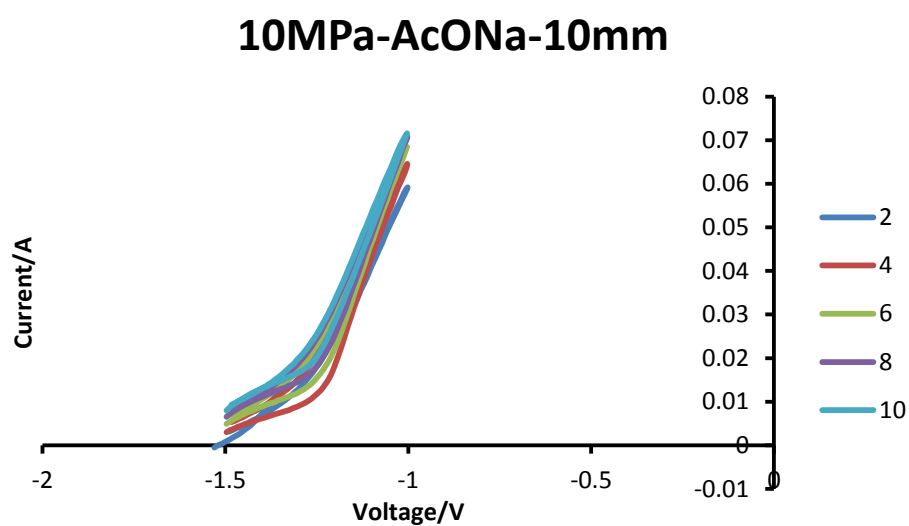


Fig. 3.11 CV curve of AcONa for 10 MPa at 10mm

### 3.2.4 CV curve of AcONa from 0 MPa to 10MPa at a distance of 2 mm

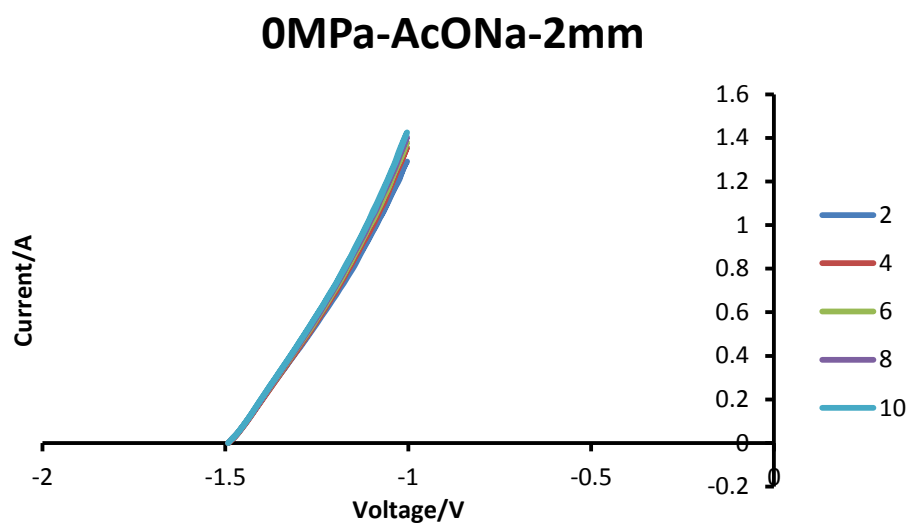


Fig. 3.12 CV curve of AcONa for 10 MPa at 2mm

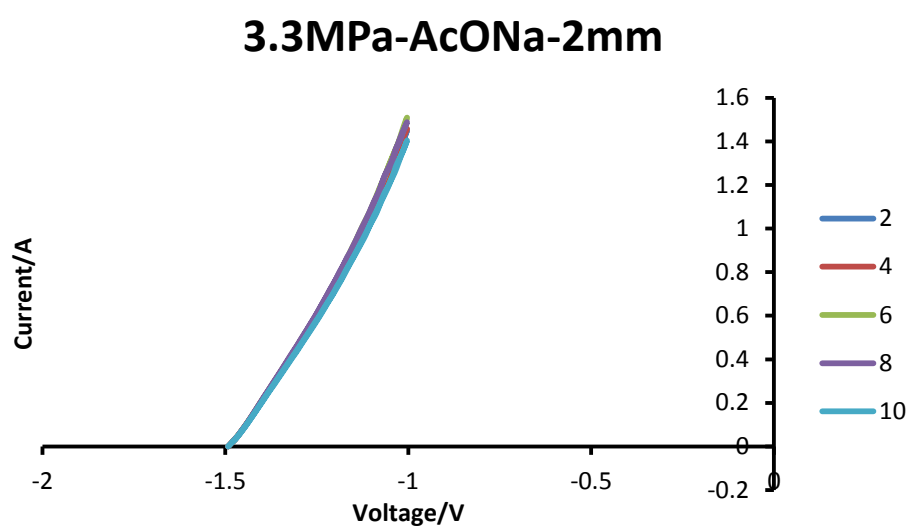


Fig. 3.13 CV curve of AcONa for 3.3 MPa at 2mm

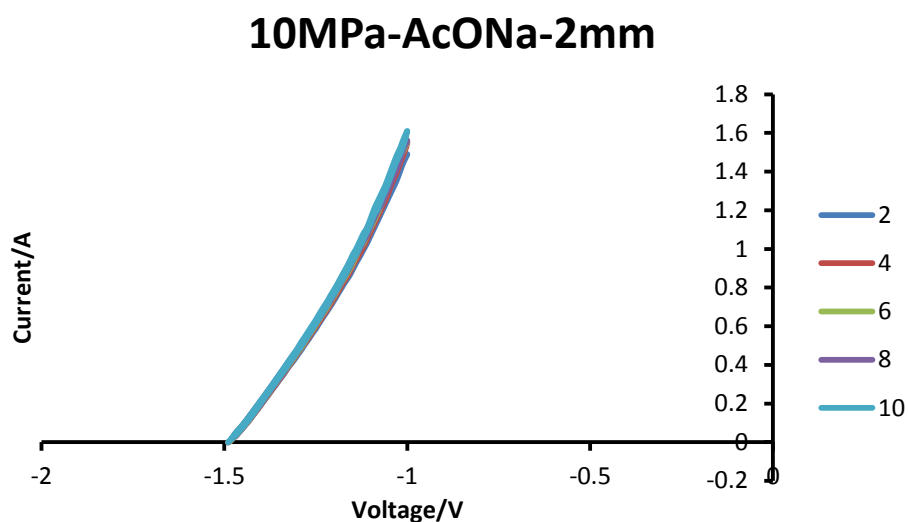


Fig. 3.14 CV curve of AcONa for 10 MPa at 2mm

When the distance of the cathode and anode of 10 mm, electrochemical properties were confirmed to be high in top current value is large for KCl. When the distance of the cathode and anode was 2 mm, was found to have high electrochemical characteristics large, top current value of AcONa. In the same type of electrolytic solution, 2mm of the distance of the cathode and anode was higher than 10 mm. All together with the raise of the whole stress, top current value has been confirmed with the increase much more. Electrochemical performance became higher.

As the distance between the cathode and the anode increases, From 10mm to 2mm, the resistance of the solution became small. The magnesium alloy in the electrochemical corrosion, the surface will form a layer of oxide film, with the tensile stress increases, these films gradually broken, making the magnesium alloy once again exposed to the electrolyte, so the electrochemical performance of the electrode with the Tensile stress increases. This can be confirmed by SEM images and impedance analysis.

### **3.3 The theory of electro-chemical chemistry and the application of the theory of the value of the study**

#### **3.3.1 Introduction**

In recent years, magnesium alloy is expected to be applied to many batteries as a negative electrode material. Among the magnesium alloys, AZ91 is one of the alloys with excellent machinability and electrochemical performance[1]. According to previous studies, we have added the compound MnS with Mg-Zn-In-Sn alloy and developed a novel electrode material Mg-Zn-In-Sn-MnS alloy. It was confirmed by the additive element that the Mg - Zn - In - Sn - MnS alloy electrode exhibited a negative voltage and a higher current than the Mg - Zn - In - Sn alloy[2]. In addition, it was possible to further enhance the electrochemical performance of the Mg - Zn - In - Sn - MnS alloy electrode by using the stress corrosion method. Therefore, it was found that the interaction between stress corrosion and electrochemical corrosion improves the electric performance of the magnesium alloy.

However, theoretical electrochemical calculations on stress corrosion of alloy electrodes are generally difficult.

In this study, we measured the concentration of magnesium ions in the corrosion solution using ICP equipment and calculated the voltage and current of the Mg - Zn - In - Sn alloy electrode by FACSIMILE software. FACSIMILE software is a program that models complex chemical reactions and can simulate efficiently[3,4]. Specifically, the reaction rate of magnesium and water was measured by an ICP apparatus and the effect of stress corrosion was investigated. In addition, the change in magnesium ion (Mg <sup>+</sup>) concentration were simulated for 1 hour by the reaction rate during stress corrosion. Then, the voltage and current of the alloy electrode were calculated and the mechanism of stress corrosion was analyzed.

#### **3.3.2 Experimental material**



Using the twin-roll continuous casting method, trace elements Zn, In, Sn, MnS were added to the AZ alloy to prepare an Mg - Zn - In - Sn - MnS alloy. The alloy plate was rolled to 0.5 mm and subjected to a heat treatment at 400 °C. for 1 hour.

The magnesium alloy negative electrode was cut as 10 cm long, 1 cm wide, and 1 mm thick. The effective electrode area was limited to 1 cm<sup>2</sup> by covering the electrodes using PVC spacers with a tetragonal hollow structure.

### 3.3.3 Measurement of Mg concentration

After conducting the stress corrosion experiment, the Mg<sup>2+</sup> concentration was measured with an ICP apparatus. Calibration curves were prepared using magnesium ion and manganese ion standard solutions of 10,20 and 30 ppm. ICP spectra of each concentration were measured using standard equations, and the results are shown in Fig3.15.

$$y=0.564x + 0.0001 \quad (3.1)$$

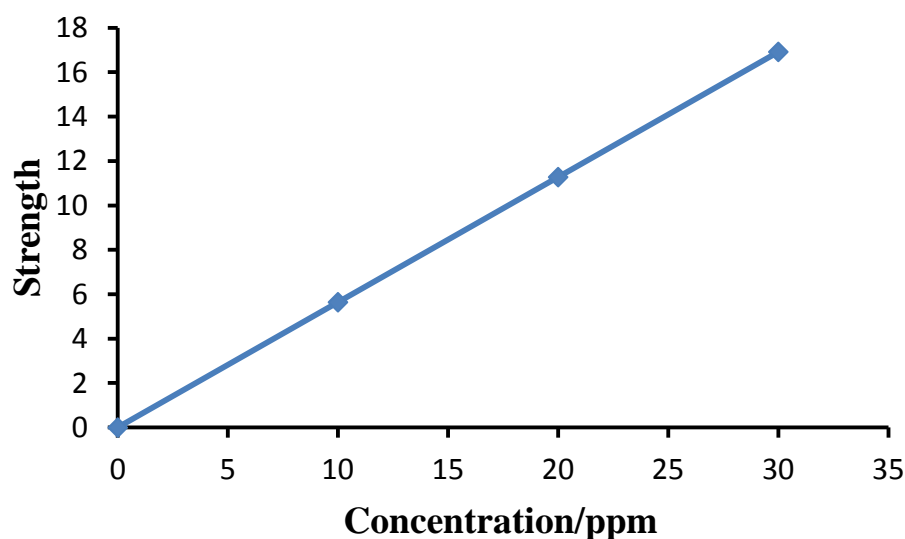


Fig. 3.15 Standard curve of Mg and Mn concentration

Based on the calibration curve, stress corrosion experiment was conducted, and  $\text{Mg}^{2+}$  concentration was measured. Then, the change of  $\text{Mg}^{2+}$  concentration during 1 hour was simulated by FACSIMILE by the reaction rate.

### 3.3.4 Proposal of hybrid model

We also proposed a hybrid model of electrochemical calculation using the reaction of magnesium and water. The corrosion reaction of the magnesium alloy follows the overall reaction formula 3.2.



Calculated by the Mg concentration measured by the reaction rate ICP. Changes in Mg concentration during 1 hour were simulated by FACSIMILE software. The voltage and current model of the alloy electrode were prepared based on the change in the reaction rate and Mg concentration.

### 3.3.5 $\text{Mg}^{2+}$ concentration changes

The  $\text{Mg}^{2+}$  concentration after 1 hour stress corrosion experiment is shown in Table 3.1. The  $\text{Mg}^{2+}$  concentration in the corrosive solution decreased with increasing stress. It was confirmed that the corrosion reaction of the Mg - Zn - In - Sn - X alloy electrode was promoted by the influence of the tension stress.

Table 3.1  $\text{Mg}^{2+}$  concentration values after stress corrosion

Tension Stress(MPa)	0	5	10	50	100
$\text{Mg}^{2+}$ concentration(mol/L)	0.0361	0.00592	0.00441	0.00312	0.00194

When no stress was applied, the corrosion reaction rate was low, so it was confirmed that the Mg concentration in the corrosive solution was high. It was also revealed that as the stress was increased, the corrosion reaction was promoted, more oxidized

corrosion products were generated, and the Mg concentration in the corrosive liquid was slightly higher.

### 3.3.6 OCP calculation

The applied stress energy improved the electrochemical potentials of alloy anode, and persisted together with stresses, because the stress did not exceed the elastic limit. The change in free energy  $\Delta G$ (per g) is given by Equation(3.3)[5]

$$\Delta G = \frac{\delta^2}{2\rho Y} \quad (3.3)$$

Where  $\delta$  is the applied stress,  $Y$  is Young's modulus, and  $\rho$  is the density of the Mg-Zn-In-Sn-X alloy. The free energy of Mg-Zn-In-Sn alloy anode increased with the applied stresses increased. The negative removal of voltage  $\Delta E$  was calculated in energy using Equation (3.4)[6,7].

$$\Delta E = -\frac{\Delta G}{nF} \quad (3.4)$$

Where  $n$  is the number of moles of electrons transferred and  $F$  is the Faraday constant. As the energy increased, the OCPs of the alloy anodes were negatively removed. The stresses are investigated to determine the OCP values of Mg-Zn-In-Sn-X alloy anode. However, the concrete values of OCP are not easy to calculated by variations of free energy[8]. Therefore, the simulated  $Mg^{2+}$  concentrations values are used to calculated the OCP values of Mg-Zn-In-Sn-X alloy anode by the Nernst equation.

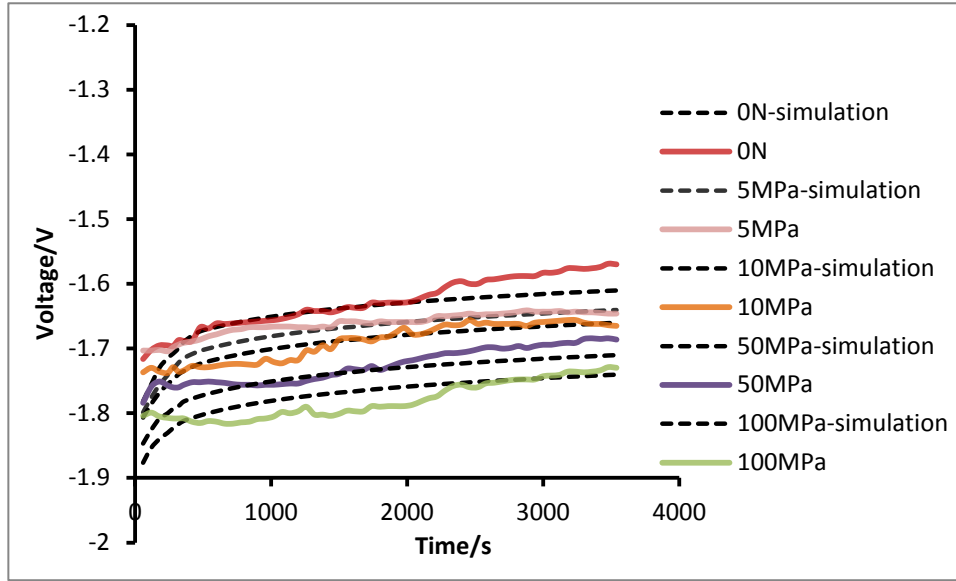


Fig. 3.16 Comparison of OCP curves for Mg-Zn-In-Sn-MnS alloy anode under stress corrosion 0MPa; 5MPa; 10MPa; 50MPa; 100Mpa

The OCPs were calculated by the following Equations(3.5)

$$E = E_0 + \frac{RT}{nF} \ln \frac{O_x}{R_{ed}} \quad (3.5)$$

Where  $E_0$  is the equilibrium potential for this reaction,  $F$  is Faraday constant,  $R$  is gas constant,  $[Ox]$  is the concentration of oxidant, and  $[Red]$  is the concentration of reductant. The calculation values of OCP are consistent with experimental results as shown in Fig. 3.16. However, the calculated value is different from the measured value. This finding can be attributed to the interference of environmental factors, such as the forming of corrosion product film and pH value of solution [9].

### 3.3.7 LC calculation

The LCs were calculated by introducing correction factor  $A$  to modify the expression of corrosion current density. Therefore, the LC density was expressed using Equations(3.4) and(3.5):  $Ai_0$

$$I = \frac{[e^{(|E| - E_0)/b_a} - e^{-(|E| - E_0)/b_c}]}{[1/Ai_0 + x]} \quad (3.6)$$

and

$$X = \frac{e^{(|E| - E_0)/b_a)}{A i_0 \exp[0.523(|E| - E_0)^5]} \quad (3.7)$$

Where  $i(0)$  is the experimental current density,  $b_a$  and  $b_c$  are the anode and cathode Tafel constants, and  $E_0$  is the equilibrium potential of the reaction calculated from the Nernst equation. This is calculated by Equation (3.8). The expression of the corrosion current density is modified by introducing the correction factor  $A$  to calculate the LC.

$$I = \frac{A i_0 \exp[0.523(|E| - E_0)^5] \left\{ \exp\left[\frac{|E| - E_0}{b_a}\right] - \exp\left[-\frac{|E| - E_0}{b_c}\right] \right\}}{\exp[0.523(|E| - E_0)^5] + \exp\left[\frac{|E| - E_0}{b_a}\right]} \quad (3.8)$$

Where  $i_0$  is the experimental current density,  $b_a$  and  $b_c$  are the anodic and cathodic Tafel constants, and  $E_0$  is the equilibrium potential for this reaction as computed from the Nernst equation, respectively.

Using equation (3.8), the current densities are calculated density under different stress corrosion conditions of 0,5,10,50 and 100MPa, respectively. And the LCs are calculated by the equation(3.9)

$$I = S \times i \quad (3.9)$$

Where  $I$  is the calculation current,  $S$  is the surface area of alloy anode.

Equations(3.8) and (3.9) were developed empirically and provide a reasonable representation of experimental results. By adjusting the Tafel factors, the calculated results were mainly consistent with the experimental results. Comparisons of the current curves between experimental and calculated values are shown in Fig. 3.17. Therefore, as shown in Table3, the stress have effects on the changes in the anode

Tafel factors increased. The modified model of the LC verifies the reliability of experimental results[10-12].

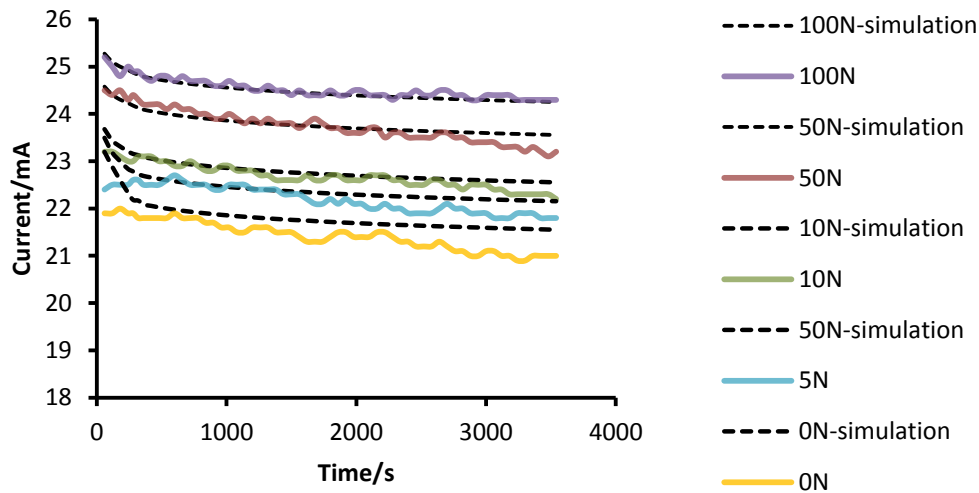


Fig. 3.17 Comparison of LC curves for Mg-Zn-In-Sn-X alloy anode under stress corrosion  
0MPa; 5MPa; 10MPa; 50MPa; 100MPa

### 3.4 Conclusion

In this chapter, it was found that Mg - Zn - In - Sn - MnS alloy has the most negative rest potential by measuring various alloys in the same electrolyte. Furthermore, using the constant stress corrosion method, the CV curve of the new magnesium alloy was measured in various solutions. When the distance between the cathode and the counter electrode was 2 mm, it was confirmed that the output performance of the novel magnesium alloy was the highest under 1 MPa stress in 1 Mol AcONa solution.

A corrosion model was developed and the electrochemical properties of the Mg - Zn - In - Sn alloy electrode were calculated. The mechanism of stress corrosion was investigated and the following conclusions were obtained.

- 1) It was found that the concentration of Mg decreases as the stress increases.
- 2) Since the calculated value of the alloy electrode voltage and the experimental value almost agreed, the mechanism of corrosion and the influence of stress were theoretically explained.

- 3) By adjusting the Tafel coefficient, the calculation value of the alloy electrode current almost agrees with the experiment value. The relationship between stress and Tafel coefficient was clarified.

## Reference

- [1] Z. Yu, D. Y. Ju, H. Y. Zhao, and X. D. Hu, Journal of Environmental Sciences.23(2011):95
- [2] Z. Yu, H. Y. Zhao, X. D. Hu, and D. Y. Ju, Transactions of Nonferrous Metals Society of China. 20(2010):318
- [3] T. D. Gregory, R. J. Hoffman and R. C. Winterton, Journal of Electrochemical Society. 137(1990): 775
- [4] D. D. Macdonald, Science. 48(1992):194.
- [5] Y. B. Unigovski, L. Riber, and E. M. Gutman, Journal of Metals, Materials and Minerals. 17(2007):7.
- [6] T. Shibata, Journal of the Society of Materials Science. 55(2006):979.
- [7] P. L. Bonora, M. Andrei, A. Eliezer and E. M. Gutman, Corrosion Science. 44(2002): 729
- [8] M. Clarke, Corrosion Science. 10(1970):671
- [9] Y. B. Unigovcki, L. Riber, and E. M. Gutman, J. Metals, Mater. Minerals. 17(2007): 7.
- [10] T. Shibata, J.Soc. Mater. Sci.. 55(2006): 979
- [11] P. L. Bonora, M. Andrei, A. Eliezer and E. M. Gutman, Corr. Sci.. 44(2002):729
- [12] J. Q. Wang, J. Chen, E. Han and W. Ke, Mater. Transaction. 49(2008):1052.

## **Chapter 4 Application of stress corrosion - Development of primary battery**

### **4.1 Introduction**

Magnesium is expected to be a candidate of negative battery-active materials with high energy density due to its highly negative redox potential and small specific gravity. There are mainly two types of batteries, commercially available and under developing; the former is a magnesium-air battery using aqueous solutions of inorganic salts, such as sea water, and the latter is a secondary battery with organic electrolytes as well as lithium ion batteries. Magnesium-air batteries are originally classified in primary batteries, exemplified by sea water batteries. However, it could be recharged by exchanging magnesium anodes [1]—[4].

Some of batteries have been proposed already as the mechanical recharging type, available to the electric vehicle application. It would be very important for these magnesium batteries to keep the activity of the anodic surface preventing from the passive state. Much attention has been paid to the selection of components of magnesium alloys for the negative active materials, and some electrochemical characteristics, such as electrode potentials and anodic current densities, would be important factors on screening alloys for the anode material. In the process of discharging for the magnesium anodes, mechanical stress could be expected to prevent the formation of inactive surface layer in the region between electrolytes and alloys, which would be important characteristics for metal alloy-air batteries to keep the anodic activity by applying such stresses. At the result of studies for screening to date, the series of AZ91 is one of the most possible candidates for the anode materials. The novel alloy for magnesium-air batteries, presented in this study, shows suitable electrochemical characteristics in electrode potentials and anodic current densities on applying the tensile stresses to the magnesium sheet anode. And the quick response time on stressing could make the batteries possible for wide range of applications, such as electric vehicles and energy storage systems for load levelling and peak shaving in the utility networks [5]—[9].



## 4.2 Experimental

### 4.2.1 The electrochemical reaction process of corrosion simulation diagram

The experiment is based on the continuous casting process in adding MnS to Mg-In-Sn-Zn alloy. As shown in Fig. 4.1, it can be determined by electrochemical measurement system made CV curves and rest voltage curves, as well as constant voltage curve which measured by current.

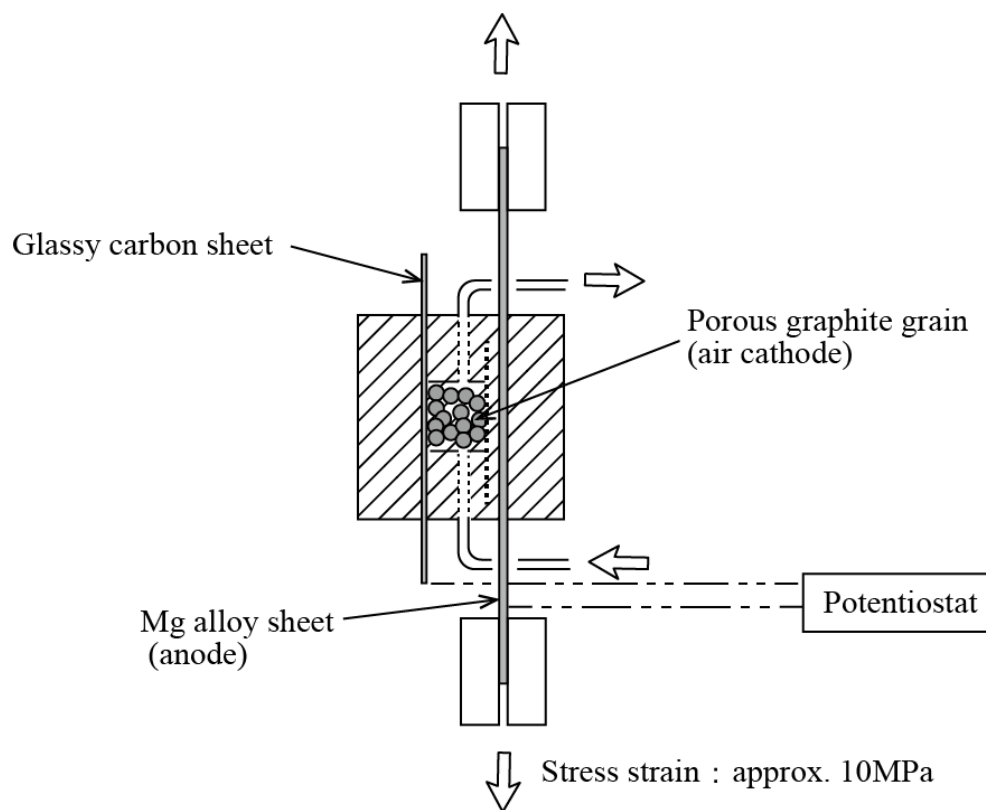


Fig. 4.1 The electrochemical system for single cell tests

### 4.2.2 Measurements of single electrode characteristics

Electrochemical behavior was observed by the tension test equipment, EZ (Tokuto Denko Electrochem Measurement System HZAP-3003A HZ-7000), Shimadzu (Modulab XM electrochemical system solartron Analytical, AMETEK Advanced Measurement Technology, Inc.) was evaluated by the results of potential sweep methods and impedance analyses.

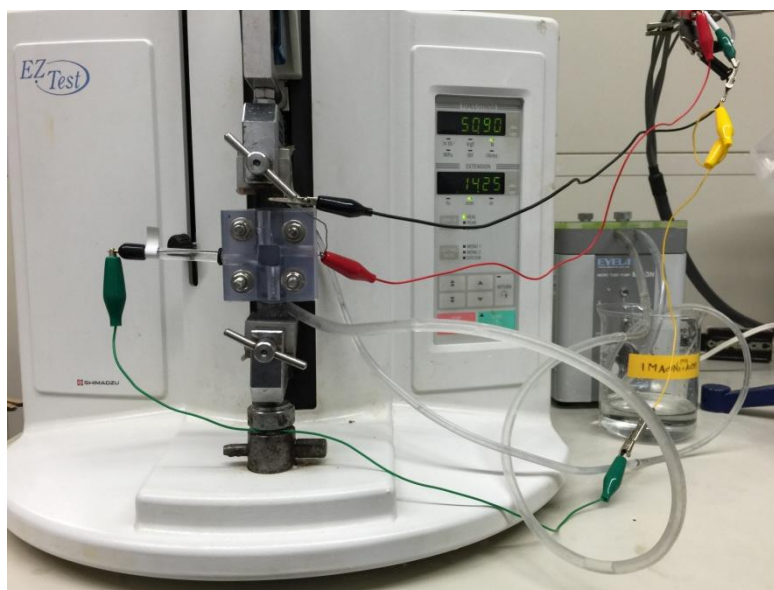


Fig. 4.2 A small single cell for the tension test

### 4.2.3 Morphologies of the magnesium alloy electrodes after tensile stress tests

Magnesium alloy were observed by SEM, XPS and micro-Raman spectroscopy, before and after tensile stress tests. SEM (Scanning Electron Microscope JSM-5500LV) was used in this experiment to observe the fracture surface and the surface of the Mg sheet which had been corroded.

XPS (PHYSICAL ELECTRONICS QUANTUM 2000 SCANNING ESCA MICROPROBE) : X-ray Source is monochromatic Al K $\alpha$  (1486.6eV). X-ray Beam

Diameter is 100 $\mu$ m, 25W, 15kV. Raman spectroscopy is a spectroscopic technique used to observe vibrational, rotational, and other low-frequency modes in a system. Raman spectroscopy is commonly used in chemistry to provide a fingerprint by which molecules can be identified. The SEM was used in this experiment to observe the fracture surface and the surface of the Mg sheet which had been corroded.

## **4.3 Result and discussion**

### **4.3.1. Measurements of single electrode characteristics**

The anodic reactivity of magnesium alloys was examined by the current-potential curves under a certain tensile stress in a electrolytic solution. Fig.4.4 shows a result of current curves in the potential range of -0.95 to -1.10VvsAg/AgCl under 10MPa of tensile stress in a sodium acetate - acetic acid (Total acetate concentration:2M, pH8.5) aqueous solution. Pump circulation of the electrolyte made the anodic current stable and maintained hi-rate anodic currents, such as 500mA cm<sup>-2</sup> for the alloy sheets. Larger anodic currents could be obtained in the coexistence of chloride ions, however, electrolytes, such as acetates or carbonates, are much suitable to control the anodic dissolution on applying the tensile stress, compared with solutions containing chloride ions, especially in the point of response time on removing the tensile stress from the alloy sheet.

At least, more than 2MPa of tensile stress was necessary for the alloy sheet to perform hi-rate discharge currents in the sodium acetate - acetic acid solution, as shown in Fig. 4.3.

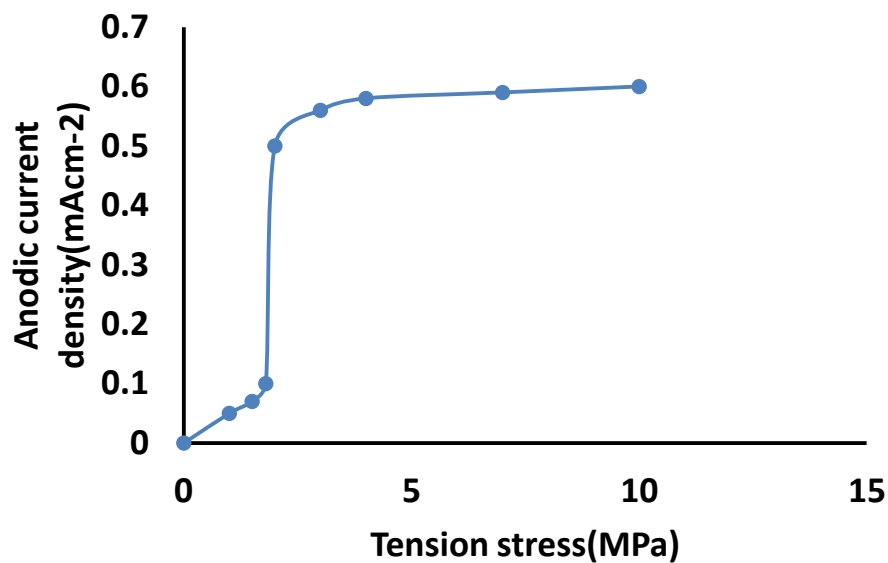


Fig. 4.3 Anodes current change for cyclic potential sweep between -0.95V to -1.10V vsAg/AgCl under 2-10MPa stretching

Figure 4.3 shows the effect of tensile stress on the Mg alloy, and it was found that the anodes current could be controlled by loading at least 2MPa tensile stress

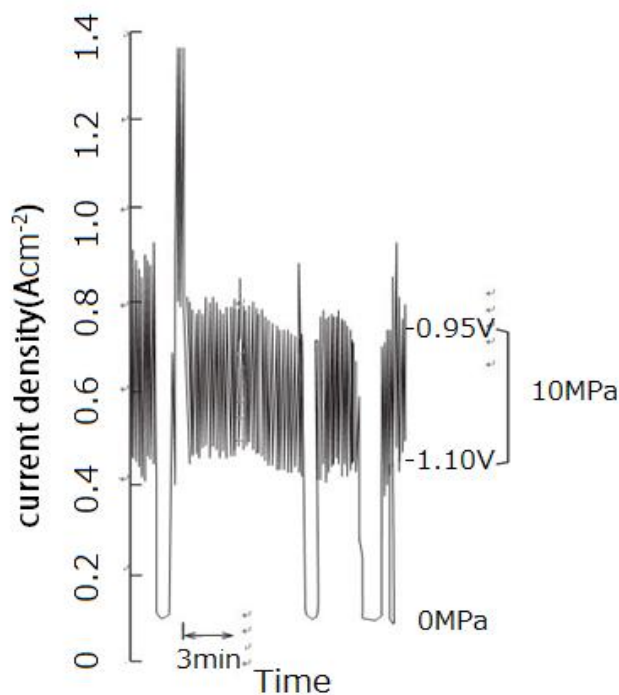


Fig. 4.4 An anodic current change responding to tensile stress under cyclic voltage range from -0.95V to -1.10V

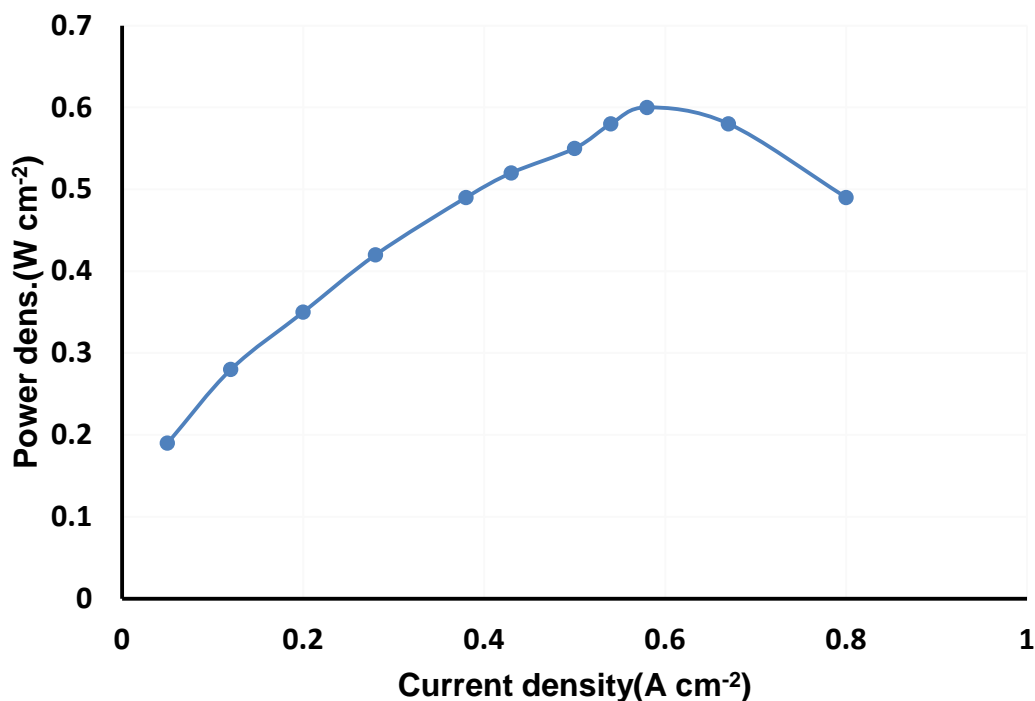


Fig. 4.5 Relationship of the current density and output power

Figure 4.4 shows an example of anodes current controlling in sodium acetate solution. For sodium acetate – acetic acid media (pH7), output power of magnesium anode was measured by assuming standard electrode potentials as output voltages; and the result was obtained as Fig. 4.5.

A magnesium-air fuel cell was assembled and demonstrated. Granular type electro-conductive activated carbon was employed as oxygen cathode. In this demonstration, the rate determining reaction was oxygen reduction in the cathode.

#### 4.3.2. Estimation of power densities for the magnesium alloy batteries

The power densities were estimated by assuming the cathode potential was the same as that of Ag/AgCl reference electrode, approximate +0.2V vs normal hydrogen electrode. 0.6W cm<sup>-2</sup> of the power peak was expected to obtain for magnesium alloy batteries under tensile stress in in a sodium acetate - acetic acid solution at pH7, as shown in Fig. 4.5.

### 4.3.3. Morphologies of the stressed magnesium electrodes

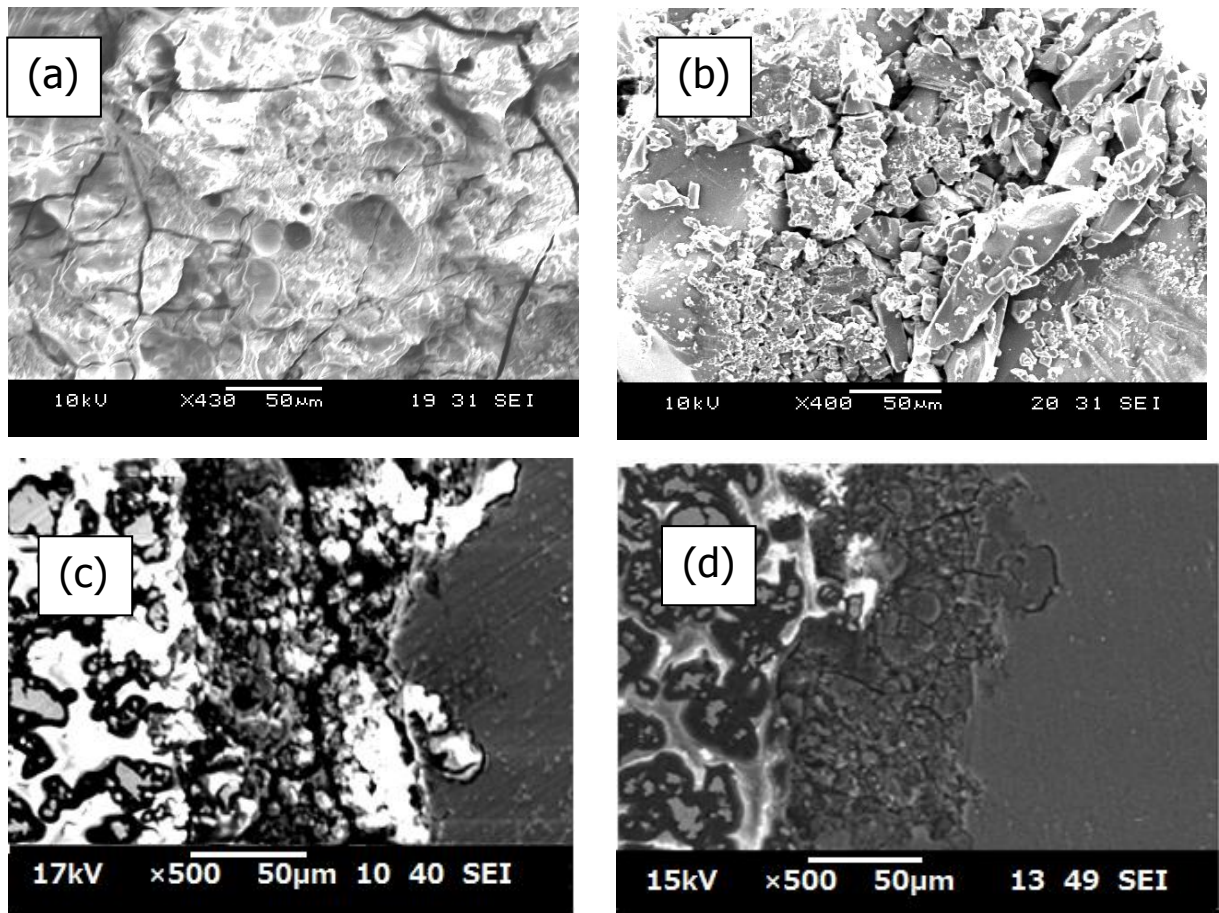
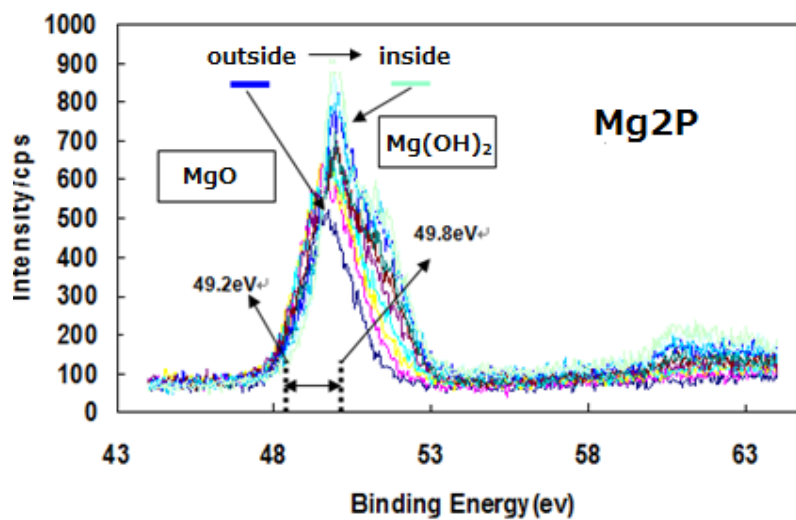


Fig. 4.6 SEM images of the magnesium alloy sheets: (a) surface of the corrosion layer after the application of 10 MPa tensile stress; (b) surface of the corrosion layer after no tensile stress; (c) cross-section after the application of 10 MPa tensile stress; (d) cross-section after the no-load test;



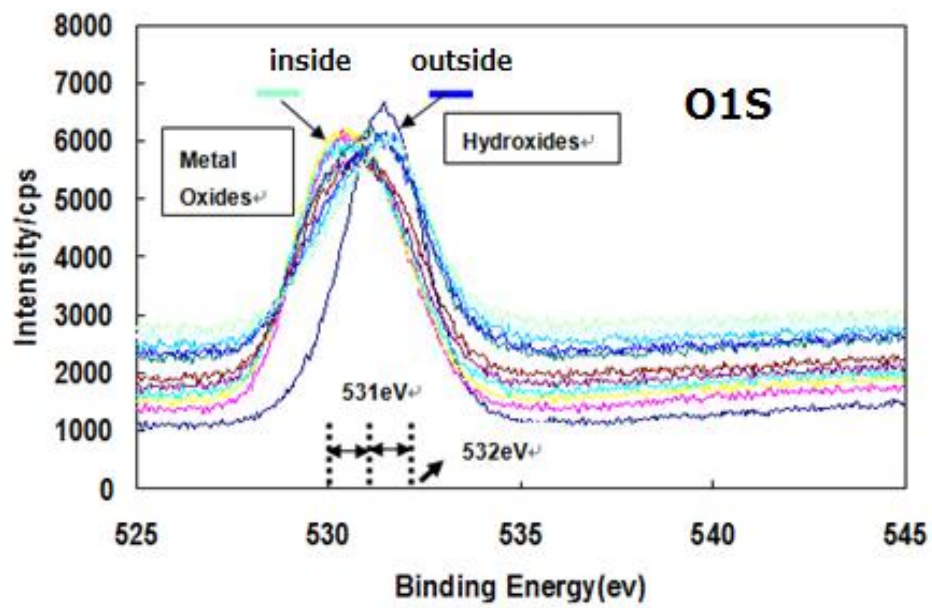


Fig. 4.7.2 XPS analysis of O1S

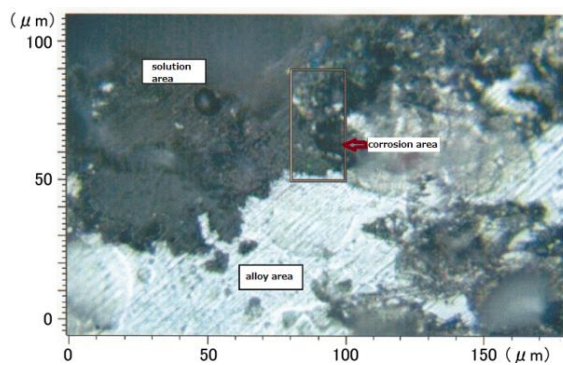


Fig. 4.8.1 The figure of the Mg alloy which had been measured by Raman spectroscopy(10MPa)

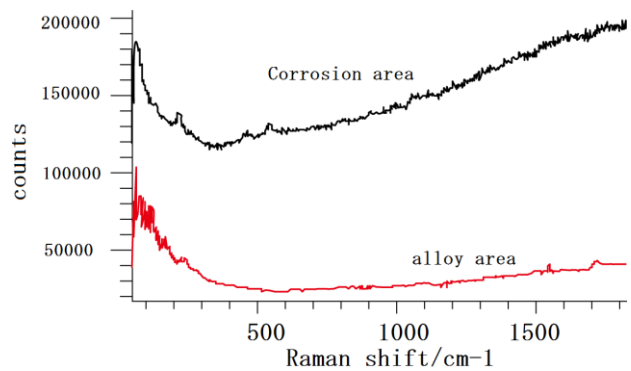


Fig. 4.8.2 The data of the Mg alloy Which had been measured by Roman Spectroscopy(10MPa)



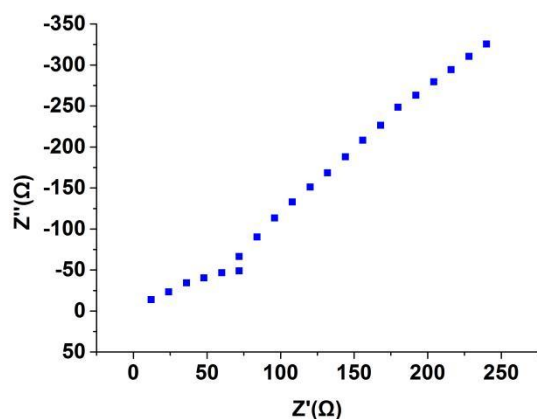


Fig. 4.9.1 The Impedance analysis of the Mg Alloy without stress

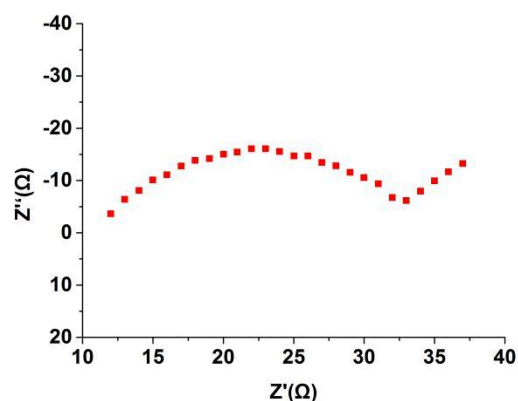


Fig. 4.9.2 The Impedance analysis of the alloy with the loading of 10MPa

SEM images, Figure 4.6(a) and Figure 4.6(b) show the difference in corrosion layer thickness between the loaded and non-loaded magnesium alloy sheets. The surface of the alloy was covered with fine particles for the sheets of non-loading tensile stress, on the other hand, the surface of the alloy sheets could be observed clearly on loading 10MPa of tensile stress. The SEM images of cross section, Figure 4.6(c) and Figure 4.6(d) show the difference of corrosion layer thickness between them, too[11]-[12]. The corrosion layer was confirmed by XPS analyses, and its main component was basic salts, such as hydroxides, of magnesium. Figure 4.7.1 and Figure 4.7.2 show the Mg 2P and O1S spectra of XPS for the alloy sheets loaded tensile stress.

The same result was obtained by the measurements of micro-Raman spectroscopy for the cross sections of tensile stress loaded alloys. Figure 4.8 shows Raman spectra of a corrosion layer and a layer of metallographic structure, and clear discrimination could be possible by micro-Raman analysis(10MPa for Fig. 4.8.1 and 4.8.2 )

The fine particles of magnesium basic salts was not observed for the alloys loaded tensile stress, since dissolution rate of magnesium seemed to be higher than the case of non-loaded tensile stress. The concentrations of magnesium in the electrolytes, sodium acetate - acetic acid solution, were determined by turbidimetry with 400nm wave length, using magnesium hydroxide as the standard suspended solid. The turbidity of the electrolyte was being concentrated clearly according to the progress of discharging, and 0.015g magnesium dm<sup>-3</sup> was determined in contrast with 0.018g magnesium, calculated from anodic current and its discharging time.



Specific surface areas of the alloy electrode were considered to expand extremely to the level of a millicoulomb per  $\text{cm}^2$  from the result of impedance analyses, whereas only dozens of coulombs for fresh magnesium alloys. In the magnesium alloy sheets, the increase of surface area was considered to linked to the increase of electrostatic capacity, which would make it possible to discharge with large current densities. Examples of impedance spectra were shown in Fig. 4.9.

#### 4.3.4 Magnesium air battery

A small single cell performance was shown in Fig. 4.10, on assembling a magnesium-air battery. After slow increase of the apparent current density for about one hour half, stable  $0.1\text{W cm}^{-2}$  of output power was obtained, which apparent current density was approximate  $100\text{mA cm}^{-2}$ . And the current decreased to approximate half value on releasing the anode sheet of magnesium alloy from 10MPa of tensile stress. By assembling the tensile stress structure of magnesium anode, a battery with higher power density could be composed compared with conventional magnesium-air batteries, such as sea water batteries, their apparent current densities were levels of several or  $10\text{mA cm}^{-2}$ .

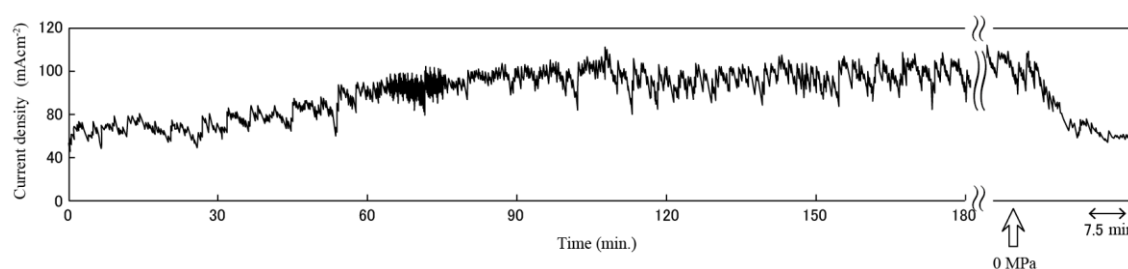


Fig. 4.10 A small single cell performance of magnesium-air battery

## 4.4 Conclusion

The anodes dissolution was controlled by loading 2 to 10MPa of tensile strain on the modified AZ91 alloy for a magnesium – air fuel cell. 0.6Acm<sup>-2</sup> of the current density and 0.5Wcm<sup>-2</sup> of output power were obtained under the condition of -1.0V vs Ag/AgCl of the negative electrode and sodium acetate - acetic acid solution. Screening of electrolytes was very important due to controlling of the corrosion layer thickness. A small single cell was assembled and demonstrated by combining oxygen cathode of electro-conductive activated carbons with the magnesium alloy anode.

## Reference

- [1] Z.Yu, D.Y.Ju,H.Y.Zhao and X.D.Hu. Effect of Zn-Sn-In elements on micro-structural performances of AZ91 Mg alloy .The Chinese Journal of Nonferrous Metals,20(2010):318.
- [2] C.J.Bettles, M.A.Gibson and K.Venkatesan.Enhanced age-hardening behaviors in Mg-4%Zn micro-alloyed with Ca.Scripta Materialia,51(2004):193.
- [3] Y.Zhang, C.Yan, F.Wang, H.Lou and C.Cao. Study on the environmentally friendly anodizing of AZ91D alloy magnesium alloy. Surface and Coatings Technology,161(2002):36.
- [4] C.E.Barchiche, E.Roocca and J.Hazan. Corrosion behavior of Sn-containing oxide layer on Az91D alloy formed by plasma electrolytic oxide. Surface and Coatings Technology, 202(2008):4145-4152.
- [5] J.Q.Wang, J.Chen, E.H.Han and W.Ke. Investigation of stress corrosion cracking behaviours of an AZ9 magnesium alloy in 0.1kmol/m<sup>3</sup> Na<sub>2</sub>SO<sub>4</sub> solution using slow strain rate test. Materials Transactions, 49(2008):1052.
- [6] H.Uchida, M.Yamashita, S.Hanaki and T.Nozaki.Susceptibility to stress corrosion cracking of AZ31B magnesium alloy by slow strain-rate technique.Journal of the Society of Materials Science, Japan, 57(2008):1091.

- [7] L.R.Cheng, Z.Y.Cao, Y.B.Liu, L.Zhang,T.Q.Li and G.H.Su. Microstructure and strain rate sensitivity of Mg-11Li-3Al-1Ca alloy. Materials Transactions, 51(2010):2325.
- [8] Z.Yu, D. Y. Ju, H.Y.Zhao and X.D.Hu. Effects of Zn-In-Sn elements on the electric properties of magnesium alloy anode materials. Journal of Environmental Sciences.23(2011):95-99.
- [9] Z. Yu, D. Y. Ju, and H. Y. Zhao. Effect of stress on the electrochemical corrosion behavior of Mg-Zn-In-Sn alloy. International Journal of Electrochemical Science. in press.
- [10] R. W. Cahn, P. Hassen and E. J. Kramer, Materials science and technology structure and properties of nonferrous alloys, UCH, NewYork, 1996
- [11] K.W.Guo. A review of magnesium/magnesium alloys corrosion and its protection. Recent Patents on Corrosion Science.2(2010):13.
- [12] L .R. Cheng, Z.Y.Cao and G. H. Su. Microstructure and strain rate sensitivity of Mg-11Li-3Al-1Ca alloy. Materials Transactions.51(2010):2325

## **Chapter 5 Mechanical control of magnesium alloy electrodes under the tensile stress for applications in non-aqueous battery electrolyte solution**

### **5.1 Introduction**

The vast majority of current electrochemical studies are directed toward the promising lead-acid, nickel-cadmium and lithium-ion systems. But magnesium alloy possess a number of characteristics which make it be an attractive material with the properties of relatively low equivalent weight, high melting point, low cost, relative abundance, high safety and ease of handling which was allowed for urban waste disposal. It has been considered a suitable anode material for high energy density batteries. Similar to stress corrosion, the electrochemical characteristics of metal surfaces change under tensile stress. Such surfaces are expected to be applicable in electrode activation to synthesize batteries, electrolytes, and chemical detectors. However, because of its favourable mechanical strength such as the yield stress and Young's modulus[1], magnesium alloy still can be used as a good electrode material when tensile stress was loaded in the plate.

In a lot of research works, magnesium alloys are applied to various types of batteries as the negative-electrode materials of batteries[2,3]. Magnesium negative electrodes are used in seawater batteries and button batteries; excellent and stable electrochemical results were obtained and confirmed by Facsimile simulation [4-6]. For the aqueous-solution-type battery, since it can only be discharged and cannot be charged, it can only be called a primary battery. The secondary battery, which can be both charged and discharged, can only occur in an organic solvent in case of magnesium batteries. Thus, it is believed that these electrodes can have practical applications as secondary batteries with high energy density because of their negative redox potential and small specific gravity[7,8]. However, the output voltage of

magnesium negative electrodes has limited values: e.g., -1.8 V vs. Ag/AgCl [9,10] in the case of aqueous electrolytes. These electrodes can only be recharged by the so-called mechanical charging method for aqueous electrolyte batteries.

However, although no dendrites form during the electro-deposition of magnesium ions, the surface of magnesium negative electrodes forms passivation film during electro-dissolution. The electrochemical behaviours of magnesium alloys change depending on the alloying elements [9]. AZ91 with additional elements such as components of Zn, In, and Sn shows relatively high negative open circuit potential and anodic reactivity in aqueous electrolytes under 3–10 MPa tensile stress [6]. The elements increase the over-potential of the hydrogen evolution reaction with Hg, Pb, Sn, etc. Low-melting-point elements such as Ga and Sn can decrease the negative electrode potential because of the increasing electrochemical reaction active site. The Sn addition can also increase the tensile effect for the electrochemical properties of magnesium alloys [11]. The elements that contain components of Al, Zn, and Mn can improve the corrosion resistance of magnesium alloys [12]. Rare earth elements such as In and Ti can refine grains. Many batteries are usually improved by the hydrogen over potential and can obtain stable discharge voltage by adding Hg and Pb. However, in this study, non-toxic elements in the components of Zn, Sn and In were added to the developed magnesium alloy electrodes to produce stable currents and high electrode potentials for environmental protection [9,13,14].

As a continuation of a previous study, we develop a new type of magnesium alloy with Zn, In, Sn, and MnS components based on the AZ91 alloy as a negative electrode material of a secondary battery in this paper. However, a problem with the use of the negative electrode of magnesium alloy in battery applications is the formation of a passivation film on its surface, Since this film is insulating and difficult to be dissolved in the organic electrolyte, it isolates the metal from contacting the external electrolyte so that the reaction can not be proceeded. So the magnesium alloy battery charge and discharge performance are both affected, especially the charge is difficult to continue. To solve the problem of passive-film formation on the surface of the negative electrode, the stress control method was used to verify the effect of stress on the charging and discharging process when the electrode material and organic electrolyte are applied to the secondary battery. The surface and cross-section of the magnesium alloy electrode after the reaction were observed by SEM, and EDS

analyses were performed on the corrosion area. A small cell was assembled with  $V_2O_5$ -supported carbon felt positive counter electrodes to evaluate the possibility of their practical development. The study showed that the secondary battery using the present cell configuration can obtain greater potential power density than 100 W/kg. The performance evaluation under stress control shows that this method can effectively improve the performance of magnesium batteries. Furthermore, two types of battery structures with a single cell and two cells were designed by substituting the organic solvent for the aqueous electrolyte solution and using the magnesium alloy as the negative electrode and the  $V_2O_5$ -supported carbon fibre felt as the counter electrode to form the current loop. By measuring the current-voltage curves, Nyquist plots and other electrochemical properties, we verified the characteristics of the proposed secondary battery. The charge and discharge performance of the battery was evaluated. Finally, as a practical application, a two-single-cell stack battery with a bending stress of 3.3 MPa was used to verify the effect of stress control. The main innovation of this paper is to add compounds MnS into the Mg-Zn-In-Sn alloy, and the new material is used as a cathode of a secondary battery with organic solvents. The effect of the additional tensile stress on the cathode is also verified.

## 5.2 Experimental

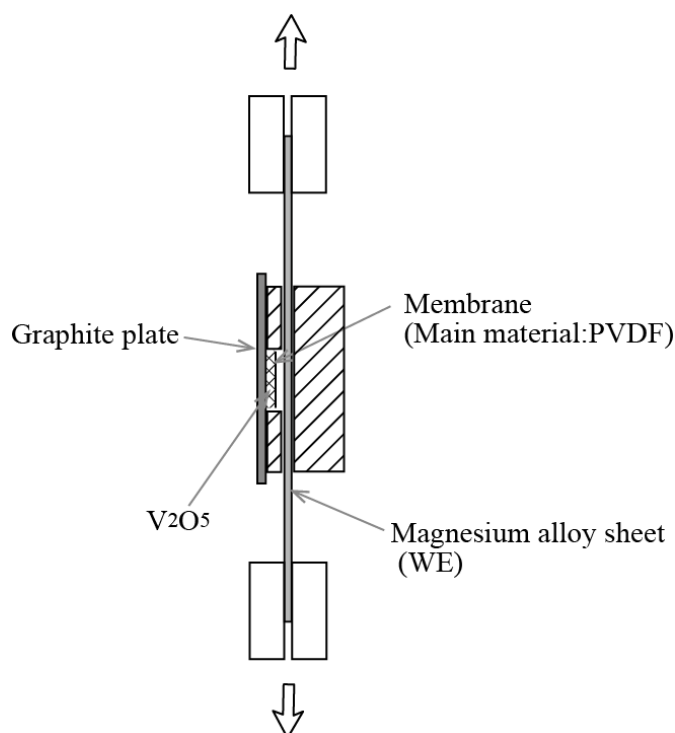


Fig. 5.1 Tensile test system for the measurement of magnesium alloy electrodes

In this research work, A small single-cell system was assembled to confirm the effect of tensile stress application, as shown in Fig. 5.1. The cell consisted of the following components: a magnesium alloy sheet (negative electrode), a carbon felt sheet, spacers, and a counter electrode (positive electrode). The magnesium alloy negative electrode was 10 cm long, 1 cm wide, and 0.5 mm thick. The effective electrode area was limited to 1 cm<sup>2</sup> by covering the electrodes using PVC spacers with a tetragonal hollow structure. Both ends of the magnesium alloy sheet were fixed using a stretch-forming machine (EZ-TEST CE, SHIMADZU Corp.), and a tensile stress of 50–150 N (3–10 MPa) was applied to the magnesium alloy electrode.

First, the static voltage of the magnesium alloy of various components was measured to select the alloy with the best electrochemical performance. The Mg alloy sheets with the best electrochemical performance were produced using the twin-roll continuous casting method. AZ91 alloy and additional element Zn-In-Sn-MnS were mixed in tundish well and the tundish project was controlled and heated up. Then, the melted liquid from the tundish is passed through the rotating twin roll and poured into the lower oil tank. And it is flowed into the lower oil tank through the twin roll that the liquid which dissolved turns by the tundish. Two shells which hardened go along

the place to thicken from the smallest gap of the roll. Since the rolled alloy plate is relatively thick and not smooth enough, the alloy is pressed to a thickness of 0.5 mm by the method of calendering. Magnesium - manganese equilibrium diagram shown in Fig. 5.2.

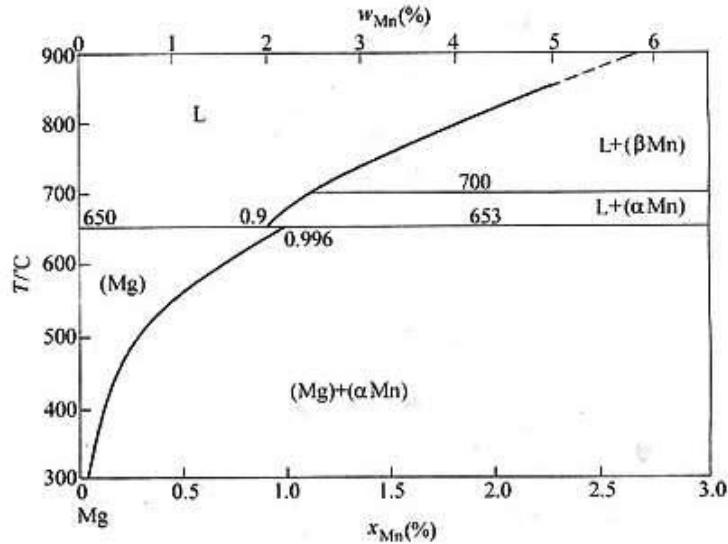


Fig. 5.2 The equilibrium phase diagram between Mg and Mn.

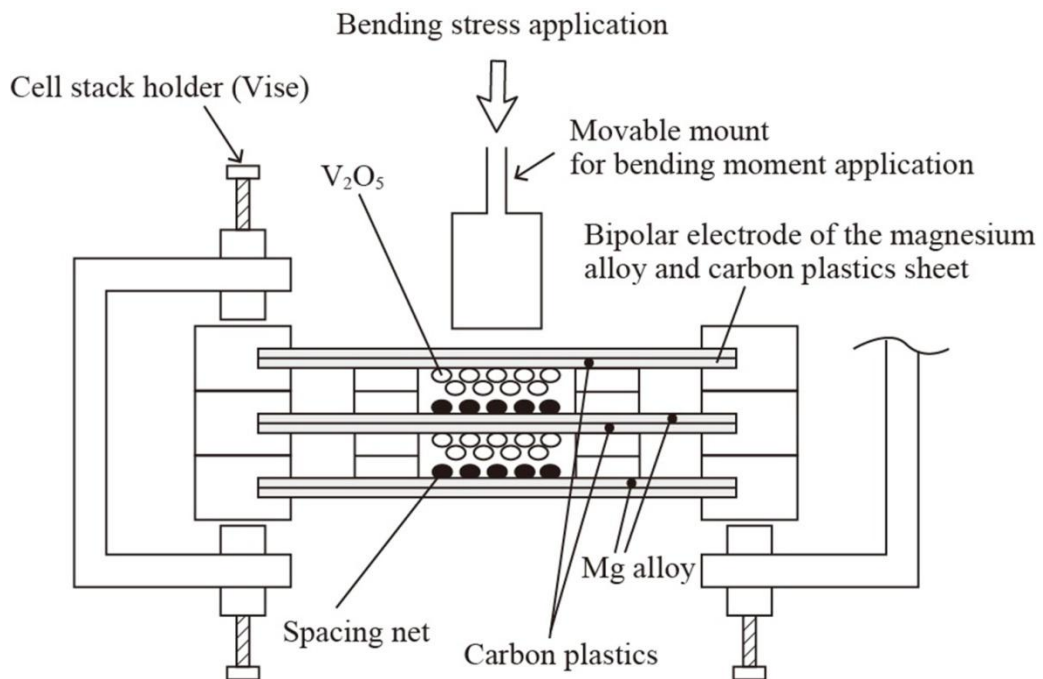


Fig. 5.3 Tensile-stress-applied cell using bending moments



The electrolytes were prepared by dissolving tetramethylammonium perchlorate (TMAP, 0.1 M) and saturated magnesium perchlorate (pure grade, Wako Pure Chemical Industries, Ltd.) in dimethyl sulfoxide (DMSO, special grade, Wako Pure Chemical Industries, Ltd.) or propylene carbonate (PC, battery grade, Highchem Co., Ltd.). TMAP was added to the electrolytes to improve their ionic conductivities.

The current-potential curves were measured using an electrochemical measurement system (HZ7000, HOKUTO DENKO Co., Ltd.) and a potentio/galvanostat (HA151, HOKUTO DENKO Co., Ltd.) for small single cells.

In order to explain the electrochemical behaviour of the battery in principle, resistance testing is very important. So An impedance analyser (ModuLab-XM, Solortron) was used to estimate the internal resistance distribution in the small single cells of the non-aqueous media. In order to observe the microstructure of the electrode after the corrosion reaction under the conditions of the tensile test, we placed the sample in SEM-EDX for observation and analysis. The surface and cross-section of the magnesium alloy sheets were both observed by SEM-EDX (JSM-5500LV, JEOL Ltd.,)

The practical use of the battery for magnesium alloy battery research is a crucial role. In order to allow stress corrosion can be applied in the actual battery, a two-cell stack was assembled for use under 3.3 MPa bending stress to consider its practical application, as shown in Fig 5.3. The cell stack has the following elements: a magnesium alloy sheet, spacers, V<sub>2</sub>O<sub>5</sub>-supported carbon fibre felt, a carbon plastic sheet, a magnesium alloy sheet (bipolar plate), spacers, V<sub>2</sub>O<sub>5</sub>-supported carbon fibre felt, and a carbon plastic sheet [15]. Magnesium per-chlorate in PC was used as the electrolyte. The effect of the bending stress was examined by comparing the results of the charge and discharge tests under bending stress and no-load conditions at a constant current of 2 mA/cm<sup>2</sup>.

### 5.3 Results and Discussion

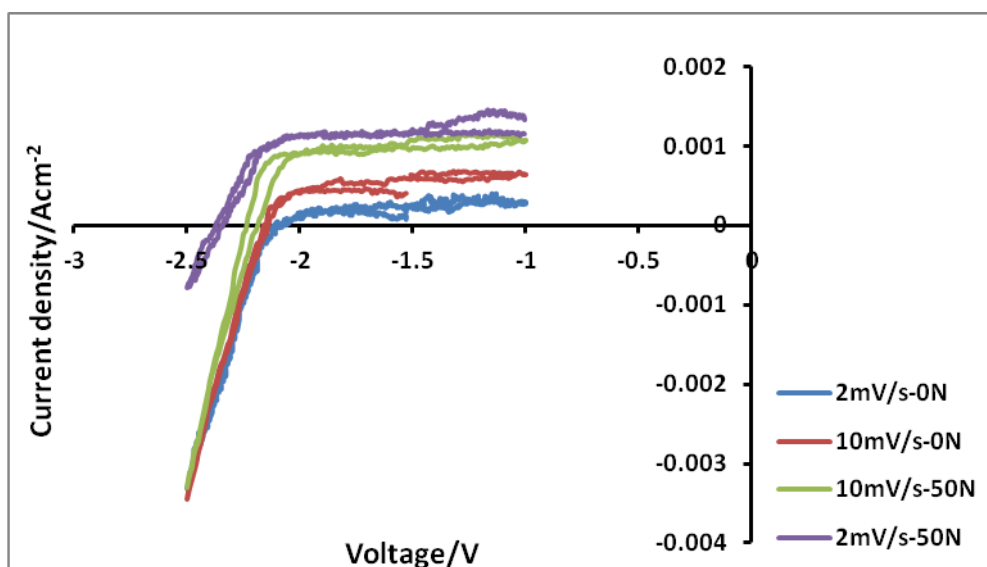


Fig. 5.4 Cyclic current voltage curves for the magnesium alloy sheet electrodes under three different conditions. at 293 K

Fig. 5.4 shows the cyclic current voltage curves for the magnesium alloy sheet electrodes under four different conditions. Above 2mA cm<sup>-2</sup> of apparent anodic current densities were obtained in the potential range from -2V to -1V for 10MPa application; whereas unstable 0.2 ~ 0.5mAcm<sup>-2</sup> of the currents were obtained in case of no tensile stress application. The difference of current level for the scanning rates, such as 2mV and 10mV a second, seemed to be caused by the anodic reaction rates of the electrodes especially for 10MPa of tensile stress application; in contrast to cases of no tensile stress application. Anodic currents, insufficient to reproducibility, were observed for no tensile stress and the difference of current caused by the scanning rates seemed to have no significant difference.

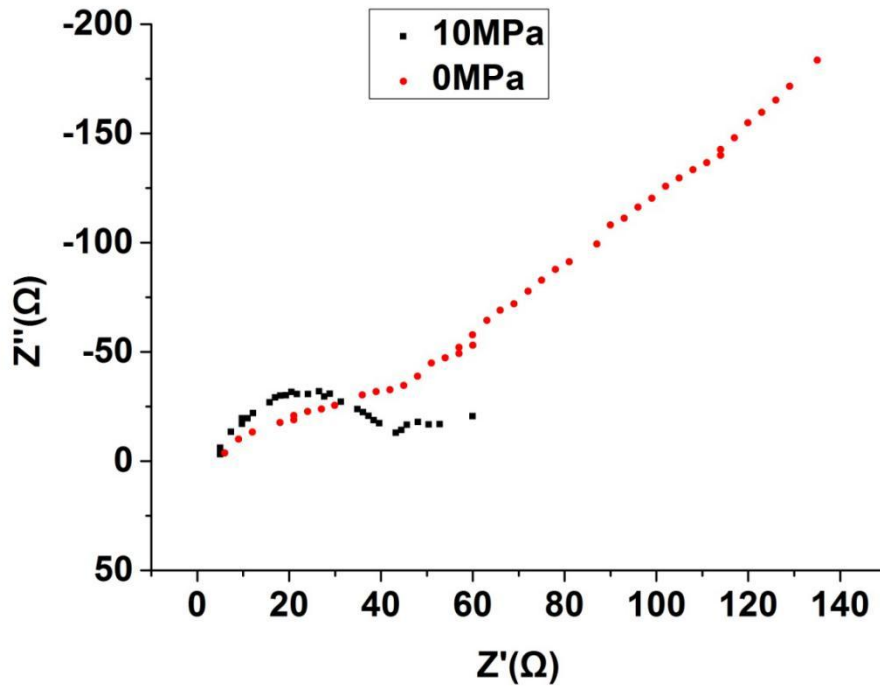


Fig. 5.5 Nyquist plots of the magnesium alloy sheet in TMAP and  $\text{MgClO}_4/\text{DMSO}$  electrolytes of the small single cell at 293 K; (a) 10 MPa tensile stress application and (b) no-load condition

The impedance analysis results in these cells under 10 MPa tensile stress and the no-load condition are shown in Fig. 5.5(a) and 5.5(b), respectively. The mass transfer condition in the electrochemical process of the magnesium alloy electrode improved under tensile stress, and the capacitance values, which were estimated from the Nyquist plots, increased to  $3 \text{ mF/cm}^2$  from  $50 \text{ }\mu\text{F/cm}^2$  because of the tensile stress.

The area resistivity, which was estimated from the inclinations of the voltage-current curves in Figs. 5.5 (curve (a): under 10 MPa stress; curve (b): without loading), was approximately  $130 \text{ }\Omega\text{cm}^2$  for curve (a) and  $60 \text{ }\Omega\text{cm}^2$  for curve (b). These values correspond to the impedance analysis results of the cell, which can be divided into the values of the charge transfer and mass transfer processes. There is a great difference in the mass transfer process under different tensile stress conditions. It is considered that the mass transfer ability increases because of the tensile stress application.

The mobility of magnesium ions appeared to be easier under 3.3 MPa tensile stress than the result without tensile stress, as shown by the clear difference in Warburg impedance in Figs. 5.6(a) and (b). When the cathode was loaded by tensile stress, the

corrosion layer of the alloy tended to become thinner, so the mass-transfer characteristics improved between the electrode surface and the electrolytes, which should accelerate charge-discharge reactions. Thus, the organic solvent resistance would be reduced and the entire battery impedance reduced. However, regardless of whether the stress is loaded, the Mg-Zn-In-Sn- MnS alloy sheet has a lower resistance in the organic solvent than the other magnesium alloy in the aqueous solution<sup>(16)</sup>.

XPS was used to determine the composition of the electrochemical corrosion before and after reaction under the condition of tensile stress as shown in Fig. 5.7. When the magnesium alloy was electrochemically corroded with an organic solvent of DMSO and TEMP, the amount of carbon and oxygen greatly increased. It was confirmed that the chemical composition of the organic substance in the corrosion layer increased. Also, the amount of magnesium was slightly lowered, it turned out that the cause was that magnesium had become an oxide.

Table 5.1 Anodic current densities under various tensile stresses at 1.4 V vs. Ag/AgCl in cyclic voltammograms from -1.2 V to -1.7 V at 298 K

Electrolytes	Solvents	Current densities (mAcm <sup>-2</sup> ) / potentials at 0 mA (V vs Ag/AgCl)				
		0.0 MPa	3.3 MPa	6.7 MPa	10 MPa	13 MPa
0.1 M tetra-ethyl ammonium perchlorate	DMSO	9 / -1.8	12 / -1.8	13 /-2.0	15 /-2.0	15 / -2.0
	PC	2 /-1.8	5 / -1.8	5.5/-1.8	6/-1.8	8/-2.0
0.1 M Magnesium perchlorate	DMSO	-3 /-1.8	5/ -1.8	6/-1.8	7 /-1.8	8/-1.8
Saturated potassium chloride	DMSO	6 / -1.8	8 /-1.8	12/-1.8	12 / -1.8	12 / -1.8
	PC	6 / -1.8	6 / -1.8	7/-1.8	8/-1.8	8/-1.8

Table 5.1 shows the comparative results of anodic current densities from -1.8V to -2.0V vs. Ag/AgCl under various tensile stresses in cyclic voltammograms at 298 K. The combinations of DMSO and TMAP were measured over 2 V, which could not be obtained in aqueous media, but other combinations were less than -1.7 V, which is identical to the case of aqueous solutions. As a high-current-density battery (10 mA/cm<sup>2</sup>), the reduction of cell resistance is notably important, which depends on the

conductivity of the electrolytic solution. The anodic currents increased with the reinforcement of the tensile stress, and the shift in voltages at the current of 0 mA showed the same tendency as the current densities for all combinations of supporting electrolytes and organic solvents.

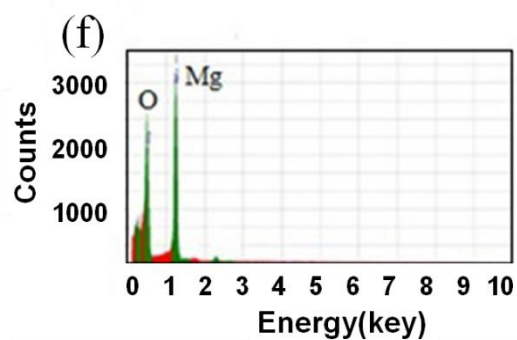
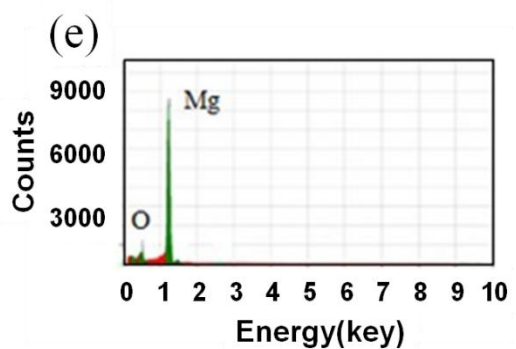
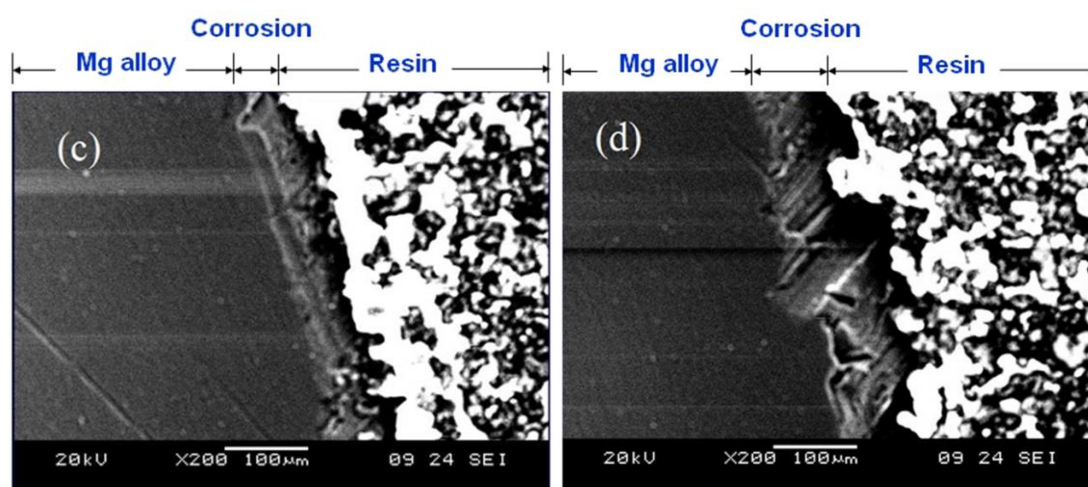
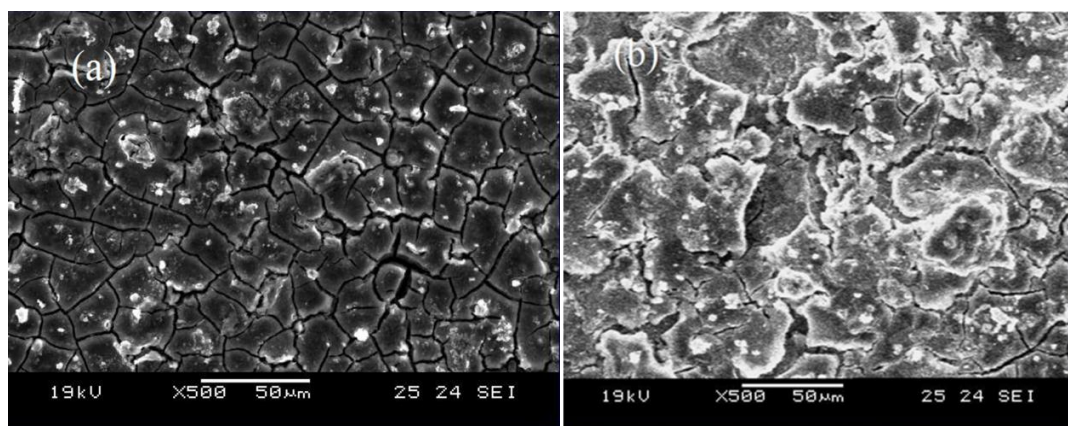


Fig. 5.6 SEM images and EDX analyses of the magnesium alloy sheets: (a) surface of the corrosion layer after the application of 3.3 MPa tensile stress; (b) surface of the corrosion layer after no tensile stress; (c) cross-section after the application of 3.3 MPa tensile stress; (d) cross-section after the no-load test; (e) EDX analysis result of the corrosion layer under 3.3 MPa tensile stress; (f) EDX analysis result of the corrosion layer after no tensile stress

Figures 5.6 (a) and (b) show the SEM images of the magnesium electrode surface after the charge and discharge tests under 3.3 MPa tensile stress (a) and the no-load condition (b). When no tensile stress was applied, bulky massive solids were observed at the electrode surface; in contrast, small aggregates of solids were observed under 3.3 MPa tensile stress. This result was similar to the observation of the corrosion tests in the aqueous solution. Figure 5.6 shows the cross-sections of the magnesium alloy electrodes after use (c: 3.3 MPa tensile stress; d: no load). A relatively thick corrosion layer was observed under no tensile stress, whereas a thinner corrosion layer was observed under 3.3 MPa tensile stress. The magnesium-to-oxygen ratio (Mg/O) after charging was different in the presence and absence of tensile stress according to the EDX analyses of the border between the alloy and the corrosion layer, as shown in Fig. 5.6 (e: 3.3 MPa; f: no load). The Mg/O ratios were 2.3 for no tensile stress and 5.3 under 3.3 MPa tensile stress. Magnesium was considered to be deposited at the border between the alloy and the corrosion layer. In order to compare the chemical composition before and after electrochemical corrosion reaction, XPS was used to determine.

Examples of the current-voltage curves of magnesium alloy electrodes are shown in Fig. 5.7, which presumes the charge-discharge performances of the Mg alloy sheet batteries. Fig. 5.7(a) was obtained for 10 mA/cm<sup>2</sup> of current density under 3.3 MPa tensile stress in the TMAP/DMSO electrolyte, and Fig. 5.7(b) was obtained for 2 mA/cm<sup>2</sup> under the same conditions as in Fig. 5.7(b). A stable voltage curve was obtained for the current density of 2 mA/cm<sup>2</sup>.

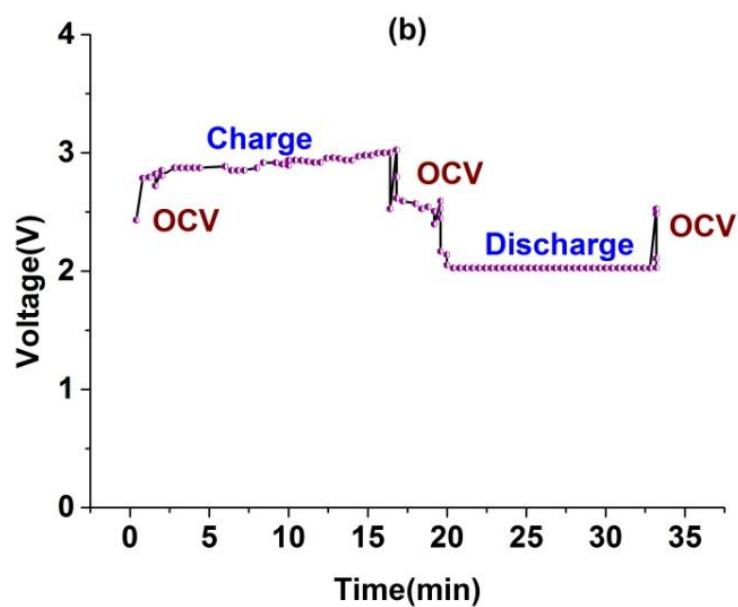
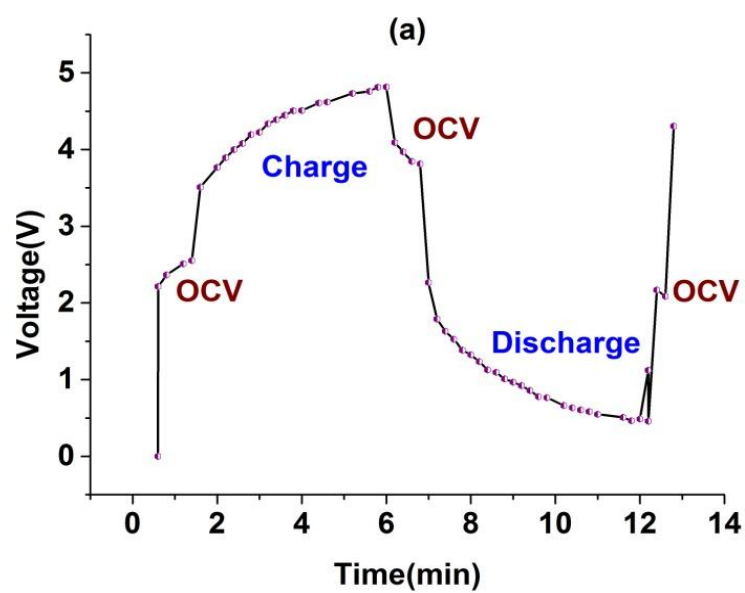


Fig. 5.7 Examples of current-voltage curves of magnesium alloy sheet electrodes using the test system in Fig. 1 under 3.3 MPa tensile stress in the TMAP/DMSO electrolyte at 298 K and a current density of (a) 10 mA/cm<sup>2</sup> or (b) 2 mA/cm<sup>2</sup>

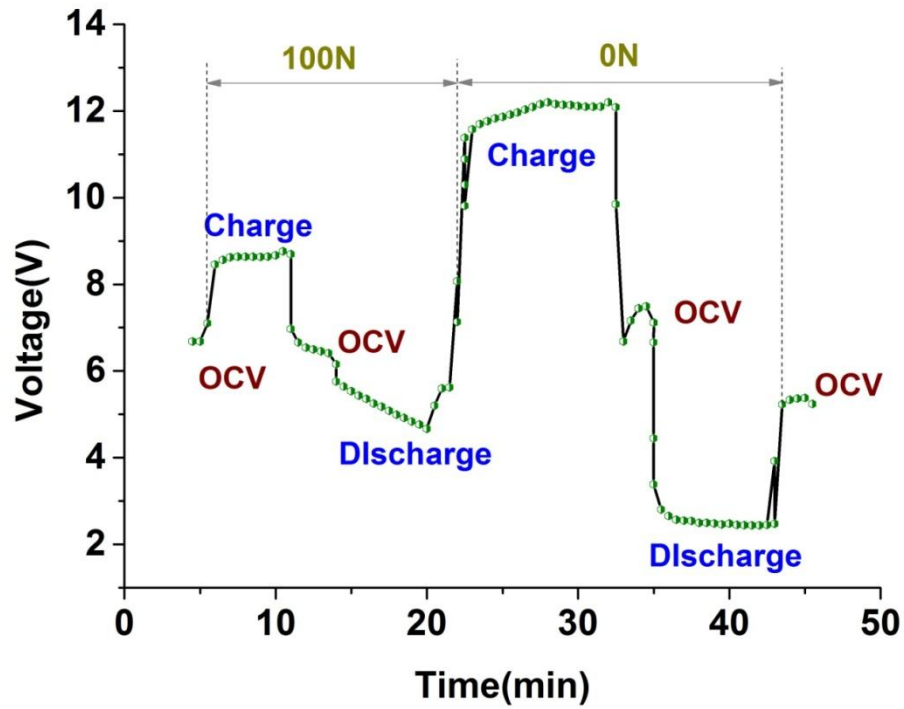


Fig. 5.8 A voltage curve presuming the charge-discharge performance for a two-single-cell stack of a magnesium alloy negative electrode and a  $V_2O_5$ -supported carbon fibre positive electrode

According to the charge-discharge performances of the two-single-cell stack in Fig. 5.8, the present cell configuration is expected to have at least 100 W/kg of power density under approximately 100 N of bending stress. The voltage for the cathodic polarization of the alloy electrode rapidly increased to above 12 V when the bending stress of 100 N was released but remained below 9 V under 100 N of bending stress. Similarly, the voltage for anodic polarization of the electrode decreased to almost 2 V despite the two-single-cell stack. Thus, the tension stress determines whether the battery can properly work. There was a positive correlation between the magnitude of the bending stress and the change in voltage. The anode and cathode chemical reactions within the battery are as follows :

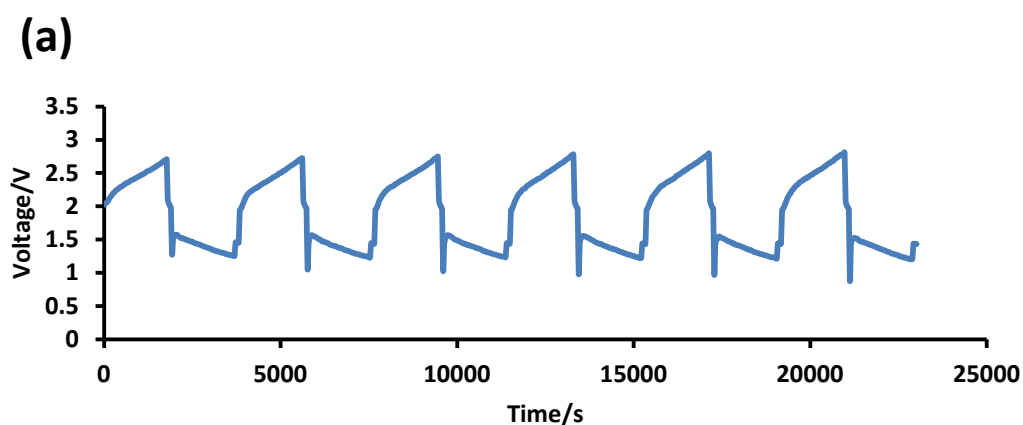




The charge and discharge life performances were shown in Fig. 5.9 (a) no tensile stress and (b) 3.3MPa of tensile stress. The setting charge periods were 40 minutes and the discharge end voltage were 1.0V with the condition of  $0.8\text{mA}/\text{cm}^2$  constant current densities for charge and discharge, and the open circuit voltage, OCV, were observed for 2 minutes every time between charge and discharge periods.

According to the differences of OCV between the case of charge and discharge, 0 and 3.3MPa of tensile stress application, the differences under tensile stress application were smaller than the case of no tensile stress, which seemed to increase the capacity of the cell. Approximate 100mV of OCV difference was estimated for this single cell corresponding the change in depth of charge, DOC, from 50% to 90%, in consideration of Nernst equations. The tensile stress application was expected to increase the rate of utilization of battery active materials remarkably, which was supposed by the results of impedance analyses. The components of Warburg impedance were extremely decreased on applying tensile stress to the cells.

The coulombic efficiencies were above 98% for both and voltaic efficiencies were 60 % for no tensile stress and 70 % for 3.3MPa of tensile stress respectively. The area resistivity of the single cell reduced by half under 3.3MPa of tensile stress.



**(b)**

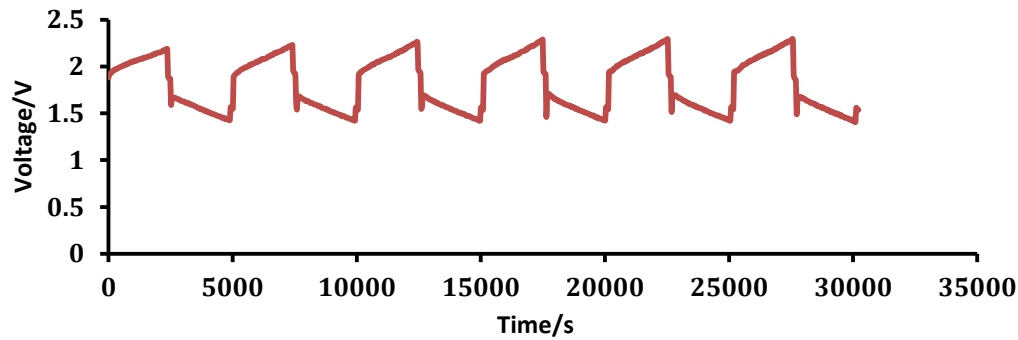


Fig. 5.9 The Charge-Discharge performance of the cell for 8 cycle(a) in case of no tensile stress application and (b) in case of 3.3MPa tensile stress application.

## 5.4 Conclusion

The effects of a new type of magnesium alloy electrode, which was selected from various components under tensile stress, were examined for magnesium secondary batteries in this paper. In addition to the charge and discharge performance, the effect under tensile stresses was also confirmed using cyclic voltammetric measurements, SEM observations and impedance analyses. Significant differences in SEM observation and impedance analysis between the cases with and without tensile stresses were obtained. The charge and discharge curve for the current density of  $2 \text{ mA/cm}^2$  in the TMAP/DMSO electrolyte was better than that for  $10 \text{ mA/cm}^2$ . When the internal resistance was reduced based on the electrolyte and positive electrode, the practical power density exceeded  $100 \text{ W/kg}$  for the secondary battery in the present cell configuration. We are conducting further studies to design practical battery systems. A two-single-cell stack battery, which can use the bending stress method, has been proposed for a practical application. In this battery structure, the role of stress control is obvious and can be expected as a new battery system. Since the calculation value of the alloy electrode voltage and the current almost agreed with the experimental value, the mechanism of corrosion and the influence of stress were explained theoretically.

## References

- [1] Z. Yu , D. Y. Ju and T. Nukii, *Int. J. Electrochem. Sci.*, 7(2012):10164-10174 .
- [2] P. Novak, R. Imhof and O. Haas, *Electrochimical. Acta*, 45(1999): 351.
- [3] E. Sheha and M. K. El-Mansy, *J. power Sources*, 185(1999):1509.
- [4] G. Shi, Z. Yu, O. Hamamoto and D. Y. Ju, 2015 Autumn Meeting of the Electrochemical Society of Japan, Abstr.,1C02. (2015) [in Japanese]
- [5] Z. Yu, G. Shi and D. Y. Ju ,*Int. J. Electrochem. Sci.*, 9(2014): 6668-6676.
- [6] Z. Yu, D.Y. Ju and H.Y. Zhao, *Int. J. Electrochem. Sci.*, 7(2012): 7098.
- [7] M. Matsui, *J. Power Sources.*, 196(2011): 7048.
- [8] D. Aurbach, Z. Lu, A. Schechter, Y. Gofer, H. Gizbar, R. Turgeman, Y. Cohen, M. Moshkovich and E. Levi, *Nature*, 407(2000): 724.
- [9] Z. Yu, D.Y. Ju, Y. H. Zhao and D. X. Hu, *J. Environ Sci.*, 23(2011): S95.
- [10] K. Yu, Q. Huang, J. Zhang and Y. L. Dai, *Trans. Nonferrous Met. Soc.*, 22(2012): 2184.
- [11] S. Sadhukhan, M. Kundu and M. Ghosh, *Advanced Materials Research.*, 828(2014): 73.
- [12] Q. Meng, G. S. Frankel, H. O. Colijn and S. H. Goss ,*Nature*. 424, 389(2003).
- [13] S. Rasul, S. Suzuki, S. Yamaguchi and M. Miyayama, 220th ECS Meeting, Boston, USA, 615(2011).
- [14] E. Kakutani, K. Fujio, M. Jotoku, A. Yamamoto and H. Tsubakino, *J. Japan Institute of Metals.*, 72, 420 (2008) [in Japanese].
- [15] A. Ghulam, Ji-H. Lee, H. O. Si, B. W. Cho, K-W. Nam and K. Y. Chung, *ACS Appl. Mater. Interfaces*, 8(2016): 6032.
- [16] K. Yu, H. Q. Xiong, L. Wen, Y. L. Dai, S. H. Yang, S. F. Fan, F. Teng and X. Y. Qiao, *Electrochimica Acta*, 194 (2015): 40-51.
- [17] Keita Umetsu, Yoshinao Hoshi, Isao Shitanda and Masayuki Itagaki, 2015 Autumn Meeting of the Electrochemical Society of Japan, Abstr., 2L11(2015). [in Japanese]

## **Chapter 6 Phosphorous Recovery by the Magnesium Alloy**

### **Electrode under Tensile Stress**

#### **6.1 Introduction**

Phosphorous in waste water or sewage sludge are expected to be removed at so called tertiary treatments in waste water treatment facilities from the point of view in environmental protection[1,2,3]. Recently, phosphorous has been considered to be recovered due to one of starved natural resources in the world[4,5]. Electrodeposition of phosphorous ions on metal electrodes is a well-known method for phosphorous removal from waste water. However, it is difficult for conventional metal electrodes, such as cast iron and aluminum, to recover phosphorous practically in the form of phosphate ions, since the separation of phosphorous from such metal electrodes is difficult due to their high affinity with phosphorous. On the other hand, stainless steels are also difficult to be phosphate adsorption electrode for phosphate recovery due to the formation of insulating phosphate layer on the surface of the steel[6,7].

Magnesium alloys, such as AZ91, have been found to be a suitable electrode material for phosphate ion recovery by being deposited from the sludge and being dissolved into concentrated solutions under tensile stress, in this study, which could control the activity of the magnesium alloy surface by means of tensile stress application. Magnesium alloys, which is effectively affected by the tensile stress for their high Young's modulus[8], were expected to be a practical electrode materials for phosphorous recovery from various solutions or slurries including phosphorous ions by the anodic deposition and succeeding cathodic dissolution on the surface of alloys. The chemical reaction equation for phosphorus recovery is as shown in Fig. 6.1:

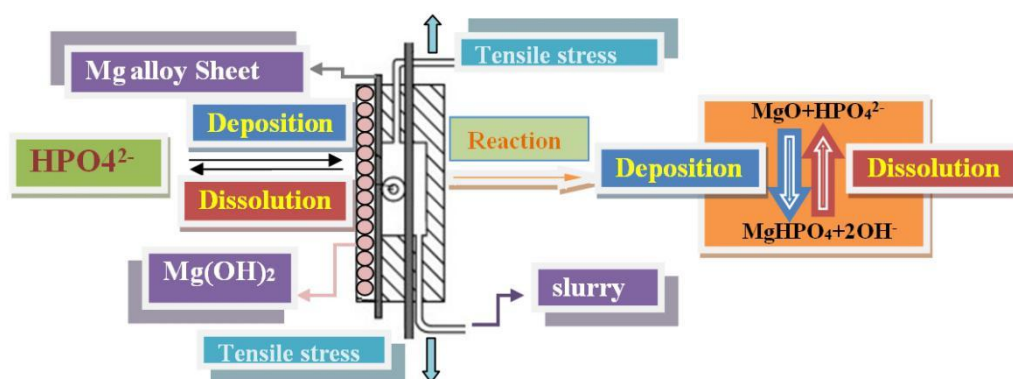


Fig. 6.1 The chemical reaction equation for phosphorus recovery

## 6.2 Experimental

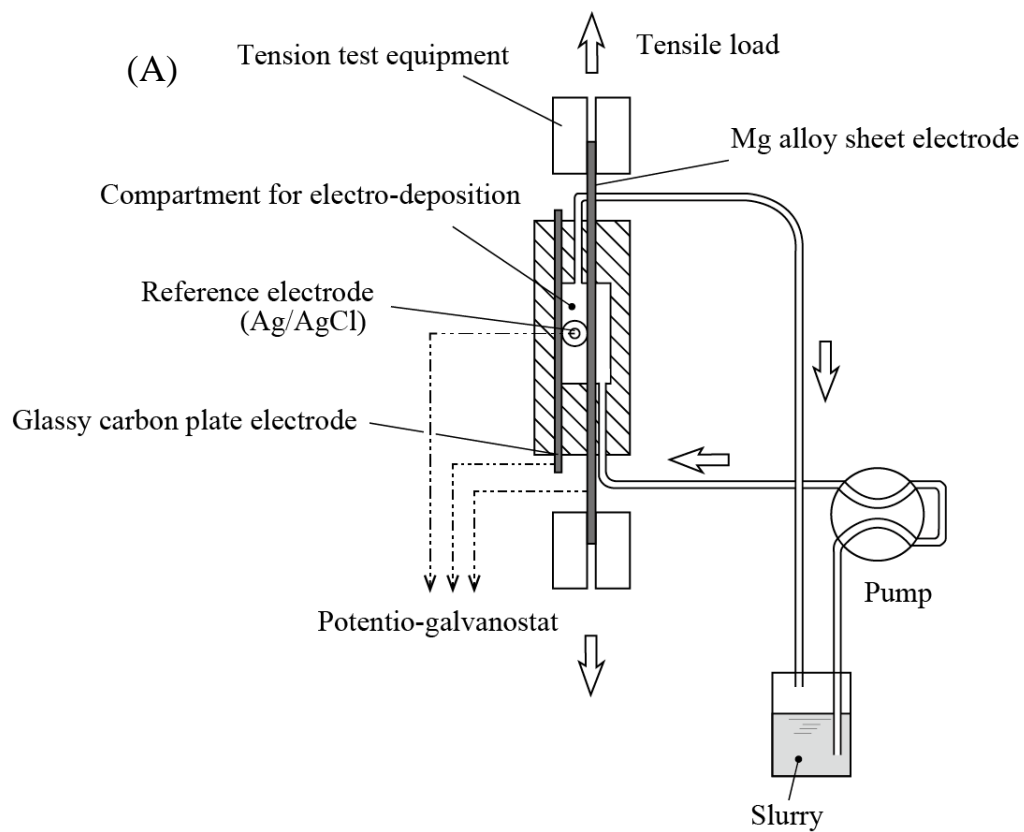
An experimental system for phosphorous recovery from the concentrated sewage sludge are shown in Fig. 6.2(A), the system flow, and (B), the photo. A sheet of magnesium alloy electrode [9,10], 10 cm in length, 1 cm in width and 1 mm in thickness, was equipped in a small single cell with 1 cm<sup>2</sup> of effective electrode area; and was stretched by tension tester (EZ-TEST CE, Shimadzu Corp.) of tensile stress condition from 1 to 10 MPa. Electrochemical measurements system (HZ-7000, Hokuto Denko Co., Ltd.) and potentiostat / galvanostst (HA-151, Hokuto Denko Co., Ltd.) were connected to the small single cell for voltage - current curves and cyclic voltammograms measurements. 20 mL of the sewage sludge was circulating in the cell by tubing pump at 2-5 ml/min for phosphorous deposition. Table 6.1 shows main components and properties of the concentrated sewage sludge. Dipotassium phosphate (special grade, Wako Pure Chemical Industries, Ltd.) was added into the sludge to adjust the approximate 340 mg/l as phosphorous ion,  $\text{PO}_4^{3-}$ , concentration. After deposition procedure of 10 mA/cm<sup>2</sup> constant current for 10 minutes, 10 mL of approximate 0.1M ( $\text{M}=\text{mol dm}^{-3}$ ) sodium acetate / acetic acid solution, pH6, was

circulated in the cell by tubing pump at 2-5 ml/min for 10 minutes. Electrode potential, -1.8V vs Ag/AgCl for the dissolution, was controlled by reference electrode of Ag/AgCl. Phosphorous ion concentrations in the solution and sludge were determined by colorimetry and deposited phosphorous on the electrodes was observed by SEM-EDX (JSM-5500LV, JEOL Ltd.,).

Table 6.1 Main components and properties of the concentrated sewage sludge.

Items	Results	Methods
<b>pH</b>	6.7	Glass electrode
<b>TS</b>	1.4 wt%	105°C drying
<b>VS</b>	0.72 wt%	600°C ignition
<b>MLSS</b>	13,600 mg/l	Filtration
<b>MLVSS</b>	6,940 mg/l	Filtration-ignition
<b>BOD</b>	2,950 mg/l	5 days method
<b>COD</b>	4,850 mg/l	Chromate titration
<b>Pb</b>	10.2 mg/l	Atomic Absorption
<b>Phosphate *</b>	340 P-mg/l	Atomic Absorption

\*: Addition of  $\text{KH}_2\text{PO}_4$



(B)

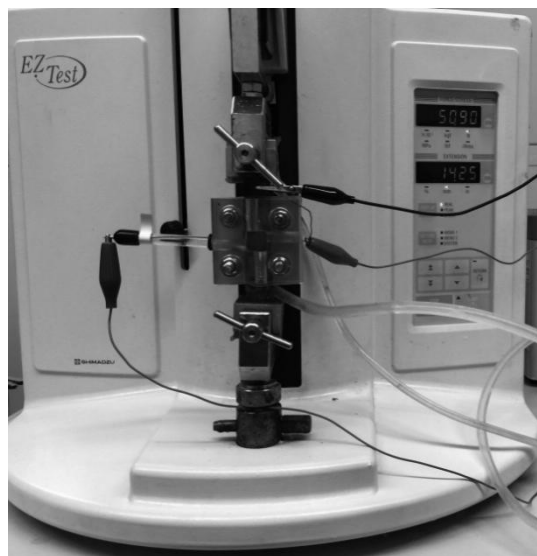


Fig. 6.2 An experimental system for phosphorous recovery from the concentrated sewage sludge.

### 6.3 Results and discussion

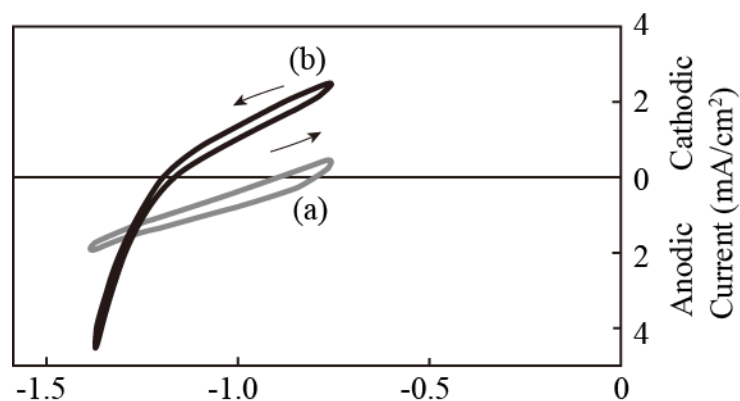


Fig. 6.3 Cyclic voltage-current curves of the magnesium alloy electrodes in 0.1M NaHCO<sub>3</sub> (curve (a)) and 260 mg/L-K<sub>2</sub>HPO<sub>4</sub> in 0.1M NaHCO<sub>3</sub> (curve (b)).

Figure 6.3 shows cyclic voltage-current curves of the magnesium alloy electrodes in 0.1M NaHCO<sub>3</sub> (curve (a)) and 260 mg/L-K<sub>2</sub>HPO<sub>4</sub> in 0.1M NaHCO<sub>3</sub> (curve (b)). The point of current 0 mA was shifted to the anodic direction by addition of dipotassium phosphate under 10 MPa tensile stress condition, considerable that the formation of basic phosphate compounds, such as magnesium phosphate tribasic salts. Magnesium hydroxides, estimated to be formed on the surface of the alloy in this study, could adsorb phosphates effectively for water quality improvement of eutrophic lakes[11]. The composition of phosphate adsorbed magnesium compounds were investigated by XRD, XPS and micro Raman spectroscopy.



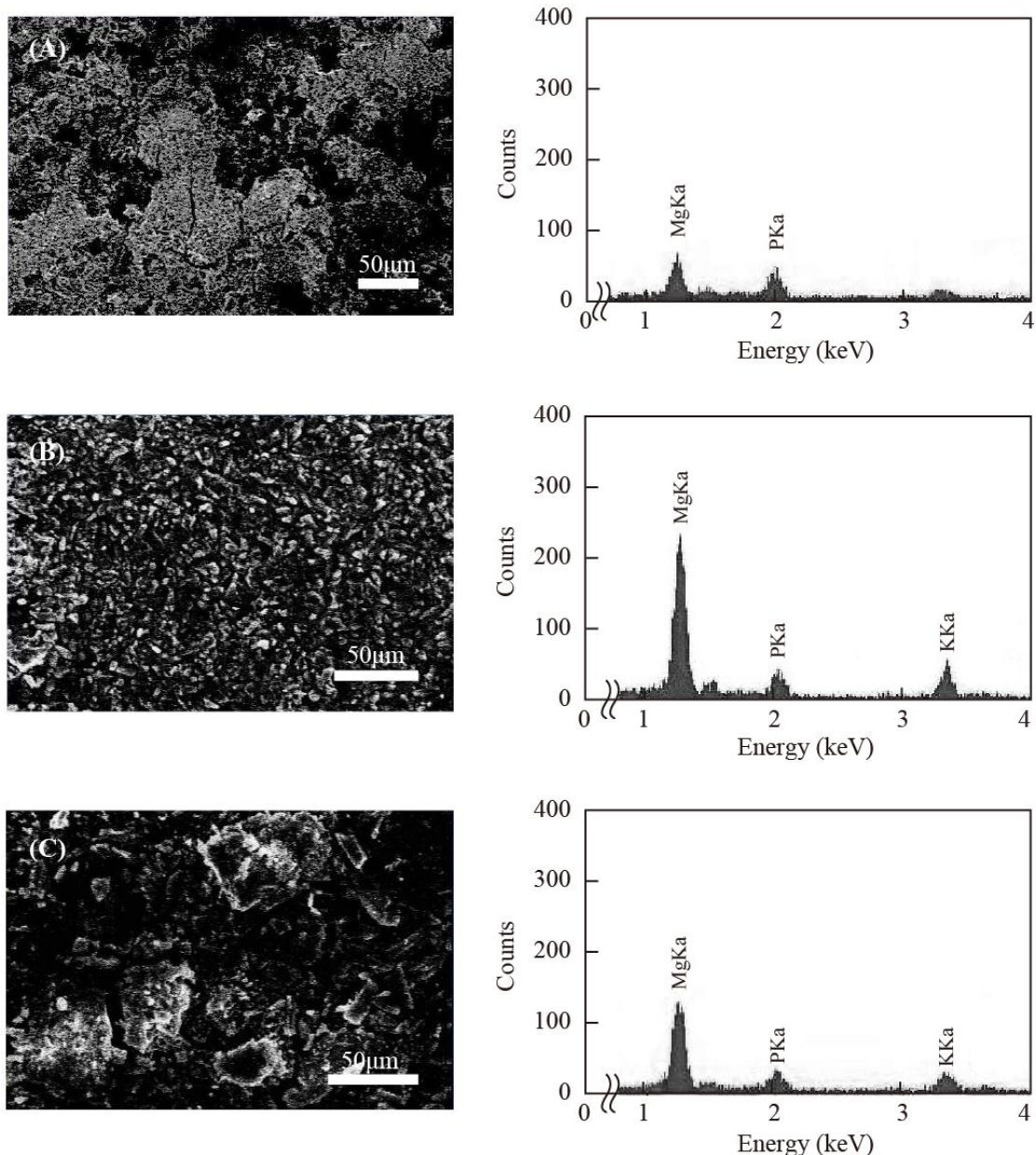


Fig. 6.4 SEM images and EDS spectra after 10 mA electro-deposition for 10 minutes under 10 MPa tensile stress(A), 10 mA electro-deposition for 10 minutes without tensile stress(B) and -1.8V vs Ag/AgCl and 10 minutes electro-dissolution under 10 MPa stress(C).

Figure 6.4 shows the SEM images and EDX spectra of the electrodes after 10 mA/cm<sup>2</sup> electro-deposition for 10 minutes under 10 MPa tensile stress condition (A), 10 mA/cm<sup>2</sup> electro-deposition for 10 minutes. without tensile stress (B) and -1.8V vs Ag/AgCl 10 minutes constant potential application for electro-dissolution of phosphate, succeeding to the electro-deposition under 10 MPa tensile stress (C).

In the EDX spectra, the ratios of numbers of elements for Mg and P, Mg/P, were 1.5 for EDX spectrum (A), 3.9 for (B) and 4.6 for (C). After the anodic adsorption of 10 MPa tensile stress condition, the abundance ratio of P was larger than other situations,

(B) and (C). A magnesium alloy may form anticorrosive composite films composed of amorphous or crystalline magnesium phosphate compounds and magnesium hydroxide on its surface[12].

Table 6.2 Concentrations of phosphorous ion in the sludge and solution after electro-deposition or dissolution.

	Concentration	
	After electro-deposition	After electro- dissolution
<b>0MPa tensile stress, deposition</b>	340 mg dm <sup>-3</sup>	No implementation
<b>10MPa tensile stress, deposition-dissolution</b>	90 mg dm <sup>-3</sup>	680 mg dm <sup>-3</sup>
<b>Remarks</b>	After deposition at 10 mA for 10 minutes	After dissolution at -1.8V for 10 minutes succeeding the electro-deposition

Table 6.2 shows an example of phosphorous recovery from the excess sludge concentrated in gravitational precipitation tank of a sewage treatment facility. The phosphorous ion concentration in the sludge was not removed at all in case of no-tensile stress condition; therefore, no dissolution test was conducted in this case. On the other hand, the phosphorous ion concentration was reduced from 340 mg dm<sup>-3</sup> to 90 mg dm<sup>-3</sup> and concentrated to 680 mg dm<sup>-3</sup> after the dissolution procedure.

The application of tensile stress was considered to be important for activation of alloys similar phenomena to stress corrosion. The activation of magnesium alloys could be realized by tensile stress application especially in magnesium batteries.<sup>8,10</sup> The results of impedance analyses showed the ratios of charge transfer process depended on the extent of tensile stress application. The larger tensile stress, the smaller ratio of charge transfer process in the real part of resistance. It seems that mechanical control, such as tensile stress application, is effective for magnesium

alloys to restrict their passivation. Other metals, such as aluminum and iron, have a problem of plastic deformation under effective tensile stress conditions. On the other hand, stainless steels with high young's modulus need stronger tensile stress, such as 20 MPa or more, which seems to be difficult to design the practical equipment for phosphorous recovery. Magnesium alloys was expected to be one of the most suitable electrode materials for phosphate recovery from sludge and solutions. A system for phosphate recovery was being designed targeting the treatment of the rock phosphate residue.

## **6.4 Conclusion**

A practical method was studied for phosphorous resource recovery from wastes, such as waste water or many kinds of sludge. It was confirmed that the magnesium alloy electrodes could remove phosphates from the sludge and dissolve them by applying reverse polarization for phosphate resources recovery. Other materials, such as stainless steels, aluminum and casting iron, were hard to be employed for the practical phosphate recovery equipment due to their mechanical characteristics. Electrolytic cells for phosphorous recovery and their processes are being designed for a sewage treatment facility and a phosphorous ore mine.

## References

- [1] K. Suzuki, Y. Tanaka, K. Kuroda, D. Hanajima, Y. Fukumoto, T. Yasuda, and M. Waki, *Bioresource technology*, 98(2007): 1573 .
- [2] K. Wang, Z. Liu, D. Lee, W. Qiu, and J. Wang, *J. Environmental Sciences*, 20(2008) :1018 .
- [3] G. K. Morse, S. W. Brett, J. A. Guy, and J. N. Lester, *Sci.Total Environ.* 212(1998): 69 .
- [4] P. Cornel, and C. Schaum, *Water Sci. Technol.*, 59(2009): 1069 .
- [5] A. Noula, and A. Christodoulou, *Proc. The World Congress on New Tech. (New Tech. 2015)*, Barcelona, Spain-July 15-17(2015): 157 .
- [6] E. Nassef, *Engineering Science and Technology*, 2(3)(2012): 403 .
- [7] T.S.N. S. Narayanan, *Rev. Adv. Mater. Sci.*, 9(2005): 130 .
- [8] G. Shi, Z. Yu, O. Hamamoto and D. Y. Ju, 2015 Autumn Annual Meeting of the Electrochemical Society of Japan, Abstr., 1C02(2015). [in Japanese]
- [9] C. J. Bettles, M. A. Gibson, and K. Venkatesan, *Scr Mater*, 51(2004): 193 .
- [10] Z. Yu, D. Y. Ju, H. Y. Zhao, and X. D. Hu, *Transactions of Nonferrous Metals Society of China*, 20(2010): 318.
- [11] F. Xie, F. Wu, G. Liu, Y. Mu, C. Feng, H. Wang and J.P. Giesy, *Environ. Sci. Technol.*, 48(2014): 582.
- [12] T. Ishizaki, R. Kudo, T. Omi, K. Teshima, T. Sonoda, I. Shigematsu and M. Sakamoto, *Materials Letters*, 68(2012): 122.

## Chapter 7 Conclusion

In this research, we have developed a novel magnesium alloy electrode that can be used as a source of next-generation eco energy by taking advantage of the excellent performance of magnesium. Compared with the commercially available magnesium alloy, it was found that it has excellent electrochemical performance. Moreover, in order to achieve higher performance, the electrochemical performance of the novel magnesium alloy electrode was improved by combining stress and corrosion.

The main innovation of this paper is to add compounds MnS into the Mg-Zn-In-Sn alloy and the new material is used as a cathode for the aqueous solution battery and secondary battery that used the organic solvents. On the other hand, the effect and influence of the additional tensile stress on the cathode is also verified. Then, according to the principle of tensile stress, material recovery, such as phosphoric acid recovery has also been the significant results.

The following conclusions are drawn from the series of experimental and theoretical studies

(1) A new magnesium alloy Mg - Zn - In - Sn - MnS was produced by adding a trace element Mn to a magnesium alloy Mg - Zn - In - Sn using a vacuum gas replacement furnace and made it by twin roll continuous casting method. Its tissue composition is also identified, and through micro-observation, the structure is better than Mg-Zn-In-Sn-MnS alloy.

(2) It was found that Mg - Zn - In - Sn - MnS alloy has the most negative rest potential by measuring various alloys in the same electrolyte. Furthermore, using the constant stress corrosion method, the CV curve of the new magnesium alloy was measured in various solutions. When the distance between the cathode and the counter electrode was 2 mm, it was confirmed that the output performance of the novel magnesium alloy was the highest under 1 MPa stress in 1 Mol AcONa solution.

(3) A corrosion model was developed and the electrochemical properties of the Mg - Zn - In - Sn alloy electrode were calculated. It was found that the concentration of Mg decreases as the stress increases. Since the calculated value of the alloy electrode voltage and current almost agreed with the experimental value, the mechanism of corrosion and the influence of stress were theoretically explained.

(4) The anodes dissolution was controlled by loading 3 to 10MPa of tensile strain on the modified AZ91 alloy for a magnesium – air fuel cell.  $0.6\text{Acm}^{-2}$  of the current density and  $0.5\text{Wcm}^{-2}$  of output power were obtained under the condition of -1.0V vs Ag/AgCl of the negative electrode and sodium acetate - acetic acid solution. A small single cell was assembled and demonstrated by combining oxygen cathode of electro-conductive activated carbons with the magnesium alloy anode.

(5) The effects of a new type of magnesium alloy electrodes which had been selected from various components under tensile stress were examined for magnesium secondary batteries in this paper. The charge and discharge curve which had been obtained for  $2\text{mA/cm}^2$  of current density at TMAP/DMSO electrolyte was better than  $10\text{mA/cm}^2$  of current density. By reducing the internal resistance based on the electrolyte and positive electrode, the practical power density of that exceed 100 W/kg will be obtained for the secondary battery in the present cell configuration.

(6) It was confirmed that the magnesium alloy electrodes could remove phosphates from the sludge and dissolve them by applying reverse polarization for phosphate resources recovery. Electrolytic cells for phosphorous recovery and their processes are being designed for a sewage treatment facility and a phosphorous ore mine.

In this paper, a novel magnesium alloy was developed by the twin roll continuous casting method. In addition, by using stress corrosion, the electrochemical performance of the alloy electrode can be improved.

Furthermore, I have studied magnesium primary batteries and secondary batteries as new magnesium alloy applications, but as we advance research on magnesium batteries that can be used in various fields in the future, I think it is necessary to apply

them to the field of 3C products such as electric cars and mobile phones for further study.

## **Acknowledgments**

I would like to express my sincere appreciations to Prof. Dr. Dongying Ju, for taking me as his student and giving me the opportunity to pursue the Ph.D. degree at Saitama Institute of Technology. I want to express my sincere thanks for his support, encouragement and guidance throughout my study. Without his support I could not have achieved so much.

I would like to appreciate the exchange program between Saitama Institute Technology in Japan and University of Science and Technology Liaoning, China. And I would like to express my sincere gratitude to all the people who have provided information to me for giving me the change to study abroad.

I would like to thank Prof. Uchida, Prof. Matsuura, Prof. Ishizaki and Prof. Saito for sparing time from their busy schedules in reviewing my dissertation and their advisable comments for revising the paper. Without their help, I could not have understood this study correctly and deeply.

I would also like to thank Professor Osamu Hamamoto and Kazuko Takahashi for their cooperation in the implementation of this research.



## **Related publications**

1. G. Shi, D. Y. Ju, O. HAMAMOTO and K. TAKAHASHI. A New Method for Phosphorous Recovery Using Magnesium Alloy Electrode under Tensile Stress. Asian Journal of Chemistry. 30(2018) No.1, 123-125

2. G. Shi and D. Y. Ju, Simulation of Electrochemical Performance on Electrode of Mg-Zn Air Cell. Applied Materials and Technologies. 833(2015), 134-137

3. Z. Yu, G. Shi and D. Y. Ju , Electrochemical Properties Evalution of a Novel Mg Alloy Anode on Mg Air Batteries. Int. J. Electrochem. Sci., 9(2014): 6668-6676.